AN ABSTRACT OF THE DISSERTATION OF

Paul E. King for the degree of Doctor of Philosophy in Civil Engineering
presented on March 8th, 2006

Title: Deterministic and Stochastic Control of Nonlinear Oscillations in Ocean Structural Systems.

Abstract approved:

Redacted for Privacy

Complex oscillations including chaotic motions have been identified in off-shore and submerged mooring systems characterized by nonlinear fluid-structure interactions and restoring forces. In this paper, a means of controlling these nonlinear oscillations is addressed. When applied, the controller is able to drive the system to periodic oscillations of arbitrary periodicity. The controller applies a perturbation to the nonlinear system at prescribed time intervals to guide a trajectory towards a stable, periodic oscillatory state. The controller utilizes the pole placement method, a state feedback rule designed to render the system asymptotically stable. An outline of the proposed method is presented and applied to the fluid-structure interaction system and several examples of the controlled system are given. The effects of random noise in the excitation force are also investigated and the subsequent influence on the controller identified. A means of extending the controller design is explored to provide adequate control

in the presence of moderate noise levels. Meanwhile, in the presence of over powering noise or system measurements that are not well defined, certain filtering and estimation techniques are investigated for their applicability. In particular, the Iterated Kalman Filter is investigated as a nonlinear state estimator of the nonlinear oscillations in these off-shore compliant structures. It is seen that although the inclusion of the nonlinearities is theoretically problematic, in practice, by applying the estimator in a judicious manner and then implementing the linear controllers outlined above, the system is able to estimate and control the nonlinear systems over a wide area of pseudo-stochastic regimes.

Deterministic and Stochastic Control of Nonlinear Oscillations in Ocean Structural Systems

By

Paul E. King

A DISSERTATION

submitted to

Oregon State University

in Partial Fulfillment of
the Requirement for the
degree of

Doctor of Philosophy

Presented March 8th, 2006
Commencement June 2006

Doctor of Philosophy dissertation of Paul E. King

presented on March 8th, 2006

APPROVED:

Redacted for Privacy 3/21/2006

Major Professor, representing Civil Engineering

Redacted for Privacy 3/21/2006

Head of the Department of Civil, Construction and Environmental Engineering

Redacted for Privacy

Dean of the Graduate School

I understand that my dissertation will become part of the permanent collection of Oregon State University libraries. My signature below authorizes release of my dissertation to any reader upon request.

Redacted for Privacy

3-21-2006

Paul E. King, Author

ACKNOWLEDGMENTS

I would like to show my appreciation for the encouragement and support of my family and friends throughout my academic career at Oregon State University. My deepest appreciation and gratitude goes to my advisor, Professor Solomon C. S. Yim, for his obvious dedication to the quest for scientific knowledge and his enthusiasm in transferring that knowledge to his students. Special thanks go to my friend and supervisor Paul C. Turner for his patience throughout this process. I would also like to thank my mother, Marianne Hawkes and my grandparents JohnD and Kay Winters who share in this accomplishment with me. Thank you all for your help, encouragement and support.

CONTRIBUTIONS OF AUTHORS

Dr. Solomon C. S. Yim assisted with the writing of Chapters 2, 3, 4, and 5.

TABLE OF CONTENTS

TABLE OF CONTENTS (Continued)

TABLE OF CONTENTS (Continued)

TABLE OF CONTENTS (Continued)

1. INTRODUCTION

1.1 General

In the recent past, nonlinear effects in dynamical systems have been of great interest. As scientists and engineers exhaust the applicability of linear analysis techniques to highly complex nonlinear systems, means and methods of analyzing these systems with other techniques are needed. Over the past several decades, an explosion of such tools has occurred. The realm of nonlinear dynamics has become one of a tremendous amount of activity. Since Edward Lorenz discovered that small variations in initial conditions can cause large changes in a system output (Lorenz, 1963), researchers have been mystified by these phenomena and challenged to understand them. The advent of computational techniques and power has given an effective tool for visualizing and studying these systems. Analytical techniques have evolved as well. Many special fields of analysis have blossomed with the increased interest in the need for nonlinear analysis techniques.

One such area of interest is that of chaotic systems. Chaotic response occurs in systems and processes in many, if not all of the engineering and scientific fields including both the physical sciences as well as the biological sciences. Some selected areas of interest where chaotic motion commonly occurs include fluid flows (Brandstäter *et. al.*, Libchaber, 1987), chemical reactors (Epstein, 1983, Smith *et. al.*, 1983), vibrations of beams and elastic structures (Olmstead, 1977, Moon and Shaw, 1983), plasmas (Horton and Reichl, 1984, Cheung and Wong,

1987, Stafford *et. al.*, 1990, King *et. al.*, 1994), feedback systems (Baillieul *et. al.*, 1980), harmonically driven electrical circuits (Murali and Lakshmanan, 1991, Testa *et. al.*, 1982, Matsumoto *et. al.*, 1984, Szemplinska-Stupnicka and Bajkowski, 1986), cardiac arrhythmias (Glass, *et al.*, 1987, Glass, *et al.*, 1983), biological populations (May, 1987) and ship stability (Thompson *et. al.*, 1990, Virgin, 1987). Nonlinear response characteristics were originally studied by such great mathematicians and physicists as Henri Poincaré (in the 3-body problem) in the late 19^{th} century. Then, there wasn't the aid of the computational power that the modern computer gives us and hence all calculations were done by hand. It is for this reason that chaos, although understood to exist at those early times, wasn't fully appreciated until much later.

Chaos, loosely defined, is the unpredictable response of deterministic systems. A chaotic system is any deterministic system that exhibits unpredictable responses to known inputs. Deterministic, by it's very definition, implies complete knowledge of the system, including the system response. However, the unpredictability of chaotic systems exists as well. It is this unusual characteristic that is of interest to scientists today. The unpredictability is both a burden as well as a tool.

Deterministic chaos refers to the unpredictable response of a nonlinear system which can be modeled by a set of deterministic differential equations. Hence, deterministic chaos comes from those systems where complete knowledge

of all of the essential properties are known. Conversely, a deterministic system may have random inputs or its state may not be well known. This type of system is sometimes called non-deterministic or stochastic chaos. For the purposes of the current work, the unpredictable responses of the deterministic system with additive noise will be of importance.

Currently, the potential for chaotic oscillations is not taken into account during the design process in many nonlinear engineering systems. The chaotic response to certain excitations can cause many undesirable effects. Catastrophic failure of the systems in question can occur due to these undesirable response characteristics, as in the over turning of equipment in the ocean or seismic environment. Alternatively, the undesirable nonlinear oscillations can create problems with position identification of moored systems when knowledge of the position is critical. These undesirable responses have been investigated with an attempt to understand the motions themselves. The current work studies the undesirable motions in an attempt to dampen them, or to get rid of them entirely. Through the application of active control techniques, it can be shown that the nonlinear oscillations can be controlled.

1.2 Problem Overview

Recently, complex nonlinear motions, including chaotic responses, have been predicted in compliant offshore structures and ocean mooring systems

(Thompson, 1983, Thompson, Bokaian and Ghaffari, 1984, Bishop and Virgin, 1988, Pan and Davies, 1997). Many of these types of systems can be characterized by a large geometric nonlinearity in the restoring force, and viscous drag and inertia excitations (Gottlieb and Yim, 1990, 1992). Nonlinear techniques to identify the parameters leading to chaotic motions for such systems have been developed (Gottlieb, Feldman and Yim, 1996, Narayanan, Yim and Palo, 1998). Isaacson and Phadke (1994) demonstrated the existence of chaotic motions in a small scale experiment of a linearly moored system with impact. A medium-scale experiment of a mooring system has been conducted at the wave research facility at Oregon State University in an attempt to validate analytical predictions (Gottlieb, Yim and Lin, 1997, Lin and Yim, 1998).

Currently, chaotic motions of these moored fluid-structure interaction systems are not considered in their design. These systems may be considered as a model of sonars, remote sensors and data collection devices deployed near the ocean floor. Stochastic analytical predictions (Lin and Yim, 1995, Lin and Yim, 1997), and preliminary analysis of experimental data of the mooring system have demonstrated the likely presence of chaotic motions under noisy environments.

Nonlinear and chaotic responses have also been identified in models of engineering systems in the offshore and seismic environments (Yim and Lin 1991a, Pompei *et al.* 1998). In the case of the free-standing equipment or structures installed on these offshore and seismic systems, it can be shown that through the

base support excitation, these "rocking blocks" can also be set into highly nonlinear complex motions (Hogan 1990, Yim and Lin 1991b). In particular, under certain periodic (Lin and Yim 1996a) or random (Lin and Yim 1996b) base motions, overturning response may occur, causing potentially catastrophic results. Should the unpredictability of the chaotic behavior observed in these and the other associated fluid-structure interaction systems be deemed undesirable, methods of real-time on-line analysis of the system response and subsequent control of the nonlinear motions are needed.

Methodology for the analysis of highly nonlinear systems has grown at a rapid pace. Understanding the mechanism for these random seeming fluctuations has given rise to the ability to begin to approach the question of controlling them as well. A need has been identified with respect to the design practice of engineers as they push the envelope of materials and implementation of their processes. This need has created the new realm of chaotic systems control. The topic of this research is to study the implementation characteristics of control systems designs to the ocean structural systems outlined above. Design and application of a control technology ensues with special attention paid to controlling the system about an harmonic cycle.

Because the ocean environment is stochastic in nature, any deterministic controller may experience problems associated with the noise. These problems may or may not be insurmountable. Further research indicates methods that can be used

to increase the effectiveness of a particular control scheme. Once the effective limit of a controller has been reached, methods of predicting or filtering the chaotic signal may be needed. This topic is addressed as well.

1.3 Control of Chaotic Systems

The previous section indicated the need for control of complex responses in ocean and associated systems. As will become evident, there has been a large movement towards easy-to-use and more importantly, easy-to-implement control algorithms. There has been a large boom in control research. The Ott-Grebogi-Yorke (1990a & b) method is just one of many methods that has been devised to render the chaotic dynamics to a predictable pattern. Many proposed control algorithms have been introduced since Ott, Grebogi and Yorke introduced their seminal work on controlling chaos. Ott *et al.* realized that the chaotic oscillations can be used to an advantage. They showed that by using the sensitivity to initial conditions exhibited by a chaotic system, a chaotic trajectory can be directed towards a stable operating state. This method of control has been demonstrated on various engineering systems, both in simulation as well as in practice. Spano *et al.* (1991) demonstrated the application of the OGY controller to the oscillations of a magneto-elastic ribbon giving possibly the first experimental evidence that control of chaos was obtainable. Meanwhile, Singer *et al.* (1991, 1992) applied the control technique to stabilize the flow within a thermal convection loop.

The OGY method has also been applied to many other experimental systems where numerical simulations have been utilized for verification of its applicability. Romeiras *et al.* (1992) successfully demonstrated the method on several distinct systems, the Henon map and the double rotor. Hong *et al.* (1997) demonstrated controlling unstable orbits in the kicked double rotor while Ding *et al.* (1994) demonstrated control for preventing the capsizing of ships due to the chaotic response in the ocean environment. Ogorzalek (1993) studied control of an electrical circuit, the Chua's Circuit, while Mehta and Henderson (1991) exhibited control to generate aperiodic orbits.

Extensions of this method have been implemented in order to expand the region and applicability of control. Shinbrot *et al.* (1990, 1992a, 1992b) demonstrated how the method could be modified in order to target a particular trajectory. Meanwhile, Epureanu and Dowell (1998) discuss the optimality of the particular implementation characteristics and indicate a means of increasing its effectiveness. Nitsche and Dressler (1992) discuss utilizing the method in the case where the system dynamics are not known *a priori* but a time history is available.

In either case, whether it is the study of control of a particular chaotic system trajectory or the study of the control technology itself, it is apparent that the need has arisen for methodology for robust, low energy and easily applicable controllers in order to render the system dynamics non-chaotic. Moreover, since systems in the ocean environment, as studied here, may be subjected to excitations

which instigate nonlinear and chaotic motions, methods of these types may be of interest to the design engineer. The implementation of an easy-to-use control algorithm is of paramount importance to the systems described above and is studied in this report.

In this study, an analysis and control procedure which uses the chaotic response to its advantage is presented. By characterizing the nonlinear system response with unstable periodic orbits (UPO's), a consistent means of investigating these strange attractors is obtained (Lathrop *et al.*, 1989, Auerbach *et al.*, 1987). Particular system trajectories are identified and then used to control the chaotic responses. The proposed control method utilizes the local linearity about an unstable cycle to maintain a periodic response within the chaotic operating regime. To maintain stability of the desired periodic response, this method applies a small perturbation about the unstable cycle at discrete time intervals (Ott *et al.*, 1990). Moreover, to better emulate the nature of the ocean and seismic environments and to determine the controller's effectiveness under the stochastic case, a random (noise) process is incorporated into the excitation model and methodology for increasing the effectiveness of the controller under these circumstances is investigated.

1.4 Organization

This dissertation is composed of four manuscripts and a series of supporting appendices. The manuscripts have been submitted to peer reviewed journals, the first already having appeared in that journal. The primary author on these manuscripts is the same as for this dissertation.

The first manuscript, Chapter 2 of this dissertation, titled "Control of Noisy Chaotic Motion in a System with Nonlinear Excitation and Restoring Forces," which appears in *Chaos*, Vol. 7, No. 2, 290-300, 1997, describes a deterministic ocean structural system, modes of oscillations for the system and subsequent control of those motions. Methods of extending the deterministic controller for increasing noise intervals are also investigated.

The second manuscript, (Chapter 3) titled "Nonlinear Rocking Responses of Free Standing Rigid Blocks: Part I - Deterministic Control" (submitted to the *Journal of Engineering Mechanics*, Manuscript Number EM/2005/024246) introduces the second system under consideration, the so-called rocking block system. Here, it is assumed that there is equipment on a platform undergoing excitation. This may arise for equipment on a ship undergoing oscillations from waves, for example. It can be shown that under certain conditions of the base excitation, the equipment can undergo periodic or chaotic oscillations as well. The difference here is that the chaotic rocking response can not be considered steady-state as in the case of the mooring system. This is due to the fact that the equipment

may topple and hence not only are the dynamics fundamentally changed, but the equipment can be damaged.

Chapter 4, "Stochastic Control of Sensitive Nonlinear Motions of an Ocean Mooring System," (submitted to the ASME Journal *of Offshore Mechanics and Arctic Engineering*, Manuscript Number OMAE-05-1071), revisits the mooring system response in an effort to gauge the effects of filtering and feedback control. In particular, the Iterated Kalman Filter is investigated in order to extend the limits of controllability under increasing noise levels. While it is known that Kalman Filtering will not work for the fully nonlinear case, in general, certain considerations are made in order to apply the filtering technique to a linearized subset of the controlled system in order to achieve the goals.

The final paper (Chapter 5) titled "Nonlinear Rocking Responses of Free Standing Rigid Blocks: Part II - Stochastic Filtering and Control" (submitted to the *Journal of Engineering Mechanics*, Manuscript Number EM/2005/0242467) re-introduces the nonlinear dynamics of the rigid rocking block system. Then, the results of applying the methodology identified in the previous papers for the control of the steady-state chaos, with and without noise, are presented including detailing the increase in controllability in the presence of increasing noise levels. The controller is then extended with the use of the Iterated Kalman Filter.

The fundamental difference between the nonlinear dynamics of the two systems is evidenced by the fact that in the Mooring System, chaos is stable while

in the Rocking Block system it is not. That is, once a chaotic state in the Mooring System is obtained, it will stay in that state until such time as a change in the dynamics occurs. However, in the Rocking Block, this is not necessarily true since the block may topple at any given time and without warning. The final chapter discusses the differences between the two systems and how the control methodology is impacted by these differences.

1.5 References

Auerbach, D., Cvitanovic, P., Eckmann, J.-P.,Gunaratne, G., and Procaccia, I., (1987) "Exploring Chaotic Motion Through Periodic Orbits," Phys. Rev. Lett., Vol. 58, No. 23, pp 2387-89..

Baillieul, J., Brockett, R. W., and Washburn, R. B. (1980). "Chaotic Motion in Nonlinear Feeback Systems," *IEEE Trans. on Circuits and Systems*, Vol. CAS-27, No. 11, 990-997.

Bishop, S. R. and Virgin, L. N. (1988). "The Onset of Chaotic Motions of a Moored Semi-Submersible," *ASME Journal of Offshore Mechanics and Arctic Engineering*, 110, 205-9.

Brandstäter, A., Swift, J., Swinney, H. L., Wolf, A., Farmer, J. D., Jen, E. and Crutchfield, P. J. (1983), "Low-Dimensional Chaos in a Hydrodynamic System," *Phys. Rev. Lett.*, Vol. 51, No. 16, 1442-45.

Cheung, P. Y. and Wong, A. Y. (1987). "Chaotic Behavior and Period Doubling in Plasmas," *Phys. Rev. Lett.*, Vol. 59, No. 5, 551-554.

Ding, M., Ott, E. and Grebogi, C. (1994). "Crisis Control: Preventing Chaos-Induced Capsizing of a Ship," *Physical Review E*, Vol. 50, No. 5, 4228-30.

Epstein, I. R. (1983). "Oscillations and chaos in chemical systems," *Physica 7D*, 47-56,

Epureanu, B. I. and Dowell, E. H. (1998). "On the Optimality of the Ott-Grebogi-Yorke Control Scheme," *Physica D*, Vol. 116, 1-7.

Glass L., Guevara M.R., Shrier A., Perez R., (1983) "Bifurcation and chaos in a periodically stimulated cardiac oscillator," Physica 7D: 89-101

Glass, L., Goldberger, A. L., Courtemanche, M. and Shrier, A. (1987). "Nonlinear Dynamics, Chaos and Complex Cardiac Arrhythmias," *Proceedings of the Royal Society of London, A*, Vol. 413, 9-26.

Gottlieb, O., and Yim, S. C. S. (1990). "Onset of Chaos in a Multi-Point Mooring System," *Proc. First (1990) European Offshore Mechanics Symposium*, Trondheim, Norway, Aug. 20-22, 6-12.

Gottlieb, O., and Yim, S. C. S. (1992). "Nonlinear Oscillations, Bifurcations and Chaos in a Multi-Point Mooring System with a Geometric Nonlinearity," *Applied Ocean Research*, Vol. 14, 241-257.

Gottlieb, O., Feldman, M., and Yim, S. C. S. (1996). "Parameter Identification of Nonlinear Ocean Mooring Systems Using the Hilbert Transform," *ASME Journal of Offshore Mechanics and Arctic Engineering*, 118, No. 1, 29-36.

Gottlieb, O., Yim, S. C. S., and Lin, H. (1997). "Analysis of Bifurcation Superstructure of Nonlinear Ocean System," *ASCE Journal of Engineering Mechanics*, 123, No. 11, 1180-87.

Hogan, S. J. (1990). "The many steady state responses of a rigid block under harmonic forcing." *Earthquake Engrg. and Struct. Dynam.*, **19**, 1057-1071.

Hong, Z., Yinghai, W. and Jie, Y. (1997). "Stabilizing Unstable Orbits," *Phys. Lett. A*, Vol 236, 53-59.

Horton, C. W. Jr. and Reichl, L. E., eds., (1984). *Statistical Physics and Chaos in Fusion Plasmas*, John Wiley & Sons, New York, 361 pps.

Isaacson, M. and Phadke, A. (1994). "Chaotic Motion of a Nonlinear Moored Structure," *Proceedings of the Fourth International Offshore and Polar Engineering Conference*, Osaka, Japan, April 10-15, Vol. III, 338-45.

King, P. E., Ochs, T. L. and Hartman, A. D. (1994). "Chaotic responses in electric arc furnaces," J. Appl. Phys., Vol. 76, No. 4, 2059-65.

King, P. E. and Yim, S. C. S (1997). Control of Noisy Chaotic Motion in a System with Nonlinear Excitation and Restoring Forces," *Chaos*, Vol. 7, No. 2, 290-300.

King, P. E. and Yim, S. C. S (2005). "Nonlinear Rocking Responses of Free Standing Rigid Blocks: Part I - Deterministic Control," submitted to the *Journal of Engineering Mechanics*, Manuscript Number EM/2005/024246.

King, P. E. and Yim, S. C. S (2005). "Stochastic Control of Sensitive Nonlinear Motions of an Ocean Mooring System," submitted to the ASME Journal *of Offshore Mechanics and Arctic Engineering*, Manuscript Number OMAE-05-1071.

King, P. E. and Yim, S. C. S (2005). "Nonlinear Rocking Responses of Free Standing Rigid Blocks: Part II - Stochastic Filtering and Control," submitted to the *Journal of Engineering Mechanics*, Manuscript Number EM/2005/0242467.

Lathrop, D. P. and Kostelich, E. J. (1989). "Characterization of an Experimental Strange Attractor by Periodic Orbits," *Phys. Rev. A*, Vol. 40, No. 7, 4028-31.

Libchaber, A. (1987). "From Chaos to Turbulence in Bénard Convection," *Proc. R. Soc. Lond. A* Vol. 413, 63-69.

Lin, H. and Yim, S.C.S. (1995). "Chaotic Roll Motion and Capsizing of Ships Under Periodic Excitation and Random Noise," *Journal of Applied Ocean Research*, 17, 3, 185-204.

Lin, H. and Yim, S. C. S. (1996a). "Nonlinear rocking motions. I: Chaos under noisy periodic excitations." *J. Engrg Mech.*, ASME, Vol. 122, No. 8, 719-727.

Lin, H. and Yim, S. C. S. (1996b). "Nonlinear rocking motions. II: Overturning under random excitations." *J. Engrg Mech.*, ASME, Vol. 122, No. 8, 728-735.

Lin, H. and Yim, S.C.S. (1997). "Noisy Nonlinear Motions of a Moored System, Part I: Analysis and Simulations," *ASCE Journal of Waterway, Port, Coastal and Ocean Engineering*, 123, 5, 287-95.

Lin, H. and Yim, S.C.S. (1998). "Experimental Calibration of Bifurcation Superstructure of a Nonlinear System," *ASCE Journal of Engineering Mechanics*, 124, No. 4, 471-75.

Lorenz, Edward N. (1963). "Deterministic Nonperiodic Flow," *Journal of the Atmospheric Sciences*, 20, 130-41.

May, R. M. (1987). "Chaos and Dynamics of Biological Populations," *Proceedings of the Royal Society of London, A*, Vol. 413, 27-44.

Matsumoto, T., Chua, L. O., and Tanaka, S. (1984). "Simplest Chaotic Nonautonomous Circuit," *Phys. Rev. A*, Vol. 3, No. 2, 1155-57.

Mehta, N. J. and Henderson, R. M. (1991). "Controlling Chaos to Generate Aperiodic Orbits," *Phys. Rev. A*, Vol. 44, No. 8, 4861-65.

Moon, F. C. and Shaw, S. W. (1983). "Chaotic Vibration of a Beam with Nonlinear Boundary Conditions," *J. Nonlinear Mech.*, Vol 18, 465-477.

Murali, K. and Lakshmanan, M. (1991). "Bifurcation and Chaos of the Sinusoidally-Driven Chua's Circuit," *International Journal of Bifurcations and Chaos*, Vol. 1, No. 2, 369-84.

Narayanan, S., Yim, S.C.S., and Palo, P.A. (1998). "Nonlinear System Identification of a Moored Structural Systems," *Proceedings of the Eighth International Offshore and Polar Engineering Conference*, Montreal, Canada, May 24-29, Vol.III, 478-84.

Nitsche, G. and Dressler, U. (1992). "Controlling Chaotic Dynamical Systems Using Time Delay Coordinates," *Physica D*, Vol. 58, 153-64.

Ogorzalek, M. J. (1993). "Taming Chaos; Part II – Control", *IEEE Trans. Circuits and Systems – I: Fundamental Theory and Applications*, Vol. 40, N0. 10, 700-6.

Olmstead, W. E. (1977). "Extent of the left branching solution to certain bifurcation problems," *SIAM J. Math. Anal.*, Vol. 8, 392-401.

Ott, E., Grebogi, C., and Yorke, J. A. (1990a). "Controlling Chaos," *Phys. Rev. Lett.*, 64, 11, 1196-99.

Ott, E., Grebogi, C., and Yorke, J. A. (1990b), "Controlling Chaotic Dynamical Systems", in *CHAOS/XAOS, Soviet-American Perspective on Nonlinear Science*, Ed. By D. Campbell, Am. Inst. Phys., New York.

Pan, R. and Davies, H. G. (1997). "Coupled Pitch-Roll Motion of a Ship with Roll Mode Excitation," *Proceedings of the 16th IASTED International Conference Modeling Identification and Control*, Feb. 17-19, 1997, Innsbruck, Austria, 32-35.

Pompei, A., Scalia, A., and Sumbatyan, M. A. (1998). "Dynamics of rigid block due to horizontal ground motion." *J. Engrg Mech.*, ASCE **124**(7), 713-717.

Romeiras, F., J., Grebogi, C., Ott, E., and Dayawansa, W., P. (1992). "Controlling Chaotic Dynamical Systems", *Physica D*, Vol. 58, 165-92.

Shinbrot, T., Ott, E., Grebogi, C. and Yorke, J. A. (1990). "Using Chaos to Direct Trajectories to Targets," *Phys. Rev. Lett.*, Vol 65, No. 26, 3215-18.

Shinbrot, T., Ott, E., Grebogi, C. and Yorke, J. A. (1992a). "Using Chaos to Direct Orbits to Targets in Systems Describable b a One-Dimensional Map," *Phys. Rev. A*, Vol. 45, No. 6, 4165-68.

Shinbrot, T., Ditto, W., Grebogi, C., Ott, E., Spano, M. and Yorke, J. A. (1992b). "Using the Sensitive Dependence of Chaos (the "Butterfly Effect") to Direct Trajectories in an Experimental Chaotic System", *Phys. Rev. Lett.*, Vol. 68, No. 19, 2863-66.

Singer, J., Wang, Y-Z. and Bau, H. H. (1991). "Controlling a Chaotic System," *Phys. Rev. Lett.*, Vol. 66, No. 9, 1123-25.

Smith, C. B., Kuszta, B., Lyberatos, G. and Bailey, J. E. (1983). "Period doubling and complex dymanics in an isothermal chemical reaction system," *Chem. Eng. Sci.*, Vol. 38, 425-430.

Spano, M. L., Ditto, W. L. and Rauseo, S. N. (1991). "Exploitation of Chaos for Active Control: An Experiment," *Journal of Intell. Mater. Syst. and Struct.*, Vol. 2, 482-93.

Stafford, S. A., Kot, M. and Roth, J. R. (1990). "Investigation of the nonlinear behavior of a partially ionized, turbulent plasma in a magnetic field," *J. Appl. Phys.*, Vol 68, No. 2, 488-499.

Szemplinska-Stupnicka, W., and Bajkowski, J. (1986). "The ½ Subharmonic Resononace and its Transition to Chaotic Motion in a Non-Linear Oscillator," *Int. J. Non-Linear Mech.*, Vol. 21, No 5., 401-419.

Testa, J., Perez, J., and Jeffries, C. (1982). "Evidence for Universal Chaotic Behavior of a Driven Nonlinear Oscillator," *Phys. Rev. Lett.*, Vol. 48, No. 11, 714-717.

Thompson, J. M. T. (1983). "Complex Dynamics of Compliant Offshore Structures," *Proceedings of the Royal Society of London*, A, 387, 407-27.

Thompson, J. M. T., Bokaian, A. R., and Ghaffari, R. (1984). "Subharmonic and chaotic motions of compliant offshore structures and articulated mooring towers." *ASME J. Energy Resources Tech.*, Vol. 106, 191-198.

Thompson, J. M. T., Rainey, R. C. T and Soliman, M. S. (1990). "Ship Stability Criteria based on Chaotic Transients from Incursive Fractals," *Phil. Trans. R. Soc. Lond. A*, Vol. 332, 149-167.

Virgin, L. N. (1987). "The Nonlinear Rolling Response of a Vessel Including Chaotic Motions Leading to Capsize in Regular Seas," *Appl. Ocean Res.*, Vol. 9, 89-95.

Yim, S. C. S. and Lin, H. (1991a). "Nonlinear impact and chaotic response of slender rocking objects." *J. Engrg Mech.*, Vol. 117, No. 9, 2079-2100.

Yim, S. C. S. and Lin, H. (1991b). "Chaotic behavior and stability of free-standing offshore equipment." *Ocean Engrg.*, Vol. 18, No. 3, 225-250.

Control of Noisy Chaotic Motion in a System with Nonlinear Excitation and Restoring Forces

Paul E. King

Solomon C. S. Yim

Published in

CHAOS Vol. 7, No. 2, pgs. 290-300

American Institute of Physics (1997)

2. Control of Noisy Chaotic Motion in a System with Nonlinear Excitation and Restoring Forces

2.1 ABSTRACT

This study examines the complex and chaotic oscillations of a dynamical system with nonlinear excitation and restoring forces for the purpose of controlling these oscillatory states. The physical system, modeled as a system of first order nonlinear ordinary differential equations, takes into account a geometric nonlinearity in the restoring force, a quadratic viscous drag and a harmonic excitation force. It is controlled using small perturbations about a selected unstable cycle and control is instigated for periodic cycles of varying periodicities. The controller, when applied on the dynamical system with additive random noise in the excitation, successfully controls the system with noise levels in excess of 5% of the total energy, giving the first evidence that (stochastic) control of these systems is possible.

2.2 LEAD PARAGRAPH

Sensitive nonlinear dynamics including chaotic oscillatory behavior has been observed in experimental data of a moored, submerged structure. This phenomenon has been verified through analysis and computer simulation of the governing dynamical system. Methods of analyzing system response to harmonic and noisy excitations and subsequent control are needed, should this unpredictability of the observed behavior be deemed undesirable. This study presents an analysis and control procedure which uses the chaotic response of the system to an advantage. By describing the nonlinear response with unstable periodic orbits (UPO's), a locally linear mapping of the dynamics is obtained. This linear mapping is subsequently employed in a controller design and the controller is applied to the moored structure. Finally, robustness of the controller is investigated under noisy conditions and modifications to the controller are made in order to maintain control of the moored structure under the conditions when noise is present in the excitation. The methods presented are equally applicable to most chaotic systems for which the response time history can be monitored.

2.3 INTRODUCTION

Recently, chaotic responses have been predicted in a system characterized by a large geometric nonlinearity in the restoring force and viscous drag excitation.[1,2] An example of a system modeled by these types of nonlinearities is a mass moored in a fluid medium subject to wave excitations. These systems include sonars, remote sensors and data collection devices deployed for mineral exploration, which are of interest to the U. S. Navy and the U. S. Bureau of Mines, are typically suspended by cables from the ocean floor. This class of fluid-structure interaction problems contain highly nonlinear drag and mooring effects. However, despite being of fluid origin, which often indicates infinite dimensionality, the overall effects of the nonlinear fluid loads on the structure can be approximated in terms of an added inertia and a nonlinear coupling of the Morison form[1,2]. The nonlinear mooring resistance force can be approximated by a low order polynomial. Hence the resulting mathematical models of these systems are reducible to a low degree system of ordinary differential equations of the Duffing type. This order of approximation is often acceptable for preliminary analysis and design of the types of fluid-structure systems considered (see Refs. 1 and 2 for detailed justifications).

Currently, chaotic motions of moored fluid-structure interaction systems

employed by the U. S. Navy and the U. S. Bureau of Mines are not considered in their design. Preliminary analysis of experimental data from such a system has demonstrated the likely presence of chaotic motions in noisy environments.[3] Should the unpredictability of the chaotic behavior observed in these and other associated fluid-structure interaction systems[4,5] be deemed undesirable, methods of analyzing system response to harmonic and noisy excitations and subsequent control of the systems are needed. The analysis and control procedure presented in this study uses the chaotic response to its advantage. By describing the nonlinear response with the unstable periodic orbits (UPO's) of the system, a consistent means of characterizing these strange attractors is obtained.[6,7,8] This characterization can include the calculation of such invariants as the topological entropy, the Hausdorff dimension,[7] the multi-fractal spectrum[9] or the Lyapunov spectrum.[10]

In this study, particular system trajectories are identified and then used to control the chaotic responses. The proposed control method utilizes the local linearity about an unstable cycle to maintain a periodic response within the chaotic operating regime. To maintain stability of the desired periodic response, this method applies a small perturbation about the unstable cycle at discrete time intervals.[11] The proposed method has been applied successfully to several physical systems, including control of a thermal convection loop[12,13] and the chaotic oscillations in a continuous stirred tank

reactor.[14] Other control methods including the use of artificial neural networks for adaptive learning of chaotic oscillations for model reference control of these oscillations has been examined in the cases of chaotic fluid flows[15] and plasmas.[16,17]

Section II describes the physical system which includes nonlinear effects of fluid structure interaction as well as nonlinear geometric stiffness. Numerical investigations show that this system possesses periodic, quasi-periodic and chaotic responses to certain combinations of driving wave amplitudes and frequencies. The regions of chaotic responses are first identified by a semi-analytical method of investigating the bifurcation structure and routes to chaos.[2] The analytical predictions are highlighted in Section III. These information are used in Section IV to numerically investigate chaotic oscillations of the system. In Section V the notion of an UPO is introduced and a method of obtaining them is outlined. This method uses only the response time series of the chaotic system and hence is applicable to many systems in which the dynamics are not precisely known *a priori,* but a chaotic time series is available. The ability of the method to identify appropriate unstable cycles in a general chaotic system, and subsequent control of the chaotic responses is investigated in Section VI.

The controller utilizes a selected UPO to maintain a trajectory in an oscillatory manner, essentially rendering the system response periodic, even though the system is

otherwise operating in a chaotic parameter regime. Section VII gives the results of applying this technique to the nonlinear oscillator defined in the previous sections.

Finally, since the proposed control scheme uses a first order approximation about an UPO, it is expected that the addition of noise may cause some stability problems with the controller. Several avenues of rendering a robust controller are available, these include filtering the noise and geometric projection. Filtering either assumes prior knowledge of the model (as in Kalman filtering[18]) or it assumes knowledge about the nature of the noise (as in statistical linearization[19]). Geometric projection,[20,21] on the other hand, uses the fuzzy image of the dynamics (via a strange attractor in phase space) to project a trajectory back onto the original phase space. However, in this study, a modification of the controller is employed to obtain the desired robustness. This modification extends the method in the case when noise is present and is discussed in Section VIII.

2.4 SYSTEM WITH GEOMETRIC AND HYDRODYNAMIC NONLINEARITIES

Figure 1 shows a system moored by cables in a fluid medium. The fluid itself is undergoing motion and an associated excitation force is described by the forcing

function $F(\ddot{x},\dot{x},t)$, where $\dot{x} = dx/dt$ and $\ddot{x} = d\dot{x}/dt$. With restraints for vertical and rotational motion, this system is modeled as a single-degree-of-freedom system for the surge, x.[2] The (nonlinear, second order ordinary differential) equation of motion is derived by using the fact that the system is hydrodynamically damped with external forcing. The forcing excitation is modeled as the sum of a constant current and an

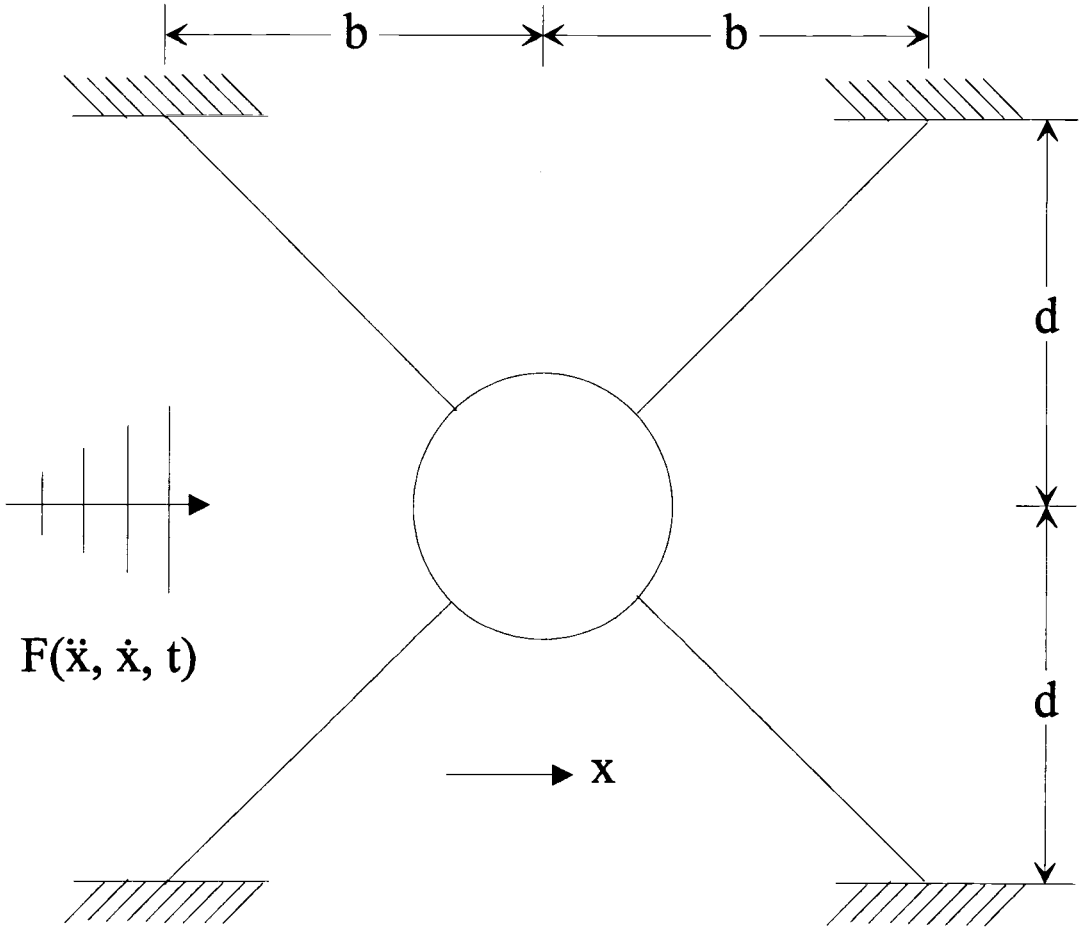

Figure 1 - A moored system suspended by cables and subject to current and wave excitation.

oscillatory wave term. Because the cables are thin and the dimensions of the mass are small compared to the orbital motions of the wave particles, the fluid-structure interaction can be modeled accurately by use of the small-body theory which assumes that the presence of the structure does not influence the wave field. This implies that the waves flowing past the structure do not change due to the fluid-structure interaction. The mooring angle produces a geometric nonlinearity in the restoring force that can become highly nonlinear for b = 0, a two-point system, or nearly linear for b $\gg$ d for the four-point system. The equation of motion for this system is given by Refs. 1 and 2 as

$$m\,\ddot{X} + c\,\dot{X} + R(X) = F(\ddot{X}, \dot{X}, t) \tag{1a}$$

where the nonlinearities are contained in the restoring force R and the excitation force F. The restoring force describes the geometric configuration of the mooring lines and assumes linear elastic behavior so that the nonlinearity is strictly due to the geometric configuration of the system. The restoring force can be shown[2] to have the form

$$R(X) = k\left(X + b\ \mathrm{sgn}(X)\right)\left[1 - \sqrt{\frac{d^2 + b^2}{d^2 + (X + b\ \mathrm{sgn}\ (X))^2}}\right] \tag{1b}$$

where sgn(X) is the signum function defined by

$$\text{sgn}(X) = \begin{cases} +1 \text{ for } X > 0 \\ 0 \text{ for } X = 0 \\ -1 \text{ for } X < 0 \end{cases}$$

The excitation force is a combination of viscous drag and inertial components based upon the interactions between the moored structure and the fluid medium. This excitation force is modeled by

$$F(\ddot{X},\dot{X},t) = \lambda(u - \dot{X})\,|u - \dot{X}| + \mu(\dot{u} - \ddot{X}) + \rho\bar{V}\dot{u} \qquad (1c)$$

The system parameters are given by the system mass m, damping c, and line stiffness k. λ, μ are the hydrodynamic viscous drag and added mass, ρ is the fluid density, $\bar{V}$ is the displaced volume of fluid, $u = u(t)$ is the fluid particle velocity under current and waves given by $u(t) = u_0 + u_1 \sin(\omega t)$ and $u_1 = u_1(a,\omega)$.

Assuming the structure does not alter the fluid flow, performing an equivalent linearization on the quadratic drag force and normalizing, a dimensionless first order autonomous nonlinear differential equation can be obtained:

$$\begin{aligned} \dot{x} &= y \\ \dot{y} &= -R(x) - \gamma\, y + F(y,x,\theta) \\ \dot{\theta} &= \omega \end{aligned} \qquad (2a)$$

where $x = X/d$ and the resulting nonlinear restoring force becomes

$$R(x) = \psi\,(x + \beta\ \mathrm{sgn}(x))\left[\frac{1}{\sqrt{1+\beta^2}} - \frac{1}{\sqrt{1+(x+\beta\ \mathrm{sgn}(x))^2}}\right] \tag{2b}$$

and the excitation force is given by

$$F(y,x,\theta) = f_0 - f_1 \sin(\theta) \tag{2c}$$

The appropriate dimensionless constants are defined by

$$\psi = \frac{k}{m+\mu}, \qquad \beta = \frac{b}{d}, \qquad \gamma = \frac{c+\lambda_1}{m+\mu} \tag{2d}$$

and the constants f_0 and f_1 depend upon the hydrodynamic characteristics of the system. Although at first glance this system appears to be significantly more complex than the simple nonlinear systems presented in standard texts, e.g. Nayfeh and Mook,[23] it turns out that, the fluid-structure system possesses nonlinear response properties very similar to those of the Duffing system[1,2].

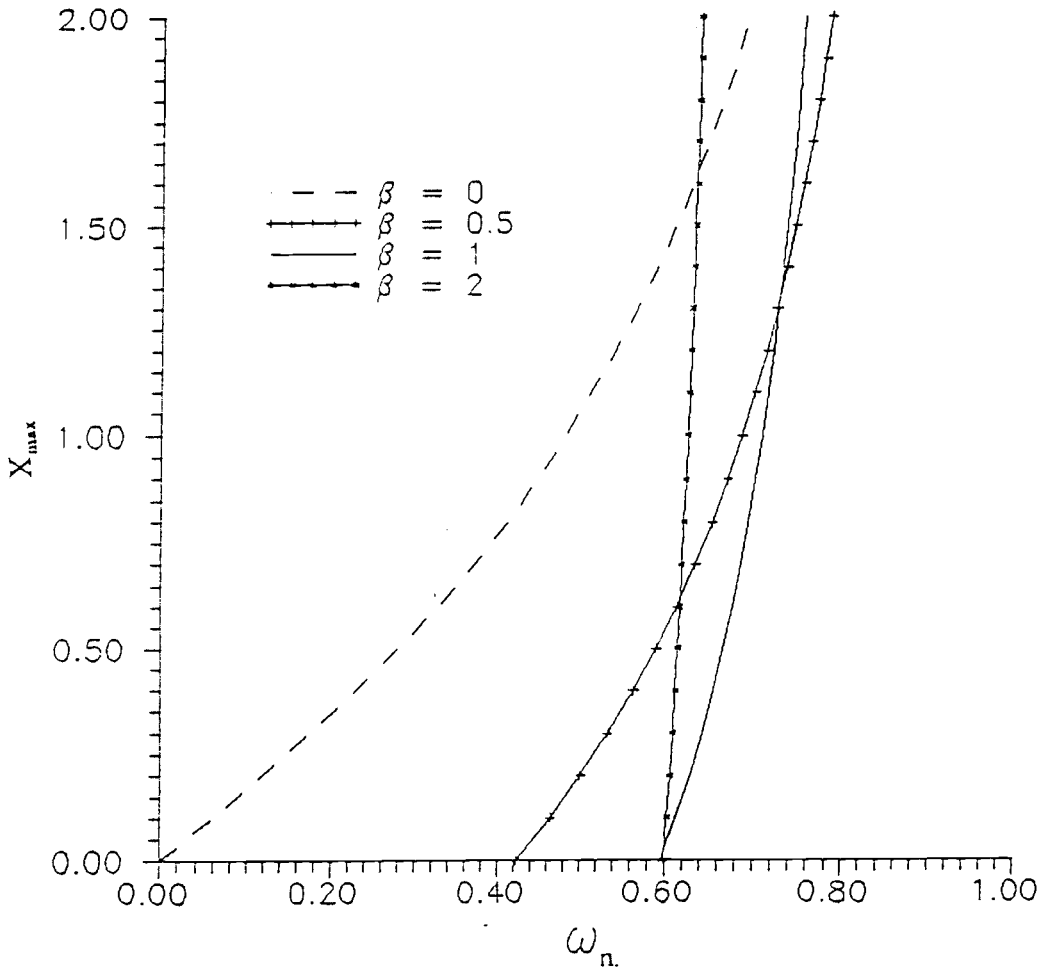

Figure 2 - Degree of geometric nonlinearity as a function of mooring angle.

2.5 ANALYTICAL PREDICTIONS

Numerical simulations of the response of the structure in the fluid medium have been shown to exhibit periodic, quasi-periodic and chaotic responses in surge motion

as depicted in Figure 1. This response has been verified through an analytical treatment of Eqs. (2a) - (2c). In this analysis, a Hamiltonian approach is employed to examine the fundamental geometric nonlinearity and a harmonic-balance method[22,23] is used to investigate the frequency response characteristics of the primary, sub- and super-harmonics.[23] A variational approach is also employed to identify a bifurcation structure and routes to chaos of the model.[1,2]

The associated Hamiltonian[24] of the system described by Eqs. (2a) - (2c) is obtained by neglecting the damping term (by setting $\gamma = 0$) and the forcing term ($F \equiv 0$). From this formulation, the natural period, T_n, of the Hamiltonian is computed from the natural period, $T_n = 2\pi/\omega_n$, where

$$\omega_n = \frac{\pi}{2}\left[\int_0^{x_{max}} \frac{dx}{y(x)}\right]^{-1} \tag{3}$$

$$y(x) = \sqrt{2}\left(V(x_0) - V(x)\right)^{\frac{1}{2}} \equiv \dot{x} \tag{4}$$

and V(x) is the potential energy and is given by

$$V(x) = \psi\left[\frac{x^2}{2} - \tau\left(\sqrt{1+(\beta+x)^2} + \sqrt{1+(\beta-x)^2}\right)\right] \tag{5}$$

a)

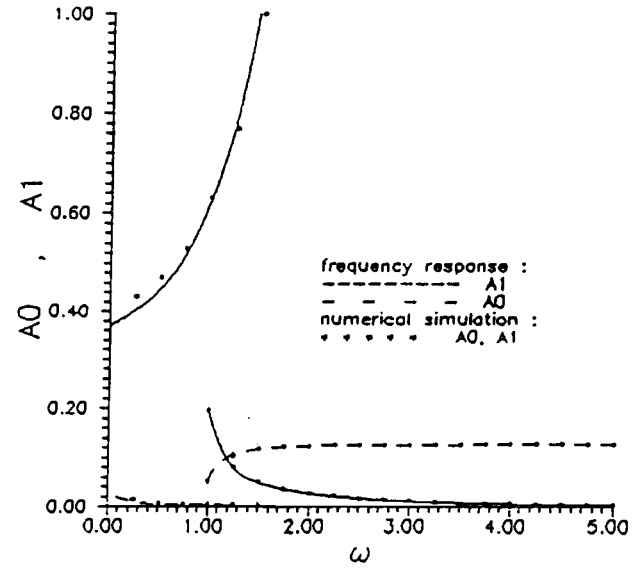

b)

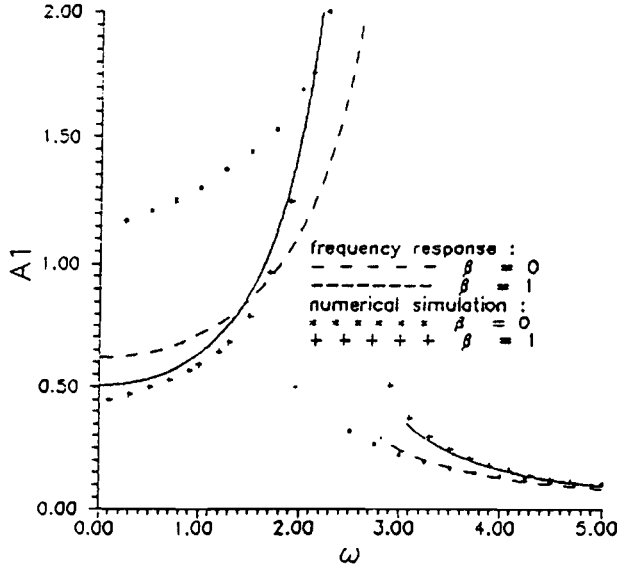

Figure 3 - Frequency response curves subject to a) current and wave excitation ($\gamma = 0.5$, $\psi = 10.0$, $f_0 = 0.01$, $f_1 = 0.1$) and b) wave excitation alone ($\gamma = 0.01$, $\psi = 10.0$, $f_0 = 0.0$, $f_1 = 2.0$).

Equation (3) characterizes the geometric nonlinearity and is sometimes called the frequency response (or backbone) curve.[23] The curvature of the backbone curve shows the degree of nonlinearity. For a weak nonlinearity the curvature is near zero and the backbone curve resembles a vertical line. For a strong nonlinearity the curvature is positive for a stiffening system and negative for a softening system. This is exhibited in Figure 2 which gives the result for Eqs. (2a) - (2c) for the stiffening case. As can be seen, the mooring angle creates a strong nonlinearity for $\beta = 0$ and a weak nonlinearity for $\beta >> 1$.

The harmonic balance[22,23] method of approximating a solution to the system [Eq. (2a) - (2c)] is applied to study the frequency response characteristics of the resonance modes. The method assumes an approximate solution of the form

$$x_0(t) = \sum_{k=0}^{M} A_k \cos(k\omega t + \phi_k) \tag{6}$$

where M is the order of the approximation and A_k is the amplitude of the k-th harmonic. This approximate solution is then substituted into the original equations and the resulting expressions are rearranged and squared. By equating the harmonic terms and the constant terms separately to zero, a set of nonlinear algebraic equations in the A_k's and ϕ_k's is obtained and subsequently solved using standard procedures.[22] Figure

3 shows the zero-th and first order amplitude as a function of frequency. As is evident, this system exhibits a jump phenomena as the frequency is swept through the values shown.[23]

The system bifurcations are identified by considering a perturbed solution of the form $x(t) = x_o(t) + \epsilon(t)$, where $x_o(t)$ is an approximate solution and $\epsilon(t)$ represents a small perturbation. Substituting this into Eqs. (2a) - (2c) and linearizing the resulting expression yields

$$\ddot{\epsilon} + \gamma\dot{\epsilon} + \psi H[x_0(t)]\epsilon = 0 \tag{7a}$$

where γ and ψ are defined in Eq. (2d) and the periodic function H is given as follows

$$H(x_0) = (1+\beta^2)^{-1/2} - \left(1 + [x_0 + \beta\,\mathrm{sgn}(x_0)]^2\right)^{-3/2} \tag{7b}$$

Performing a Fourier series expansion on H produces a generalized Hill's equation[23] of the form

$$\ddot{\epsilon} + \gamma\dot{\epsilon} + \psi H\,[\theta]\epsilon = 0 \tag{8a}$$

for

$$H[\theta] = \frac{a_0}{2} + \sum_n a_n \cos(n\theta) \tag{8b}$$

Note that Eqs. (8a) - (8b) define parametric excitation and resonant interaction where harmonics of all orders are possible. The use of Floquet Theory (described in detail in Ref. 23) gives the particular solution to the variational equation as

$$\epsilon(t) = \exp(\zeta t)Z(t) \tag{9}$$

where the real part of the constant ζ determines the stability of the approximate solution, and the complex part of ζ corresponds to the natural frequency of the periodic response. The function Z is periodic in T, i.e., $Z(t) = Z(t+T)$.

By investigating the order of the harmonic part of the solution the sub- and super-harmonic solutions can be determined. The procedure is conducted by examining the symmetric solution $Z(t) = Z(t+T/2)$ or the period doubled solution $Z(t) = Z(t+2T)$. The boundaries of the stability regions can be obtained by performing a harmonic-balance approximation to the Hill's variational Eq. (8a) at the stability limits where $d\zeta/dt = 0$. (Specific details of the solution procedure can be found in Ref. 2,

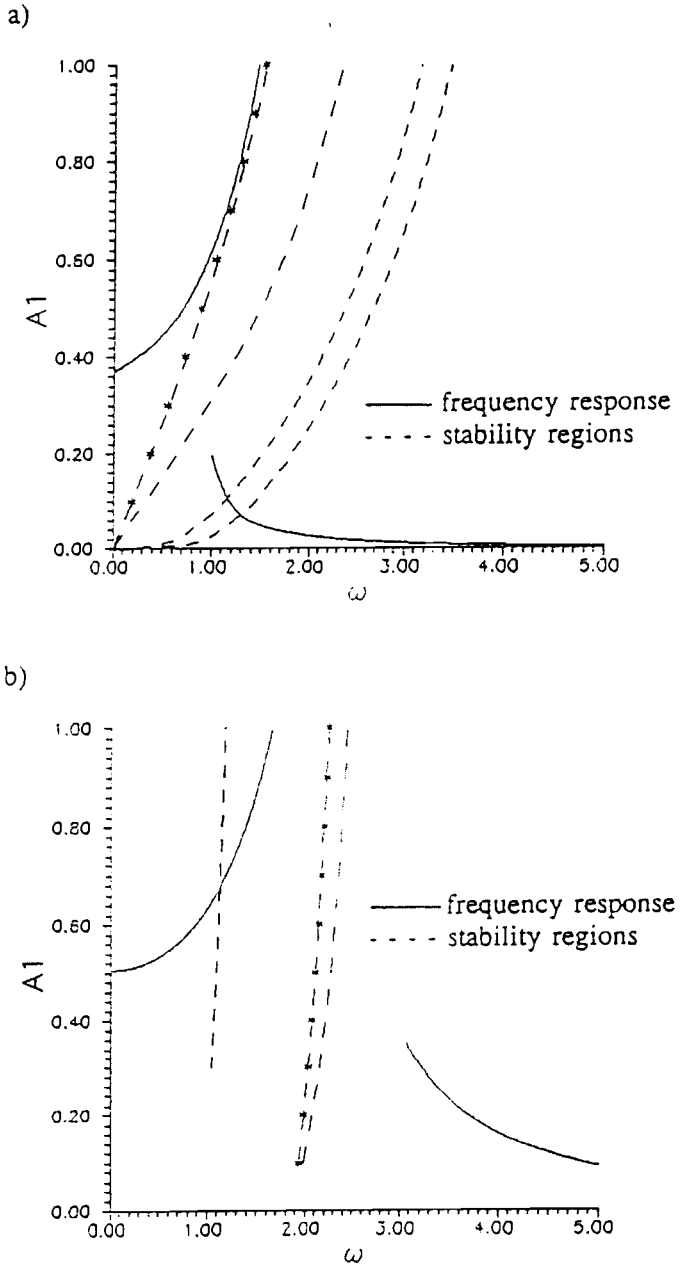

Figure 4 - Stability diagrams of the system with linearized excitation for a) current and wave excitation ($\gamma = 0.01$, $\psi = 10.0$, $\beta = 0.0$, $f_0 = 0.01$, $f_1 = 0.1$) and b) wave excitation alone ($\gamma = 0.01$, $\psi = 10.0$, $\beta = 1.0$, $f_0 = 0.0$, $f_1 = 2.0$).

while a description of the general procedure can be found in Ref. 23.) For the fluid-structure interaction systems of interest to the U. S. Navy and the U. S. Bureau of Mines, preliminary experimental results have indicated that the primary resonance is of major concern.[3] Although, the analysis procedures described in this study are equally applicable to higher order resonances, primary resonance will be employed for demonstration purpose.

The above analysis yields the frequency response curve of the primary resonance, $Z(t) = Z(t+T)$, given by

$$\omega^2 = \frac{1}{2a_0}\left[\psi(a_0^2-a_1^2) - \gamma^2 a_0 \pm \sqrt{\gamma^4 a_0^4+2\psi\gamma^2(a_1^2-a_0^2)+\psi^2(a_1^2-a_0a_1)^2}\right] \qquad (10)$$

Note that in Eq. (10), $\gamma \ll 1$. For the undamped system, $\gamma = 0$, and $\omega \approx \sqrt{(\psi a_0/2)}$. The distribution of the a_i's and their influence on system behavior had been examined[1,2].

Similarly, the stability boundaries for the ½ subharmonic can also be obtained by inserting the period-doubled solution $x_{1/2}(t) = b_{1/2}\cos(\theta/2)$ (corresponding to $Z(t) = Z(t+2T)$) into Eq. (8a). This yields the frequency response curve

$$\omega^2 = 2\left[\psi a_0 - \gamma^2 \pm \sqrt{\gamma^4-2\psi\gamma^2 a_0+\psi^2 a_1^2}\right] \qquad (11)$$

Now, the regions of bifurcations can be approximated by observing that the intersections of the frequency response curves obtained from Eq. (6) and the investigations of the stability regions which lead to the frequency response curves given by Eqs. (10) - (11) as shown in Figure 4. From this analysis, obviously the strength of the geometric nonlinearity (as evidenced by β) plays an important role in the ultimate response of the system. In fact, by examining the frequency response characteristics and equating them with the stability regions a period-doubling bifurcation structure is obtained.

2.6 NUMERICAL INVESTIGATIONS

The analytical investigations above provide a guide for a numerical search in parameter space for various types of responses including the existence and co-existence of periodic solutions, period-doubling bifurcations and chaos. Extensive numerical investigations and many examples as presented in Ref. 2 show that Eqs. (2a) - (2c) exhibit periodic, quasi-periodic and chaotic motions. These motions were verified through the analytical predictions discussed above. As a demonstration, Figure 5 shows one of the many possible chaotic responses of the system, where the parameter values used were $\omega = 0.335$, $\gamma = 0.01$, $\psi = 4.0$, $\beta = 0.0$, $f_0 = 0.0$, and $f_1 = 2.0$. In the

chaotic regime, this system exhibits both steady-state chaos and transient chaos, where the system undergoes a transient chaotic response before it settles into periodic or quasi-periodic oscillations.[2] Figures 5a - 5d show the phase space portrait, Poincaré section, frequency spectrum and a typical time series, respectively, of a chaotic response. The Poincaré sections are obtained by stroboscopically sampling the time series every $2\pi/\Gamma$ and plotting the points sequentially i.e. by plotting $x(t)$ vs. $x(t+\Gamma)$ for Γ the sampling period. One can notice the fractal structure of the Poincaré section. The presence of an abundance of these complex harmonic responses predicted by the analytical and numerical results indicate that their influence on extreme and fatigue designs of the fluid-structure interaction systems may need to be included in the future.

2.7 UNSTABLE PERIODIC ORBITS

The numerical simulations together with the analytical results show that the oscillatory nature of Eqs. (2a) - (2c) exhibit a range of modes, including periodic, sub- and super-harmonics and chaotic motions. A means of analyzing the chaotic motion by using the time series alone has been introduced by Refs. 6 and 7. The procedure utilizes the unstable periodic orbits of a system. Since a chaotic attractor contains a multitude of UPO's of varying periodicities, much of the nonlinear characteristics can

be identified through these special cycles. It is well known that UPO's are dense in a chaotic attractor,[9,11] and in fact this is a necessary condition for chaos to exist.[26] This fact is exploited in the following discussions.

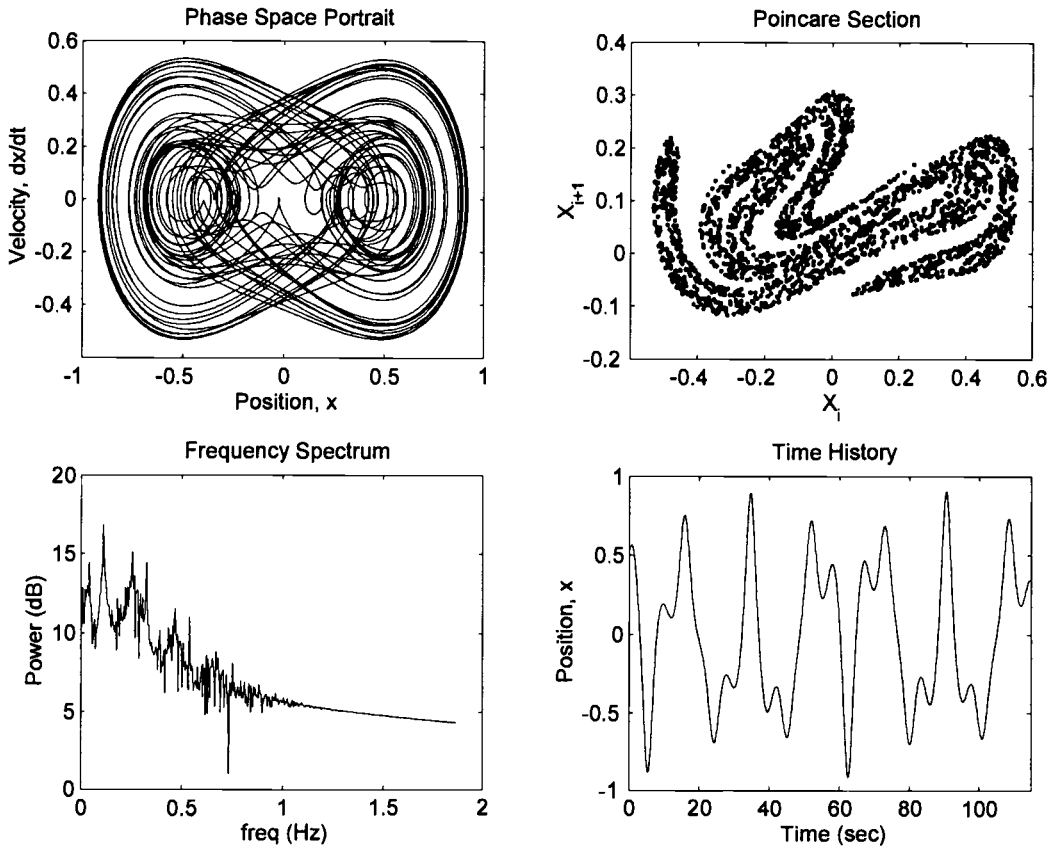

Figure 5 - Chaotic response of the nonlinear system with parameter values ω = 0.335, γ = 0.01, ψ = 4.0, β = 0.0, f_0 = 0.0, and f_1 = 2.0 exhibiting the a) chaotic attractor, b) Poincaré section, c) Power spectrum and d) time history of the (surge) position.

The basic idea behind the use of an UPO is that if the chaotic system is allowed to evolve long enough, then a trajectory will return arbitrarily close to a given unstable

cycle, arbitrarily often. This is because these cycles are dense on the attractor and that they are periodic and yet unstable. Thus, if the system is on a cycle it will remain on it for all time. However, if there is any minute deviation from the cycle, then the chaotic trajectory will diverge from this unstable cycle. Because of the "mixing" property of the chaotic attractor, some time later the trajectory will again come arbitrarily close to this UPO.

In other words, suppose that a chaotic time series x(t) is available. Let $\eta > 0$ be given, then at some time t in the time series $|x_p - x_t| < \eta$, that is the chaotic trajectory has come arbitrarily close to the UPO, x_p, of period p. At some time Γ later $|x_p - x_{t+\Gamma}| < \eta$ and the trajectory has come close to the UPO again. To identify the unstable cycle of period p, a search through the data set for all points separated by Γ time steps that are a distance of η apart is performed. To ensure that the points obtained by this search correspond to a particular unstable cycle and not another nearby unstable cycle, not only are the points that are identified used but also their images under integration (or iteration for discrete systems). This is done by restricting the points of interest to those with iterates of which are within $\delta > \eta$ of each other, $|x_{p+1} - x_{t+1}| < \delta$. That is, all points such that $|x_p - x_t| < \eta$ and $|x_p - x_{t+\Gamma}| < \eta$ are considered and that $|x_{p+1} - x_{t+1}| < \delta$ to ensure that only one cycle is included and not several nearby cycles.

In practice, this is typically performed on a Poincaré section where the

continuous flow is mapped to a discrete iterative dynamical system of one less degree of freedom. Let Z_i be a point on the Poincaré section and suppose Z_p is an unstable periodic point on the section representing the UPO of period p. Then, the algorithm for calculating the UPO consists of searching the data set on the section, $\{Z_i\}^N_{i=1}$, for all points that are within η of Z_p the set $\{\xi_i: |Z_p-Z_i| < \eta\}$. Once these points have been identified, their corresponding image, or next iterate, is investigated. The set of points whose images (i.e. the next iterates) are within δ, $|Z_p-Z_{i+p}| < \delta$, for some $\delta > \eta$, are considered to correspond to that UPO, otherwise they correspond to a different UPO and are not further examined.

The last step is to identify the stability characteristics of the UPO, which is performed by using a least squares procedure to calculate a linear map, A, which maps Z_i to Z_{i+p}, where Z_i and Z_{i+p} correspond to the periodic point Z_p. This is accomplished by creating the vectors $D = \{d_i\}$ and $E = \{e_i\}$, where the d_i's are the deviations of the points from the UPO under consideration, $d_i = Z_i - Z_p$, and the e_i's are the deviations of the iterates from the image of the UPO, $e_i = Z_{i+\Gamma} - Z_{p+\Gamma}$. The point corresponding to the UPO, Z^*, is taken as the centroid of points under consideration.

The linear map A (an n *x* n matrix, where n is the dimension of the Poincaré section, usually taken as 2) is calculated by a least squares method that minimizes the error orthogonal to the approximate solution of the matrix equation $||DA-E||^2$, which,

since D and E are vectors, has solution given by A = inv (D^TD) D^TE.[25] The stability characteristics of the UPO are governed by the eigenvalues of the map A.

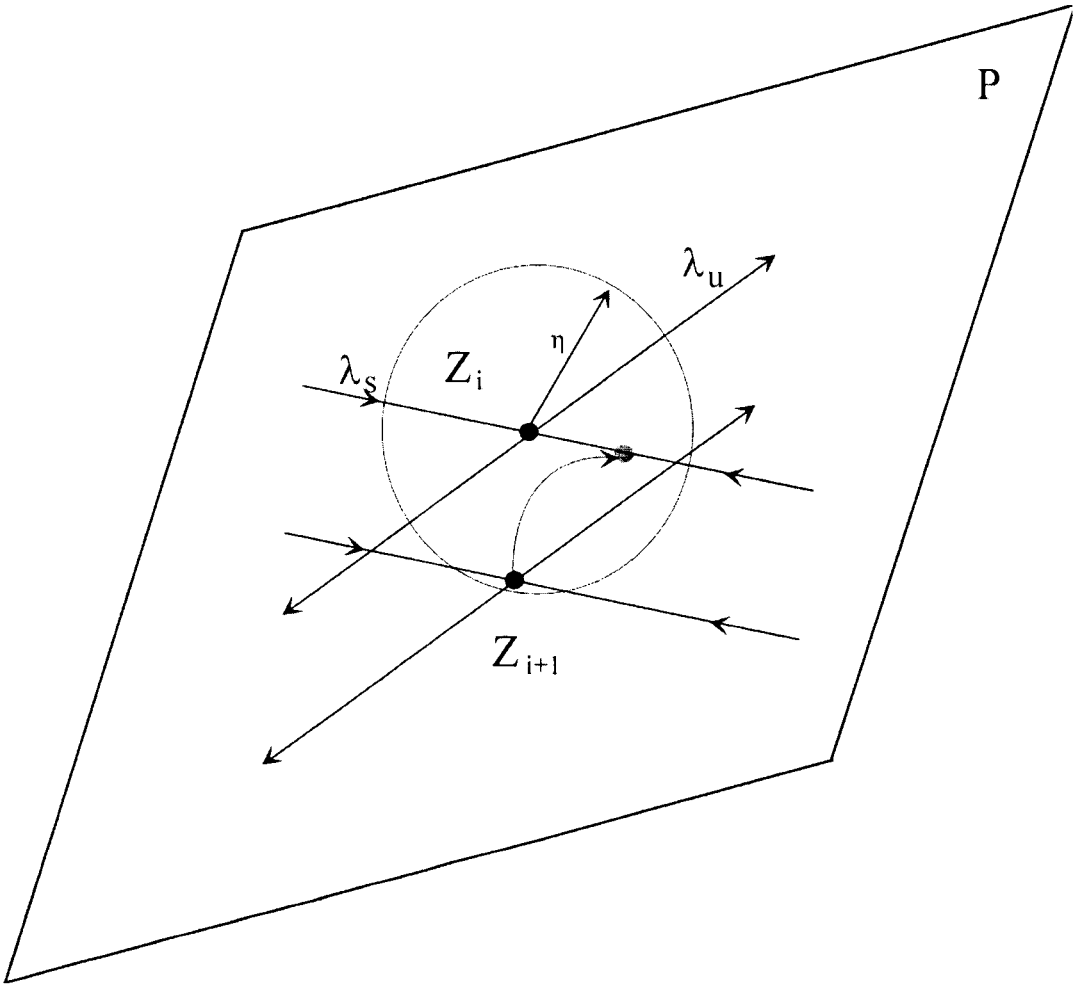

Figure 6 - Schematic of the action of the controller on a point. The control law pushes the point Z_{i+1} towards the stable eigenvector of Z_i.

2.8 CONTROL OF CHAOTIC SYSTEM RESPONSES

Once a periodic cycle has been selected for control and the corresponding linear map A has been calculated, control of the system about an unstable cycle can be maintained by applying a small perturbation to the chaotic trajectory about the UPO on the Poincaré plan. That is, the system is allowed to oscillate chaotically until the first time the trajectory enters within the η ball of the chosen UPO. Once within this ball, a small perturbation in the direction of the stable eigenvector of the linear map can be applied to ensure that upon the next return to the Poincaré section the trajectory is still within η of the UPO. Figure 6 is a schematic of this operation in which the point Z_{i+1}, is perturbed toward the stable eigenvector of the UPO.

A means of finding the magnitude and direction of the perturbation is obtained by employing the pole placement method[27,28] which is a state feedback rule devised to render the eigenvalues of the controlled system stable. A linear map describing the evolution of a trajectory from a point close to a periodic point on the Poincaré section to its next iterate is calculated as before. It remains to find a feedback rule which, when added to the linearized system, renders the nonlinear system stable.

Consider the dynamical system (linearized within the η ball as in Section V) represented by the state-space system

$$\dot{x} = Ax + By \tag{12a}$$

where x is the response of the system, y is the external forcing, A is the linear mapping and B is a column vector. Suppose that the external forcing can be written as $y = y_c + y_e$ where y_c describes a control input and y_e is the usual external excitation. Next, consider a feedback law of the form $y_c = - K^T x$, then Eq. (12a) can be rewritten as

$$\dot{x} = (A - BK^T)x + By_e \tag{12b}$$

Now, the homogeneous portion of Eq. (12b) determines the linear systems natural behavior, hence if the external excitation is ignored and the subscript from y_c is dropped, then a feedback of the form $y = - K^T x$ can be considered and Eq. (12b) takes the form

$$\dot{x} = (A - BK^T)x \tag{13}$$

The goal is to find a vector K^T such that the eigenvalues of the matrix $(A - BK^T)$ are asymptotically stable[28,29] (i.e. $|\lambda_i| < 1$ for i=1...n). This ensures that the fixed points

of the associated system, Eq. (12b), are stable. The eigenvalues of the matrix ($A - BK^T$) are called the regulator poles while the problem of placing these poles in an appropriate spot on the complex plane is called the pole placement problem.[30] The solution to this problem lies in the fact that one is free to choose K^T in an advantageous way, as long as the eigenvalues have the appropriate characteristics. If the system given by the pair (A, B) is controllable, then a solution to the pole placement problem always exists.[27] It can be shown that (A, B) is controllable when the n *x* n controllability matrix, C, has full rank, for the controllability matrix defined by

$$C = \left[B \mid AB \mid A^2B \mid \cdots \mid A^{n-1}B \right] \tag{14}$$

and where the columns of C are made up of the column vectors B, AB, A^2B, ... $A^{n-1}B$. The control law then consists of picking the entries in the vector K^T, called gains, so that the roots of the characteristic equation [Eq. (15)] are in prescribed positions. Since the λ_i's are known, this amounts to choosing the c_i's in the characteristic polynomial $\pi(\lambda)$:

$$\begin{aligned} \pi_{A-BK^T}(\lambda) &= \det\left(\lambda I - (A - BK^T)\right) = \\ &(\lambda-\lambda_1)(\lambda-\lambda_2)\cdots(\lambda-\lambda_n) = \\ &c_n + c_{n-1}\lambda + \cdots + \lambda^n \end{aligned} \tag{15}$$

A general method for calculating the c_i's is given by Ackerman's formula for pole placement in Ref. 30. The idea is to transform the pair (A, B) into controllable canonical form[27] by constructing a particular transformation matrix, solving for the gains in terms of the controllable canonical form and then transforming back. The result yields the choice of gains as $K^T = (-\sigma_n + c_n, ..., -\sigma_1 + c_1)\, G^{-1}$ where $G = C\,\Lambda$ is the transformation matrix, C is the controllability matrix and Λ has the form[27, 28, 30]

$$\Lambda = \begin{vmatrix} \sigma_{n-1} & \sigma_{n-2} & \cdots & \sigma_1 & 1 \\ \sigma_{n-2} & \sigma_{n-3} & \cdots & 1 & 0 \\ . & . & & . & . \\ . & . & & . & . \\ . & . & & . & . \\ \sigma_1 & 1 & \cdots & 0 & 0 \\ 1 & 0 & \cdots & 0 & 0 \end{vmatrix} \tag{16}$$

The c_i's are the coefficients of the characteristic polynomial $\pi_{A\text{-}BK}{}^T(\lambda)$ and the σ_i's are the coefficients of the characteristic polynomial $\pi_A(\lambda)$. For the case where A is 2×2, it can be shown that an optimal choice (in the sense of time to control) for the gain vector is $K^T = [\lambda_u, -\lambda_u\lambda_s]$, where λ_u is the unstable eigenvalue and λ_s is the stable eigenvalue of A.[11,28]

One can now formulate an algorithm to control a chaotic system utilizing this

control law on a Poincaré section. First, the linear map, A, of an unstable cycle is constructed as before and its eigenvalues identified. Then, setting $x = Z_i - Z^*$ and $\dot{x} = Z_{i+1} - Z^*$ in Eq. (13) yields the control law for the discrete UPOs on the Poincaré section as

$$Z_{i+1} = (A - BK^T)\left(Z_i - Z^*\right) + Z^* \tag{17}$$

Then, calculating the eigenvalues of A, λ_u and λ_s, choosing $K^T = [\lambda_u, -\lambda_u\lambda_s]$ and applying Eq. (17) whenever the trajectory comes within η of Z^* on the Poincaré section yields the desired stable characteristics. The final point left to consider is a relative distance on the Poincaré section a trajectory can be from Z^* and still be able to guarantee that the controller will perform adequately. The answer to this lies in the fact that since it was required that $|Z^* - Z_{i+1}| < \gamma$ by construction then, combining this with Eq. (17) yields

$$| Z_i - Z^* | < \frac{\gamma}{| A - BK^T |} \tag{18}$$

Since K^T was constructed to render the eigenvalues of the matrix $A - BK^T$ stable, and $(A - B K^T)^{-1}$ exists, this defines an area of width $2\gamma / | A - B K^T |$ about Z^* for which

the control should be applied.

2.9 APPLICATION OF CONTROL TO A MOORED STRUCTURE

Consider the chaotic oscillations of Eqs. (2a) - (2c) for the parameter values given as before ($\omega = 0.335$, $\gamma = 0.01$, $\psi = 4.0$, $\beta = 0.0$, $f_0 = 0.0$, and $f_1 = 2.0$) exhibited in Figure 5a - 5d. A search was done on the Poincaré data exhibited in Figure 5b to obtain all points that were near a period-1 orbit. This is done by comparing all points Z_i that are close and whose next iterate Z_{i+1} are also close (where the Z_i's are taken by stroboscopically sampling the position, x). Then, the UPO of period 1 is estimated as the mean of the set of points found to correspond to it (c.f. Section V). Utilizing this method, the system structural response data found a UPO of period-1 at the values $Z^* = [x, \dot{x}]^T$ where $x = 0.2623$ and $\dot{x} = -0.0677$. A linear map is constructed which maps the points near the UPO Z^* toward Z^* along the direction of the stable eigenvector as seen in Figure 6. In this case the linear map is given by

$$A = \begin{bmatrix} 0.8793 & 0.2766 \\ 0.4553 & -0.0729 \end{bmatrix} \tag{19}$$

which has a practically neutrally stable eigenvalue $\lambda_u = 0.9970$ and a stable eigenvalue

λ_s = - 0.1906. If the feedback control is applied only to the position x, this gives

$$B=\begin{bmatrix}1\\0\end{bmatrix} \tag{20}$$

Choosing the gain vector $K^T = [\lambda_u, -\lambda_u\lambda_s]$ yields the control poles at $p_{1,2}$ = [- 0.2951, 0.1044]. Thus, each time the system trajectory crosses the Poincaré section near Z^* the controller affects this point by applying the control law Eq. (17), ensuring

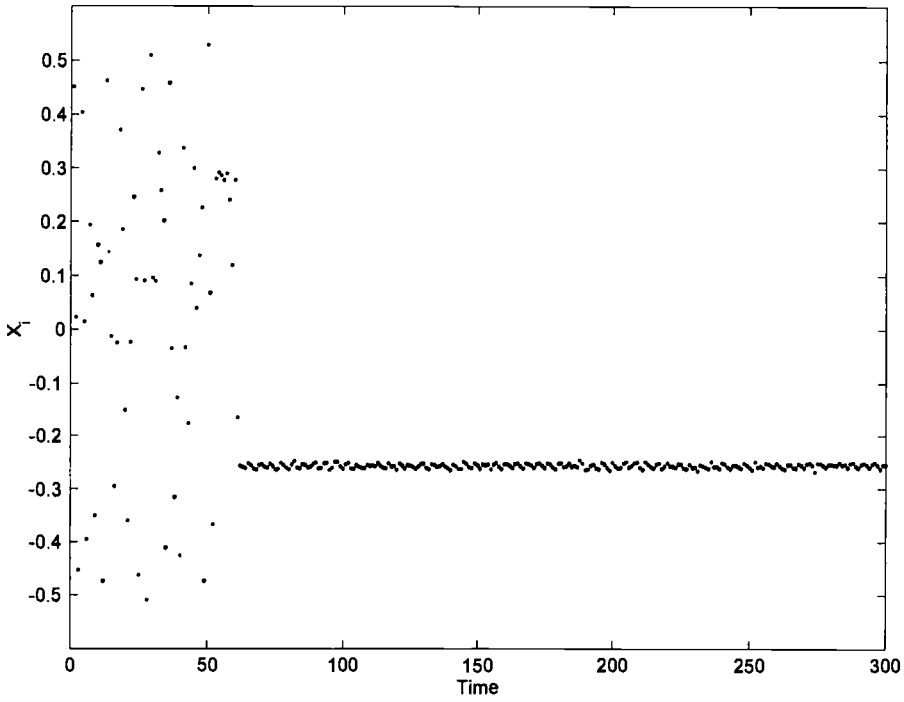

Figure 7 - Example of controlling the system about a period-1 cycle showing the Poincaré points versus time before and after control is applied.

that the trajectory returns near the point Z^* on the next return to the Poincaré section. The results of this application are shown in Figure 7, which is a plot of the Poincaré points versus time exhibiting the controlled periodic oscillation after an arbitrary duration of chaotic oscillations.

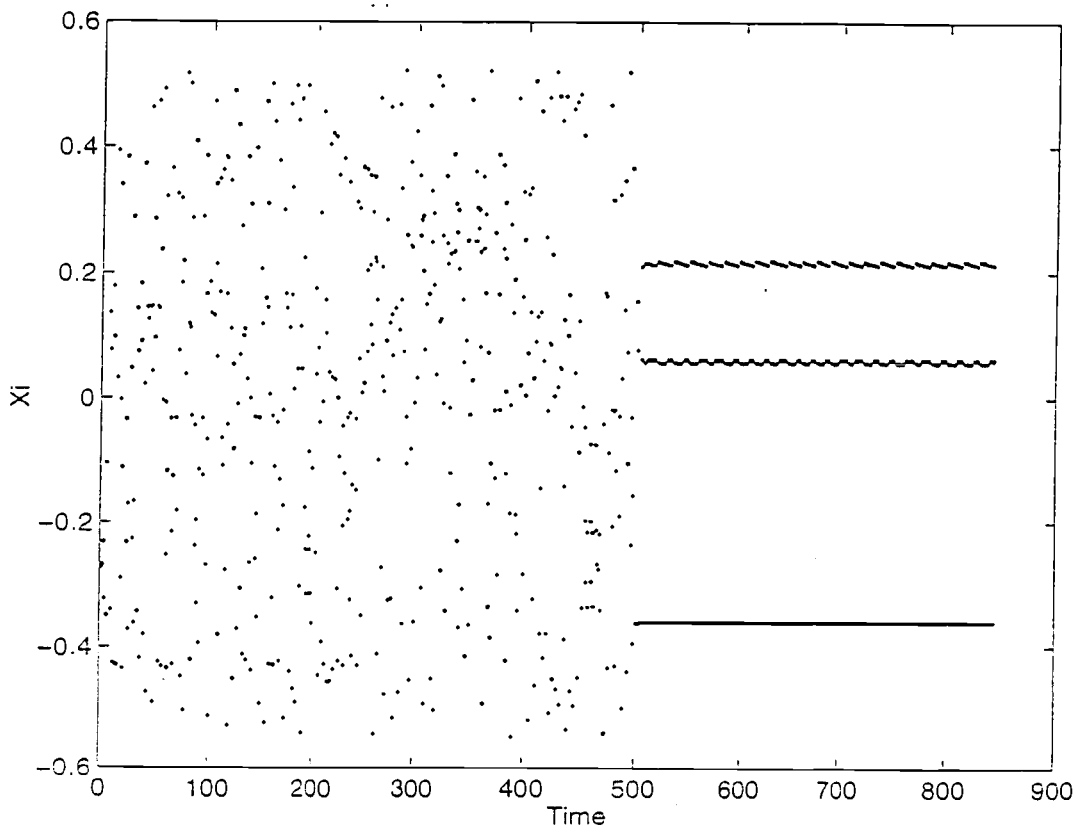

Figure 8 - Example of controlling the system about a period-3 cycle.

To further demonstrate the effectiveness of this strategy, a higher order periodicity is identified and the controller is again applied. Analysis of the higher order

motions, and in particular period-3 motion, is very similar to that of the primary resonance case treated in Section III (and has been examined in detail in Refs. 1 and 2 and, hence is not reported here). Figure 8 shows the results of this calculation for a period-3 orbit identified at the point $Z^* = [x, \dot{x}]^T$ for $x = -0.3609$ and $\dot{x} = 0.0359$. The linear map obtained for this case is given by

$$A = \begin{bmatrix} 0.9904 & -0.113 \\ -0.097 & -0.145 \end{bmatrix} \tag{21}$$

which has a neutrally stable and a stable eigenvalues $\lambda_u = 1.000$ and $\lambda_s = -0.1544$, respectively. The controller poles are placed at $p_{1,2} = [-0.6177, 0.2068]$ and the controller Eq. (17) is again applied to initiate control each time the system trajectory intersects the Poincaré section near the UPO at Z^* with period 3. The system oscillates chaotically until the trajectory comes close to the period-3 UPO at which time the controller is applied and subsequently the system oscillates between the period-3 points.

Observe that, despite the complexity of the dynamics between points in time where control is applied, the method produces a desired periodic motion through small adjustments. This method works well for arbitrary chaotic time series. The algorithm to control this chaotic system is to first obtain enough Poincaré points to be able to

characterize an unstable periodic orbit, typically a minimum of 20 points. Once the unstable orbit is identified, a linear map is obtained by a least-squares minimization of the matrix equation involving the points near the UPO and their iterates. Given this map, a feedback law is postulated that places the control poles in a stable operating regime. Finally, the system is allowed to oscillate until the trajectory enters within η of the UPO. At this time, control is applied to produce the desired periodic orbit.

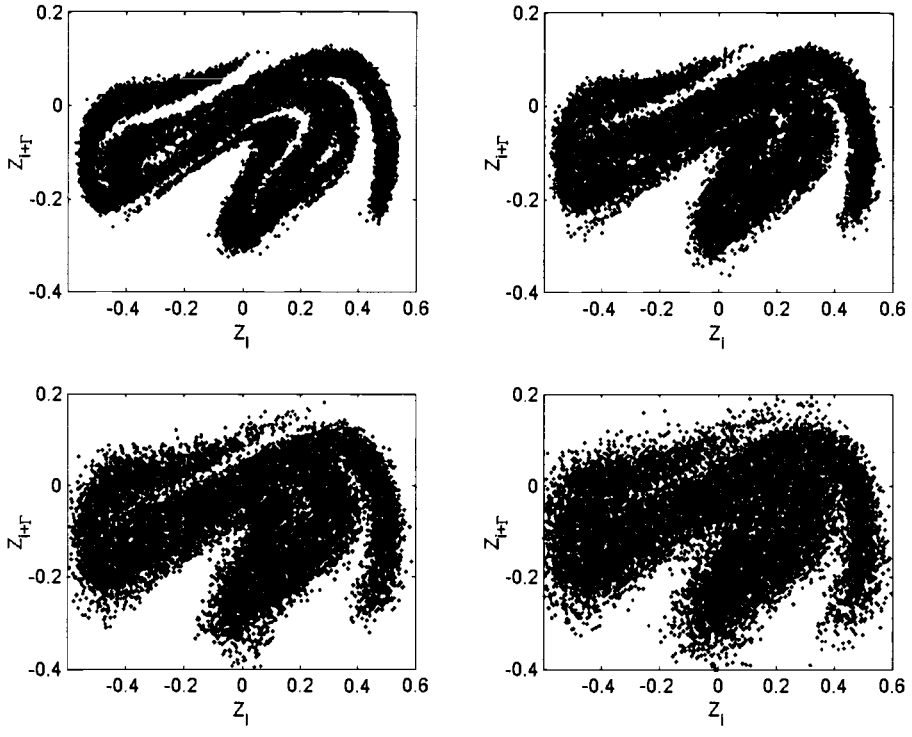

Figure 9 - Effects of increasing noise on the Poincaré portraits.

2.10 CONTROL OF SYSTEM WITH NOISE

The benefit of using small perturbations to control a deterministic nonlinear dynamical system within the chaotic operating regime has been presented above. However, for a typical real physical system such as a moored fluid-structure system, there will be noise added to the system through measurement errors as well as a random component in the excitation. For example, Figure 9 shows the Poincaré map of the noisy chaotic response obtained by adding (band-limited) white noise of finite variance to the excitation term in the deterministic case (as shown in Figure 5b). Here, the noise energy content is increased from 1.4% (Figure 9a) to 5.5% (Figure 9d) of the forcing energy. In this case a series of Poincaré sections about the chaotic attractor can be constructed by stroboscopically sampling every $2\pi/r\Gamma$, where r is the number of sections desired. This yields r separate controllers evenly distributed throughout the cycle, thus decreasing the long term effects of the noise with respect to an individual controller. By applying the above control scheme on each Poincaré section, the UPO can be targeted from one section to the next. If these sections are selected appropriately, then the effects of noise can be minimized.

Figure 10 shows the results of adding the white noise to the excitation term in the period-1 example above. Here, the noise energy level is increased from 1.4% to

5.5% of the forcing energy to exhibit the effects of the noise on the controller without making any modifications to the control scheme. Figures 10a - 10d are the Poincaré points from the controlled system as the noise is increased. Observe that, as the noise level is increased from 0% to 5.5%, the system goes from being completely controlled, to a mode where the controller appears to be effective only during limited durations, and finally to the point where the effects of noise overpowers the influence of the controller. For the system and example considered, the controller appears to have acceptable performance with no modifications for upto 2.7% noise energy.

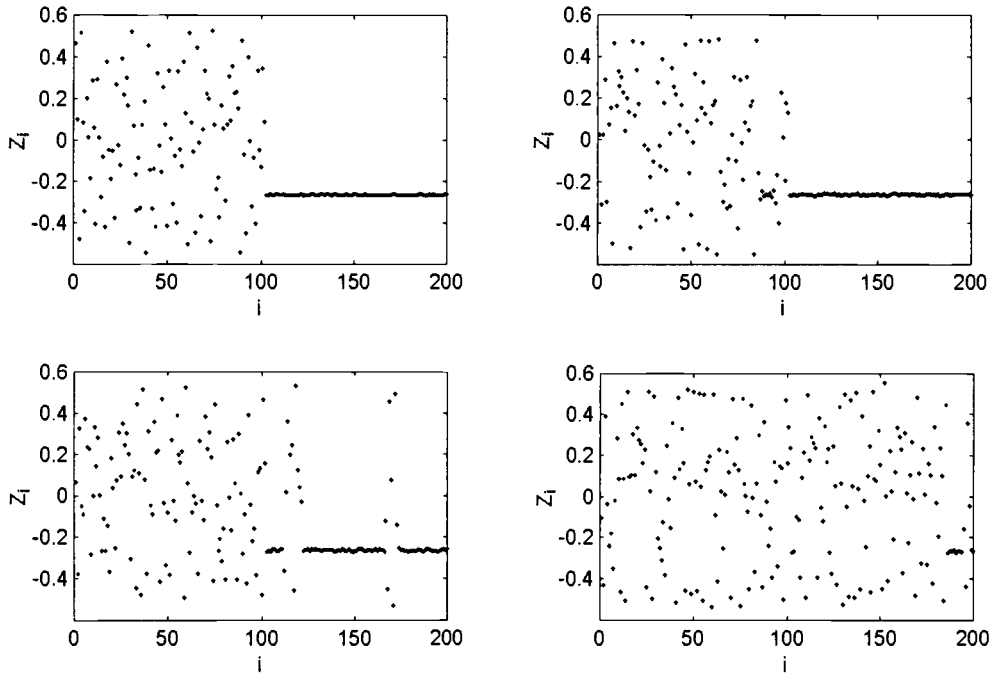

Figure 10 - Effects of increasing noise on the controller in Figure 7.

A simple modification to the control scheme can dramatically increase the controllability of the system. By taking several Poincaré sections around a single cycle, and then building a feedback controller on each section, the effects of the noise are reduced proportionally to the number of sections the controller is applied on per cycle.

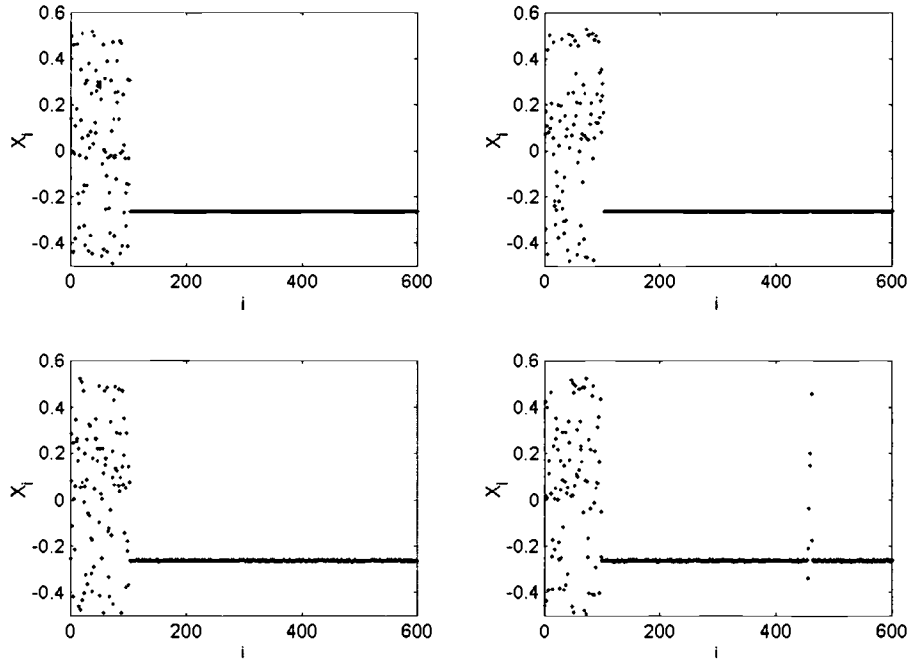

Figure 11 - Control of noisy chaos when control is applied on 4 control sections and the noise levels go from 1.4%-5.5%.

Figure 11 shows the results of the previous example with 4 control sections. Each of the 4 sections has been created by sampling the same time series data set at 4

times the rate of that in Figure 10, r = 4. Then, using the scheme outlined above, a linear map on each section is constructed, finally, each time a trajectory crosses a section within the control tolerance, Eq. (17) is applied for that section. Figure 11 shows the results for one of the sections and the varying noise levels. With 4 control sections, an increase from 2.7% to 4.15% noise can be acceptably controlled.

The number of control sections verses the amount of noise that the system controller is able to handle are shown in Figure 12. Here, two levels of control influence, i.e. two different values of η (0.05 and 0.1), are employed. It is assumed that the system is fully controlled if it can be controlled for 100 Poincaré points (or about

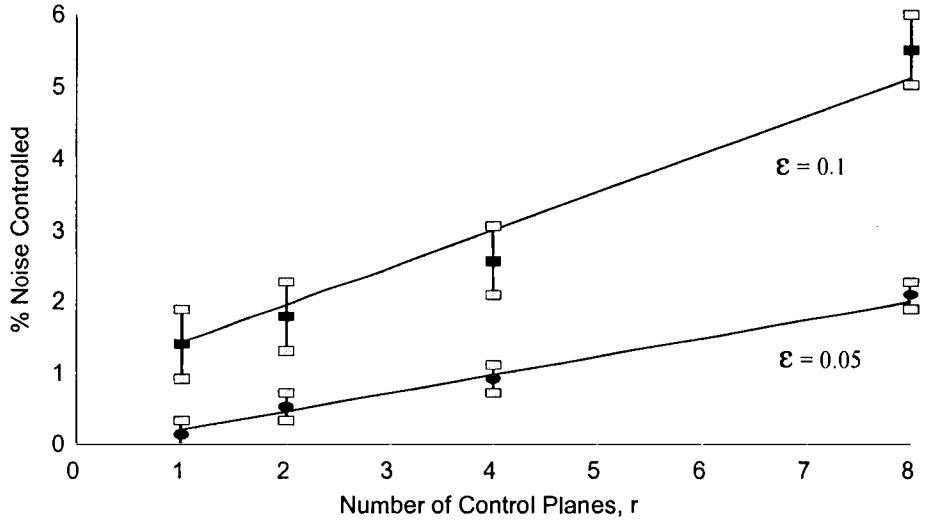

Figure 12 - Effects of increasing number of control sections on the increasing amounts of controllable noise for several control tolerances.

85,000 time series data points). Figure 12 indicates an approximately linear relationship between the controllable level of the energy of the noise versus the number of sections required for complete control.

2.11 CONCLUDING REMARKS

This study examines control of the chaotic oscillations of a fluid-structure interaction system. The system under consideration, although of fluid origin, is modeled as a low degree of freedom system by considering cases for which the small body theory applies. This assumes that the structure does not influence the wave field, allowing for the nonlinear fluid loads to be approximated in terms of an added inertia and a nonlinear coupling. This, together with restraints on vertical and rotational motion and, by approximating the nonlinear mooring resistance with a low order polynomial, yields the desired low order system.

The nonlinear dynamics of the fluid-structure interaction system have been demonstrated to exhibit chaotic oscillations under certain environmental conditions and verified on data obtained from experiments. This fact is used to an advantage in the design of a controller. This study outlines a method for controlling chaotic systems, in general, with the use of the systems dynamics and small perturbations. The method

uses a chaotic time series to categorize unstable periodic orbits. This is done by mapping the time series to a Poincaré section and then obtaining the unstable periodic orbits through an exhaustive search of the Poincaré points. This produces a linear map for which the pole placement method of feedback control can be applied. The method was first applied to the model to verify control. Then, the method was applied to the model in the case that band-limited white noise of finite variation was added to the excitation term, producing the first indications that (stochastic) control of moored systems is possible.

An unstable periodic point can be identified by realizing that after p iterations (where p is the periodicity of the cycle), a trajectory will return to a neighborhood of its corresponding unstable cycle. By investigating all of the points that are a small distance apart after every p iterates the set of UPO's of period p can be obtained.

Given a UPO of period p, control can be applied by taking advantage of the local linearity of the UPO. A linear map is constructed from the set of points about the periodic cycle and then the stability of this map is investigated. The controller uses the pole placement procedure to perturb a trajectory toward the periodic cycle along the stable direction of the linear map. This ensures that the linear system dynamics are locally stable and system control is achieved. This control amounts to small perturbations to the system trajectory at prescribed times to maintain the desired

oscillatory characteristics. The control algorithm is then applied to the fluid-structure interaction system. The controller was able to stabilize the chaotic oscillations of the system about periodic orbits of arbitrary periodicity. As examples, the control of a period-1 orbit and a period-3 orbit were demonstrated.

An extension of the system was investigated to achieve a more robust controller under the circumstances that additive noise is present in the excitation force. This extension applies the same algorithm of control design to a series of Poincaré sections produced by stroboscopically sampling every $2\pi/r\Gamma$, where r is the number of sections desired. This yields r separate controllers evenly distributed, thus decreasing the long term effects of the noise with respect to an individual controller. This method appears to yield a linear growth in the amount of noise that the system is able to handle. More robust control schemes will be examined in the near future.

Finally, should the responses of the prototypes corresponding to the model tests mentioned in the beginning of this study confirm the existence of chaotic motions in the (noisy) field environments, the analysis and control method presented in this study can be applied to suppress these motions if desired. Extensions of this study to the multi-degree-of-freedom physical models and subsequent design of practical controllers for experimental tests are being examined.

2.12 ACKNOWLEDGMENTS

The authors wish to acknowledge the financial support of the U. S. Bureau of Mines process control-program (AL-92-A-001) and the United States Office of Naval Research (Grant No. N0001-92-J-1221).

2.13 BIBLIOGRAPHY

1. Gottlieb, O., and Yim, S. C. S., "Deterministic Motions of Nonlinear Mooring Systems Part I: Analysis and Predictions", Ocean Engineering Report No. OE-93-02, Oregon State University, Corvallis, OR, 1993.

2. Gottlieb, O., and Yim, S. C. S., "Onset of Chaos in a Multi-Point Mooring System", Proc. First (1990) European Offshore Mechanics Symposium, Trondheim, Norway, Aug. 20-22, 1990, pp. 6-12.

3. Yim, S. C. S., Myrum, M. A., Gottlieb, O., Lin, H., and Shih, I. M., "Summary and Preliminary Analysis of Nonlinear Oscillations in a Submerged Mooring System Experiment", Ocean Engineering Report No. OE-93-03, Oregon State University, Corvallis, OR, 1993.

4. Yim, S. C. S. and Lin, H., "'Chaotic Behavior and Stability of Free Standing Offshore Equipment", Ocean Engineering, Vol. 18, No. 3, pp. 225-250, 1991.

5. Yim, S. C. S., and Lin, H., "Nonlinear Impact and Chaotic Response of Slender Rocking Objects", J. Eng. Mech., Vol. 117, No. 9, Sept. 1991, pp. 2079-2100.

6. Lathrop, D. P. and Kostelich, E. J., "Characterization of an Experimental Strange Attractor by Periodic Orbits.', Phys. Rev. A, Vol. 40, No. 7, pp 4028-31, Oct. 1989.

7. Auerbach, D., Cvitanovic, P., Eckmann, J.-P.,Gunaratne, G., and Procaccia, I., "Exploring Chaotic Motion Through Periodic Orbits", Phys. Rev. Lett., Vol. 58, No. 23, June 1987, pp 2387-89.

8. Cvitanovic, P., "Invariant Measurement of Strange Sets in Terms of Cycles", Phys. Rev. Lett., Vol. 61, No. 24, Dec. 1988, pp. 2729-32.

9. Grebogi, C., Ott, E., and Yorke, J. A., "Unstable Periodic Orbits and the Dimensions of Multi-fractal Chaotic Attractors", Phys. Rev. A, Vol. 37, No. 5, March 1988, pp. 1711-24.

10. Sano, M., and Sawada, Y., "Measurement of the Lyapunov Spectrum from a Chaotic Time Series", Phys. Rev. Lett., Vol. 55, No. 10, Sept., 1985, pp. 1082-85.

11. Ott, E., Grebogi, C., and Yorke, J. A., "Controlling Chaos", Phys. Rev. Lett., Vol. 64, No. 11, Mar. 1990, pp. 1196-99.

12. Singer, J., Wang, Y.-Z., and Bau, H. H., "Controlling a Chaotic System", Phys. Rev. Lett., Vol. 66, No. 9, Mar. 1991, pp. 1123-25.

13. Wang, Y., Singer, J., and Bau, H. H., "Controlling Chaos in a Thermal Convection

Loop", J. Fluid Mech., Vol. 237, pp. 479-98, 1992.

14. Petrov, V., Gaspar, V., Masere, J., and Showalter, K., "Controlling Chaos in the Belousov-Zhabotinsky Reaction", Nature, Vol. 361, Jan. 21, 1993, pp. 240-43.

15. Einerson, C. J., Smartt, H. B., Moore, K. L., and King, P. E., " Modeling and Control of Nonlinear Chaotic Systems Using a Feedforward Neural Network", *Intelligent Engineering Systems Through Artificial Neural Networks, Vol. 2,* ed. C. H. Dagli et. al., ASME Press, New York, 1992.

16. King, P. E., Ochs, T. L., and Hartman, A. D., "Chaotic Responses in Electric Arc Furnaces", J. Appl. Phys. Vol. 76, No. 4, Aug., 1994

17. King, P. E., Nyman, A. D., Ochs, T. L. and Einerson, C. J., "Modeling for Control of an electric Arc Furnace Using a Feedforward Artificial Neural Network", *Intelligent Engineering Systems Through Artificial Neural Networks, Vol. 3,* ed. C. H. Dagli et. al., New York, 1993.

18. Anderson, B. D. O., and Moore, J., B., *Optimal Filtering,* Prentice Hall, 1979, 357 pps.

19. Roberts, J. B., and Spanos, P. D., *Random Vibration and Statistical Linearization,* John Wiley & Sons, New York, 1990, 407 pps .

20. Cawley, R., and Hsu, G.-H., "Noise Reduction for Chaotic Data by Geometric Projection", in *Applications of Digital Image Processing XV,* ed. by Andrew G. Tescher,

Proc. SPIE 1771, pps. 368-76, 1993.

21. Cawley, R., and Hsu, G.-H., "Another New Noise Reduction Method for Chaotic Time Series", in *Proc. of the 1st Experimental Chaos Conference,* Oct. 1-3, 1993, eds. Arlington, V., Vohra, S., Spano, M., Shlesinger, M., Pecora, L., and Ditto, W., World Scientific Press, Singapore, 1992, pps. 38-46.

22. Jordan, D. W. And Smith, P., *Nonlinear Ordinary Differential Equations*, 2nd ed., Clarendon Press, 1987, 381 pps.

23. Nayfeh, A. H., and Mook, D. T., *Nonlinear Oscillations,* John Wiley & Sons, New York, 1979 704 pps.

24. Wiggins, S., *Introduction to Applied Nonlinear Dynamical Systems and Chaos,* Springer-Verlag, 1990, 672 pps.

25. Strang, *G., Introduction to Applied Mathematics,* Wellesley-Cambridge Press, Wellesley, Mass, 1986, pp. 37-8.

26. Devaney, R., *An Introduction to Chaotic Dynamical Systems*, Addison-Wesley Publ. Co., 1987, 320 pps.

27. DeCarlo, R., A., *Linear Systems, A State Variable pproach with Numerical Implementation,* Prentice Hall, New Jersey, 1989, pp. 335-45.

28. Romeiras, F., J., Grebogi, C., Ott, E., and Dayawansa, W., P., "Controlling Chaotic Dynamical Systems", Physica D, Vol. 58, 1992, pp. 165-92.

29. Nitsche, G., and Dressler, U., "Controlling Chaotic Dynamical Systems Using Time Delay Coordinates", Physica D, Vol. 58, 1992, pp. 153-64.

30. Franklin, G. F., Powell, J. D., and Emami-Naeimi, A., *Feedback Control of Dynamic Systems,* 2nd ed., Addison-Weseley, New York, 1991, pps. 377-96.

2.14 LIST OF FIGURES

Nonlinear Rocking Responses of Free Standing Rigid Blocks, Part I - Deterministic Control

P. E. King[1]

Solomon S. C. Yim[2]

Submitted to

Journal of Engineering Mechanics

ASCE Publications

Manuscript Number EM/2005/024246

3.1 Abstract:

An understanding of the rocking response and overturning stability of rigid blocks is of importance to the preservation of free-standing equipment and structures placed in the ocean and seismic environments. Previous studies have indicated a wide spectrum of possible responses under support excitation including periodic, quasi-periodic and chaotic motions, which may lead to overturning. To avoid potentially catastrophic chaotic responses, a means of actively controlling the nonlinear oscillations is presented. Part I of this two-part study presents system responses to purely deterministic excitations while Part II presents the case where a low intensity additive random noise component is included in the excitation. The controller is able to maintain the dynamical system in a periodic oscillatory state of arbitrary periodicity for prescribed cases in the corresponding chaotic region of the uncontrolled system. The proposed control methodology applies a force to induce small perturbations about the nonlinear system trajectory at prescribed times in order to guide it towards a stable operating state. This is accomplished by creating a locally linear map about a desired trajectory. Then, a feedback controller is designed to guide the system trajectory towards the associated stable eigenvector of the linearized system, ensuring that the trajectory is maintained in a neighborhood of the desired periodic motion during the interval between sampling. This paper outlines the proposed method using a simple, standard control algorithm (pole placement) to emphasize the ease of which control of these highly sensitive,

nonlinear systems can be maintained as exhibited by an application to the free-standing rocking blocks. Estimates of the energy required to maintain control of the rocking motions are given.

[1]Research Program Leader, U. S. Department of Energy, Albany Research Center, Albany, OR 97321
[2]Professor, Civil, Construction and Environmental Engineering Dept., Oregon State University, Corvallis, OR 97331.

3.2 Introduction

Nonlinear and chaotic responses have been identified in models of engineering systems in the offshore and seismic environments (Thompson 1983 and 1984, Gottlieb and Yim 1990 and 1991a, Pompei *et al* 1998, Jeong, *et al* 2003, and Lenci and Stega 2005). In the case that free-standing equipment or structures should be installed on these offshore and seismic systems, it can be shown that through the base support excitation, these "rocking blocks" can also be set into highly nonlinear complex motions (Hogan 1990 and Yim and Lin 1991b). In particular, under certain periodic (Yim and Lin 1996a) or random (Yim and Lin 1996b) base motions, overturning response may occur, causing potentially catastrophic results. In an effort to avoid this scenario, a means of effectively controlling the rocking block motions is needed to preserve the integrity of the systems under all modes of excitations. Moreover, to better emulate the nature of the ocean and seismic environments and to determine the controller's effectiveness under the stochastic case, a random (noise) process needs to be incorporated into the excitation model.

In this study, it is assumed that the supporting base of the rigid blocks is either under going periodic oscillations (Part I) or is periodic with low amplitude, band limited white noise component (Part II, Yim and Lin 1996a). Under these conditions, it can be shown that these base motions may cause highly sensitive, nonlinear (quasi-periodic or chaotic) responses in the free standing rigid blocks.

Due to the intrinsic characteristics of these types of nonlinear motions (including topological transitivity and sensitivity to initial conditions), a means of efficiently achieving the desired control is possible. By applying small forces to induce perturbations to the nonlinear system response at prescribed intervals, one may effectively control the nonlinear oscillations.

Control of the rocking motions can be accomplished by applying relatively small generalized forces, in this case moments, about the rocking edge of the block. This can be achieved by attaching a small mass at the top of the block and inducing relative accelerations of the mass via a control mechanism. By creating a locally linear map of the nonlinear system about a desired trajectory identified as an unstable periodic cycle, the necessary displacements of the mass can be calculated to achieve control (Lathrop and Kostelich 1989, Auerbach *et al* 1987, Ott Grebogi and York 1990, Romeiras *et al* 1992). This can be performed on a Poincaré section (Bergé, Pomeau and Vidal 1984) which is a mapping of the continuous dynamical system to that of a discrete dynamical system of one less degree of freedom. Because of the nature of these types of nonlinear systems, this mapping preserves many of the interesting characteristics and dynamic invariants that are indicative of highly sensitive systems, including chaotic systems. Thus, the unstable periodic cycles are preserved and their dynamic characteristics maintained. Moreover, the locally linear map will necessarily contain both stable and unstable eigenvalues defining the directions for which the continuous dynamical system expands or

contracts. These eigen-directions are used to design a feedback controller which ensures that the linearized system has stable eigenvalues. The pole placement method is employed to ensure the required stability (Franklin, Powell and Emami-Naeimi 1991). This simple, standard method is chosen to emphasize the ease of which control of highly nonlinear systems such as the rocking block can be maintained.

This work follows along the same line as the seminal one proposed by Ott, Grebogi and York (1990). However, in their work, the assumption was made that a system parameter is available which can be altered, giving an effective means of making minor changes to the dynamics of the system. For the rocking block system such a parameter is not available for control. In this study, the control method is modified by applying a moment to induce desired perturbations to an observable of the system, the angular position. It is assumed that an external means of applying the moment is available and many such mechanical control systems are conceivable as mentioned above.

This paper introduces a mathematical description of the rocking block system. Then, an outline of the proposed control methodology is presented and the method is applied to the rocking object in order to minimize the over turning probability of the system. In Part II, extensions to the methodology are indicated for the case with low intensity randomness in the excitation and the resulting controller is applied to

the system when there is additive noise present. Finally, an estimate of the relative magnitude of the perturbation energy required to maintain control is given.

3.3 Rocking Response of Rigid Blocks

The system under consideration is that of a free standing rectangular rigid body subject to horizontal base excitation as shown in Figure 1. Considering only cases where the coefficient of friction is substantial enough that there will be no slipping between the rigid body and its base, the block may move rigidly about one of the two centers of rotation represented as O and O'. If rocking should occur, it is assumed that the body will oscillate rigidly about these centers of rotation until toppling occurs or the body comes to rest again. The governing equations of motion for the rigid body with positive and negative angular displacement are given by

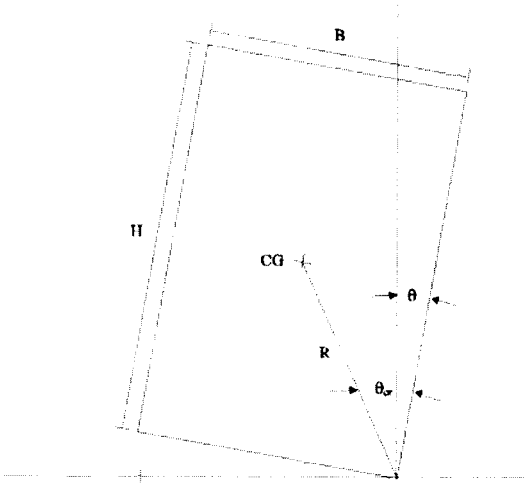

Figure 1 - A free standing rigid body subject to horizontal base excitation.

$$I_O\ddot{\theta} + MgR\sin(\theta_{cr} - \theta) + MRa_{gx}\cos(\theta_{cr} - \theta) = 0 \quad \theta > 0 \tag{1a}$$

$$I_o\ddot{\theta} + MgR\sin(\theta_{cr} + \theta) + MRa_{gx}\cos(\theta_{cr} + \theta) = 0 \quad \theta < 0 \tag{1b}$$

where I_o is the moment of inertia about the center of rotation O (or O') M is the mass of the rigid body, g is the force of gravity, R is the distance from O (or O') to the center of mass, a_{gx} is the base excitation, H and B are the height and width of the object and $\theta_{cr} = cot^{-1}$(H/B) is the critical angle defining the angular position for which toppling occurs under static conditions.

The transition between rocking motions about O and O' is accompanied by an instantaneous impact when the angular displacement crosses zero either from the positive or the negative direction. Associated with the impact is a finite amount of energy loss which is accounted for by a reduction in the angular velocity of the object after impact. It is assumed that the angular velocity after impact is related to the angular velocity before impact through the impact parameter, e, defined by the following relationship:

$$\dot{\theta}(t^+) = e\dot{\theta}(t^-), \quad 0 \le e \le 1 \tag{2}$$

where e is the coefficient of restitution, t^+ is the time just after impact and t^- is the time just prior to impact. In this study, the base excitation a_{gx} is assumed to be harmonic with constant amplitude a_x and single frequency ω ($\zeta(t)$=0) or harmonic with additive noise ($\zeta(t)\neq 0$).

$$a_{gx} = a_x \cos(\omega t + \phi) + \xi(t) \tag{3}$$

Note that there are four sources of nonlinearities present in this system. The first nonlinearity is the righting moment about the edges which gives rise to the nonlinear restoring forces as a function of angular displacement, θ. The second is associated with the coupled parametric excitation. The third is associated with the energy loss at impact and is represented as a jump discontinuity in the angular momentum while the fourth is due to the change in centers of rotation resulting in a transformation from one governing equation to the other.

Many of the nonlinear responses of this type of systems have been identified and their importance reported in the literature (e.g., Hogan 1989 and 1990, Iyengar 1996, Jeong 2003, Lenci 2005, Lin 1996a, b, Yim 1980, 1991a, b) and hence will not be repeated here. For this study it is sufficient to identify certain responses to the base excitation and their effect on the motion of the rigid block. In particular, it has been shown that this system undergoes responses ranging from periodic, quasi-periodic, chaotic to overturning.

It is convenient to normalize the angular displacement and angular velocity with respect to the critical angle θ_{cr} for plotting and interpretation of the results as follows:

$$\Theta = \theta / \theta_{cr}, \qquad \dot{\Theta} = \dot{\theta} / \theta_{cr} \tag{4}$$

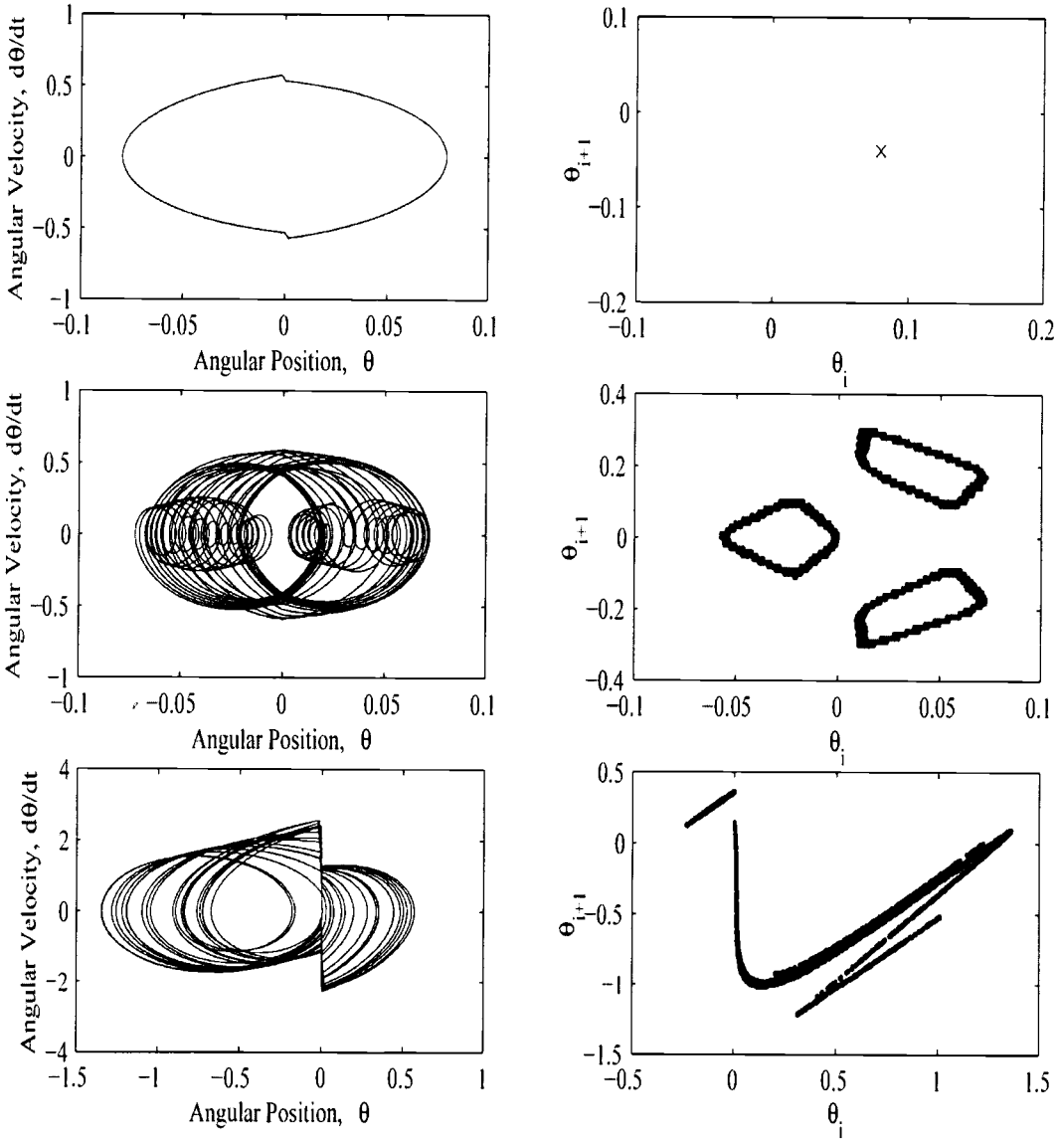

Figure 2 - The response of the rigid rocking object subject to base excitation for the cases a) periodic phase space (A_x=6.5, ω=15.70796, e=0.925), b) periodic Poincaré section, c) quasi-periodic phase space (A_x=4.0, ω=15.70796, e=1.0), d) quasi-periodic Poincaré section, e) chaotic phase space (A_x=4.6, ω=2.7, e=0.5) and f), chaotic Poincaré section.

This results in the normalized horizontal base excitation amplitude $A_x = a_{gx}/(g\theta_{cr})$. Figure 2 shows the phase space portraits and the corresponding[e)] Poincaré sections[f)] for some of these various responses. Specifically, Figs.2a & b show the periodic response, Figs.2c & d the quasi-periodic response and Figs.2e & f the chaotic response. The Poincaré surface of sections is an alternate way of representing the responses and is obtained by stroboscopically sampling the time series at $2\pi/\Gamma$ intervals and then plotting the points sequentially, i.e., by plotting $\Theta(t)$ vs. $\Theta(t+\Gamma)$, for Γ the sampling period. This technique gives a suitable means of viewing the geometric complexity of the time histories. In this study, it is assumed that the nonlinear motion observed in Figs.2e & f is deemed undesirable, and means of rendering these nonlinear oscillatory states periodic are necessary.

3.4 Unstable Periodic Orbits

The numerical simulations together with the analytical results presented in the literature show that the oscillatory nature of the rocking block system described by Eqs.(1)-(3) exhibit a range of modes. A means of analyzing the chaotic motion by using the time series alone has been introduced Auerbach *et al* (1987) and Lathrop and Kostelich (1989). The procedure utilizes the unstable periodic orbits (UPO's) of a system. Since a chaotic attractor contains a multitude of UPO's of varying periodicities, much of the nonlinear characteristics can be identified through these

special cycles. It is well known that UPO's are dense in a chaotic attractor (Grebogi, Ott and York 1988), and in fact this is a necessary condition for chaos to exist (Devaney 1987). This fact is exploited in the following discussions.

The characteristic of importance in the use of an UPO is that if the chaotic system is allowed to evolve long enough, then a trajectory will return arbitrarily close to a given unstable cycle, arbitrarily often. This is because these cycles are dense on the attractor and that they are periodic and yet unstable. Thus, if the system is on a cycle, it will remain on it for all time. However, if there is any minute deviation from the cycle, then the chaotic trajectory will diverge from this unstable cycle. Because of the "mixing" property of the chaotic attractor, at some time later the trajectory will again come arbitrarily close to this UPO.

In other words, suppose that a chaotic time series x(t) is available. Let an arbitrarily small scalar "distance" $\varepsilon > 0$ be given, then at some time t in the time series $|x_p - x_t| < \varepsilon$, and the chaotic trajectory has come arbitrarily close to the UPO, x_p, of period p. At some time Γ later $|x_p - x_{t+\Gamma}| < \varepsilon$ and the trajectory has come close to the UPO again. To identify the unstable cycle of period p, a search through the data set for all points separated by Γ time steps that are a distance of ε apart is performed. To ensure that the points obtained by this search correspond to a particular unstable cycle and not another nearby unstable cycle, not only are the points that are identified used but also their images under integration (or iteration for discrete systems). This is done by restricting the points of interest to those with

iterates of which are within $\eta > \varepsilon$ of each other, $|x_{p+1}-x_{t+1}|< \eta$. That is, all points such that $|x_p-x_t| < \varepsilon$ and $|x_p-x_{t+\Gamma}| < \varepsilon$ are considered and that $|x_{p+1}-x_{t+1}|< \eta$ to ensure that only one cycle is included and not several nearby cycles. Figure 3 is a schematic of this operation. The points which fall within the ε-ball and whose iterates fall within the η-ball are picked for future calculations while the points outside the η-ball are discarded from future consideration.

In practice, this is typically performed on a Poincaré section where the continuous flow is mapped to a discrete iterative dynamical system of one less degree of freedom. Let Z_i be a point on the Poincaré section and suppose Z_p is an unstable periodic point on the section representing the UPO of period p. Then, the algorithm for calculating the UPO consists of searching the data set on the section, $\{Z_i\}^N_{i=1}$, for all points that are within ε of Z_p, the set $\{\xi_i: |Z_p-Z_i| < \varepsilon\}$. Once these points have been identified, their corresponding image, or next iterate, is investigated. The set of points whose images are within η, $|Z_p-Z_{i+p}| < \eta$,

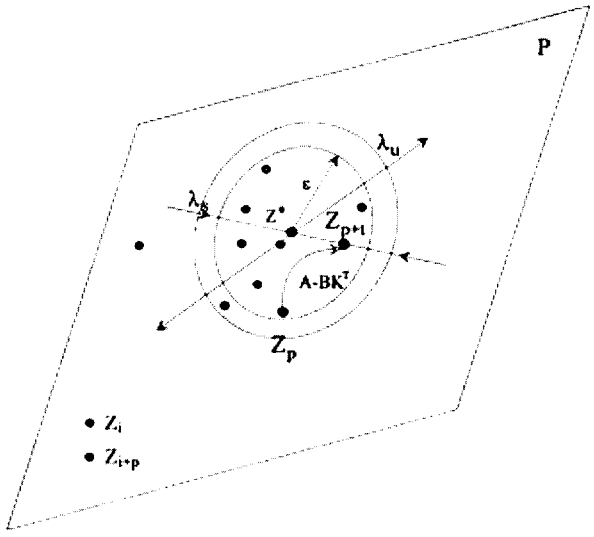

Figure 3 - Schematic of selection of Poincaré points corresponding to an UPO and the corresponding controller action on the locally linear system.

for some scalar "distance" $\eta > \varepsilon$, are considered to correspond to that UPO, otherwise they correspond to a different UPO and are not further examined.

The last step is to identify the stability characteristics of the UPO, which is performed by using a least squares procedure to calculate a linear map, A, which maps Z_i to Z_{i+p}, where Z_i and Z_{i+p} correspond to the periodic point Z_p. This is accomplished by creating the vectors $D = \{d_i\}$ and $E = \{e_i\}$, where the d_i's are the deviations of the points from the UPO under consideration, $d_i = Z_i - Z_p$, and the e_i's are the deviations of the iterates from the image of the UPO, $e_i = Z_{i+r} - Z_{p+r}$. The point corresponding to the UPO, Z^*, is taken as the centroid of points under consideration.

The linear map A (an $n \times n$ matrix, where n is the dimension of the Poincaré section, usually taken as 2) is calculated by a least squares method that minimizes the error orthogonal to the approximate solution of the matrix equation $\|DA-E\|^2$, which, since D and E are vectors, has solution given by $A = \text{inv}\,(D^TD)\,D^TE$ (Strang 1986). The stability characteristics of the UPO are governed by the eigenvalues of the map A.

3.5 Control of Chaotic Responses

Once a periodic cycle has been selected and the corresponding linear map, A, calculated, control of the system about this cycle can be maintained by applying any number of control schemes. Potential controllers that have appeared in the literature for these types of systems include the pole placement control employed in Auerbach *et al*, the linear quadratic regulator and H^{∞} control (Hammand *et al* 1996), optimal control (Abarbanel *et al* 1997), and stochastic control (Fowler 1988). In each case, a state feedback control law is formulated which either places physical constraints on the system poles or minimizes a predefined cost function for the system. Figure 4 is a state feedback diagram indicating the control strategy outlined. For the problem under consideration, the state feedback controller is designed to apply a small perturbation to the chaotic trajectory about the UPO on the Poincaré plan. That is, the system is allowed to oscillate chaotically until the first time the trajectory enters within the η ball of the chosen UPO. Once within this ball, the feedback controller applies a small perturbation to the measured signal, in the direction of the stable eigenvector of the linear map. This action ensures that upon the next return to the Poincaré section, the trajectory is still within η of the UPO. By referring again to Figure 3, the application of the control is clearly identified in this schematic of the operation.

Recall that the control is applied only on the Poincaré section in which the point Z_{i+1} is perturbed toward the stable eigenvector of the UPO while the system is left untouched otherwise. Because of this discrete application of the control and due to the fact that the "perturbations" are small in comparison to the amplitude of the system structural response, this methodology requires very little energy to obtain the desired system response.

A means of finding the magnitude and direction of the perturbation is obtained by employing the pole placement method (Romeiras *et al* 1992 and DeCarlo 1989), a state feedback rule devised to render the eigenvalues of the controlled system stable. Mathematically, the goal of this method is to construct a matrix, called a gain matrix, which assigns the poles of the controlled system in prescribed positions, i.e. the spectral assignability problem. In order to solve the general problem of spectral assignability, the canonical single input case is first considered. Then, a means of constructing a transformation matrix from a general single-input system to the canonical single-input system is explored. Next, the general multi-input case

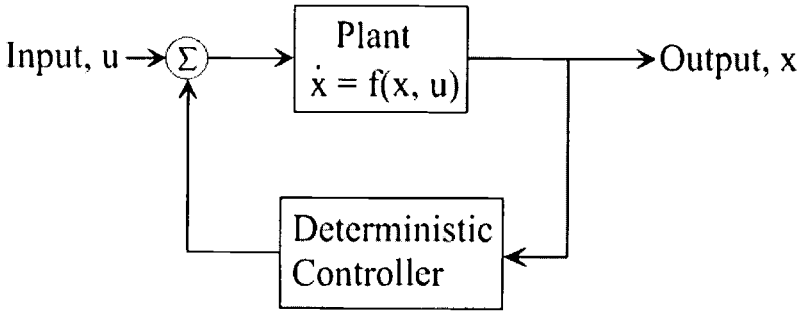

Figure 4 - State feedback diagram for control of the nonlinear system.

becomes an exercise in transforming the multi-input case into the canonical single input case. Using the spectral assignability technique identified for the canonical single input case, a feedback matrix is constructed and the feedback matrix for the multi-input case is found by taking the appropriate inverse transformations.

The controllable canonical form is a convenient means of representing the linear dynamical system in question. The controllable canonical form is the system defined by the state model

$$\dot{x} = (\hat{A} - \hat{b}K^T)x \tag{5}$$

where the matrices $\hat{A}$ and $\hat{b}$ are given by the special forms

$$\hat{A} = \begin{bmatrix} 0 & 1 & 0 & \cdots & 0 & 0 \\ 0 & 0 & 1 & \cdots & 0 & 0 \\ \vdots & \vdots & \vdots & & \vdots & \vdots \\ 0 & 0 & 0 & \cdots & 0 & 1 \\ -\hat{a}_n & -\hat{a}_{n-1} & -\hat{a}_{n-2} & \cdots & -\hat{a}_2 & -\hat{a}_1 \end{bmatrix} \quad \hat{b} = \begin{bmatrix} 0 \\ 0 \\ \vdots \\ 0 \\ 1 \end{bmatrix} \tag{6}$$

Then, by expanding the determinant of $\hat{A}$-λI about the bottom row, we see that the characteristic polynomial $\pi_{\hat{A}}(\lambda) = \det\{\hat{A} - \lambda I\}$ is

$$\pi_{\hat{A}}(\lambda) = (\lambda - \lambda_1)(\lambda - \lambda_1)\cdots(\lambda - \lambda_1) = \hat{a}_n + \hat{a}_{n-1}\lambda + \hat{a}_{n-2}\lambda^2 + \cdots + \hat{a}_1\lambda^{n-1} + \lambda^n \tag{7}$$

Now, consider the dynamical system (linearized within the ε ball) represented by the state-space system

$$\dot{x} = Ax + by \tag{8a}$$

where x is the response of the system, y is the external forcing, A is a linear map and b is the input vector. Assume, furthermore, that the pair (A, b) is in controllable canonical form, Eq.(6). Suppose that the external forcing can be written as $y = y_c + y_e$ where y_c describes a control input and y_e is the usual external excitation. Next, consider a feedback law of the form $y_c = -K^T x$, then Eq.(8a) can be rewritten as

$$\dot{x} = (A - bK^T)x + by_e \tag{8b}$$

Now, the homogeneous portion of Eq.(8b) determines the linear systems natural behavior hence, if the external excitation is ignored and the subscript from y_c is dropped, then a feedback of the form $y = -K^T x$ can be considered and Eq.(8b) takes the form

$$\dot{x} = \hat{A}x + \hat{b}y \tag{9}$$

The goal is to find a gain vector K^T such that the eigenvalues of the matrix $(A - bK^T)$ are asymptotically stable (i.e. $|\lambda_i| < 1$ for i=1...n). This ensures that the fixed points of the associated linearized system are stable. The eigenvalues of the matrix $(A-bK^T)$ are called the regulator poles while the problem of placing these poles in an appropriate spot on the complex plane is called the pole placement problem (Franklin *et al* 1991). The solution to this problem lies in the fact that one is free to choose K^T in an advantageous way, as long as the eigenvalues have the appropriate characteristics. Notice that the state feedback matrix is

$$\hat{A} = A - bK^T = \begin{bmatrix} 0 & 1 & 0 & \cdots & 0 & 0 \\ 0 & 0 & 1 & \cdots & 0 & 0 \\ \vdots & \vdots & \vdots & & \vdots & \vdots \\ 0 & 0 & 0 & \cdots & 0 & 1 \\ (-\hat{a}_n - k_n) & & & \cdots & & (-\hat{a}_1 - k_1) \end{bmatrix} \tag{10}$$

which has characteristic polynomial

$$\begin{aligned} &\pi_{(A-bK^T)}(\lambda) = \\ &(\hat{a}_n + k_n) + (\hat{a}_{n-1} + k_{n-1})\lambda + \cdots + (\hat{a}_1 + k_1)\lambda^{n-1} + \lambda^n \\ &= (\lambda - \lambda_1)(\lambda - \lambda_2)\cdots(\lambda - \lambda_n) \\ &= \hat{\alpha}_n + \hat{\alpha}_{n-1}\lambda + \hat{\alpha}_{n-2}\lambda^2 + \cdots + \hat{\alpha}_1\lambda^{n-1} + \lambda^n \end{aligned} \tag{11}$$

and where the λ_i's specify the coefficients of the desired characteristic polynomial. Assigning the spectrum of the characteristic polynomial is equivalent to specifying the coefficients α_i's. This in turn solves the spectral assignability problem for the system in controllable canonical form.

Now, suppose the pair (A, b) is not in controllable canonical form. Assume that the system is still a single input system ($b = \hat{b}$) and that the system is controllable, then a solution to the pole placement problem always exists (Romeiras *et al* 1992). It can be shown that (A, b) is controllable when the n x n controllability matrix, C, has full rank, for the controllability matrix defined as

$$C = \left[b \mid Ab \mid A^2 b \mid \cdots \mid A^{n-1} b \right] \tag{12}$$

and where the columns of C are made up of the column vectors b, Ab, A^2b, ... $A^{n-1}b$. The system (A, b) can be transformed into controllable canonical form by introducing the transformation matrix constructed as follows. Let v be the last row of C^{-1} (notice that C^{-1} exists by assumption). Define the state transformation matrix Y such that $z = Yx$ by

$$Y^T = \left[v \quad vA \quad vA^2 \quad \cdots \quad vA^{n-1} \right] \tag{13}$$

Then, Y^{-1} exists by construction. Applying the state transformation to the original system yields the transformed system

$$\dot{z} = YAY^{-1} + Yby \tag{14}$$

Define $\hat{A}=YAY^{-1}$ and $\hat{b} = Yb$, then the pair $(\hat{A}, \hat{b})$ has the controllable canonical form and the spectral assignability follows as before. Now, should the pair (A, b) not be completely controllable as assumed, then the part that is not completely controllable can still be assigned an arbitrary spectrum. The solution here relies on a non-singular transformation which converts the state model to the Kalman controllable canonical form. The Kalman controllable canonical form identifies and extracts the completely controllable modes of the system and then builds a state feedback controller for this part of the problem. This is mentioned here for completeness, however, for the current problem, this generalization is not required.

The control law then consists of picking the entries in the gain vector K^T so that the roots of the characteristic equation are in prescribed positions. Since the λ_i's are known, this amounts to choosing the $\hat{a}_i$'s in the characteristic polynomial $\pi_{A\text{-}bK}{}^{T}(\lambda)$. Then, applying the inverse transformation yields the desired control law for the original system. Notice that the eigenvalues for the original system and the transformed system are the same since the particular transformation matrix constructed is a similarity transformation matrix. This procedure is called

Ackerman's formula for pole placement. For the case where A is 2 x 2, it can be shown that an optimal choice (in the sense of time to control) for the gain vector is $K^T = [\lambda_u, -\lambda_u\lambda_s]$, where λ_u is the unstable eigenvalue and λ_s is the stable eigenvalue of (Nitsche and Dressler 1992).

One can now formulate an algorithm to control a chaotic system utilizing this control law on a Poincaré section. First, the linear map, A, of an unstable cycle is constructed as before and its eigenvalues identified. Then, setting $x = Z_i - Z^*$ and $x = Z_{i+1} - Z^*$ in Eq.(9) yields the control law for the discrete UPOs on the Poincaré section as

$$Z_{i+1} = (A - bK^T)(Z_i - Z^*) + Z^* \tag{15}$$

Then, calculating the eigenvalues of A, λ_u and λ_s, choosing $K^T = [\lambda_u, -\lambda_u\lambda_s]$ or some other equally acceptable poles for control of the nonlinear system values, and then applying Eq.(15) whenever the trajectory comes within ε of Z^* on the Poincaré section yields the desired stability characteristics.

Finally, it is necessary to determine the relative distance on the Poincaré section a trajectory can deviate from Z^* and still be able to guarantee that the controller will perform adequately. The answer to this lies in the fact that since it was required that $|Z^* - Z_{i+1}| < \eta$ by construction then, combining this with Eq.(15) yields

$$| Z_i - Z^* | = \frac{\eta}{| A - bK^T |} \tag{16}$$

Since K^T was constructed to render the eigenvalues of the matrix $(A - bK^T)$ stable, and $(A - bK^T)^{-1}$ exists, this defines an area of width $2\eta / | A - b K^T |$ about Z^* for which the control can be successfully applied.

3.6 Application to Rocking Response

The controller presented above was applied to the rocking response of the rigid block. Several cases of the nonlinear oscillations are considered with low order oscillations of primary importance. For this system, we mainly will demonstrate the control application to the primary resonance case. However, other periodic responses can be controlled in a similar fashion as shown.

3.6.1 Primary Resonance

Since primary resonance is of importance as previously described, the first example exhibits the effectiveness of the methodology with respect to this oscillatory state. By searching the data set seen in Fig.2f for all period-1 oscillations and then calculating a first return map, A, as outlined, the method found a primary resonance case at $Z^* = [0.5977, -0.6812]$. The first return map is given by

$$A = \begin{bmatrix} 5.3467 & 1.7973 \\ -4.2966 & -0.8651 \end{bmatrix} \tag{17}$$

An interesting artifact of this problem is that the stable eigenvector is apparently strongly attracting while the unstable eigenvector is strongly repelling. The stable and unstable eigenvalues are given by λ_s=0.8536 and λ_u=3.6279. This artifact is most evident by studying the Poincaré section, Fig.2f, and by noticing the extent of the apparent linearity of the chaotic attractor in the region of Z^*. This indicates that the stable and unstable directions can be decoupled from one another, making the control matrix (A-bK^T) diagonal. For this case, the control matrix used was

$$A - bK^T = \begin{bmatrix} -0.251 & 0 \\ 0 & 0.390 \end{bmatrix} \tag{18}$$

with regulator poles read directly as $p_{1,2}$=[-0.251, 0.390].

Fig.5 plots the results of controlling the chaotic system using the control law defined by Eq.(15) for Z^* and with the control matrix given by Eq.(18) to maintain the period-1 oscillation. Fig.5a is a plot of the phase space portrait for the controlled system. A circle is placed at the point on the phase space where control is applied for reference. Fig.5b plots the Poincaré points versus time. Notice the random-like response prior to the time at which control is applied. This arbitrary

duration of chaotic response prior to control is due to the fact that the system is allowed to oscillate in a chaotic fashion until the trajectory falls within the ε-ball. Once there, the controller is applied at each crossing of the Poincaré plane, maintaining the stable oscillations seen in Fig.5. The next example investigates a different primary resonance case.

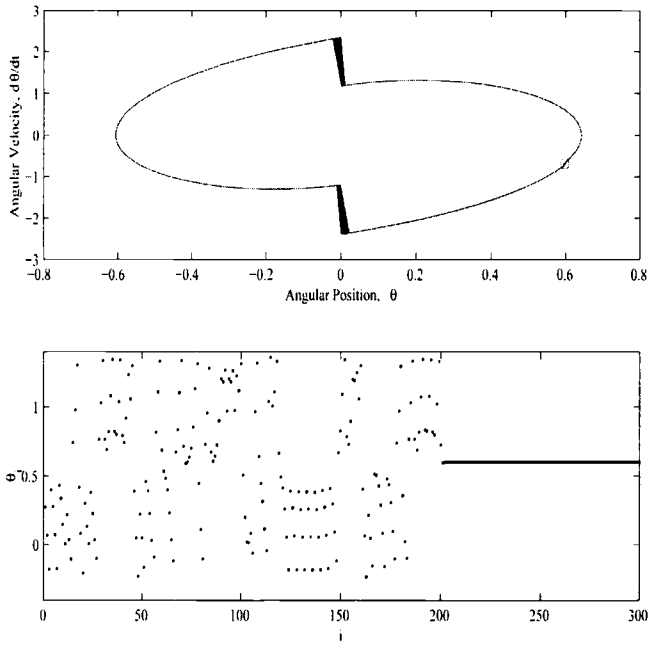

Figure 5 - Control of a primary resonance case for the rocking of the free standing equipment, a) the phase space plot and b) the Poincaré points plotted as a function of time.

3.6.2 Secondary Period-1 Oscillation

A second period-1 oscillation was found at Z^*=[0.0167, -0.645]. Again, for this case, the controller can be decoupled due to the apparent strong attraction of the stable eigenvalue. The control matrix used for this example was

$$A - bK^T = \begin{bmatrix} 0.60 & 0 \\ 0 & 1.00 \end{bmatrix} \tag{19}$$

Fig.6 plots the results of this simulation. The control action allows the block to oscillate about both centers, however, for the positive angular momentum, the oscillation amplitude is small while for the negative angular momentum the amplitude is large.

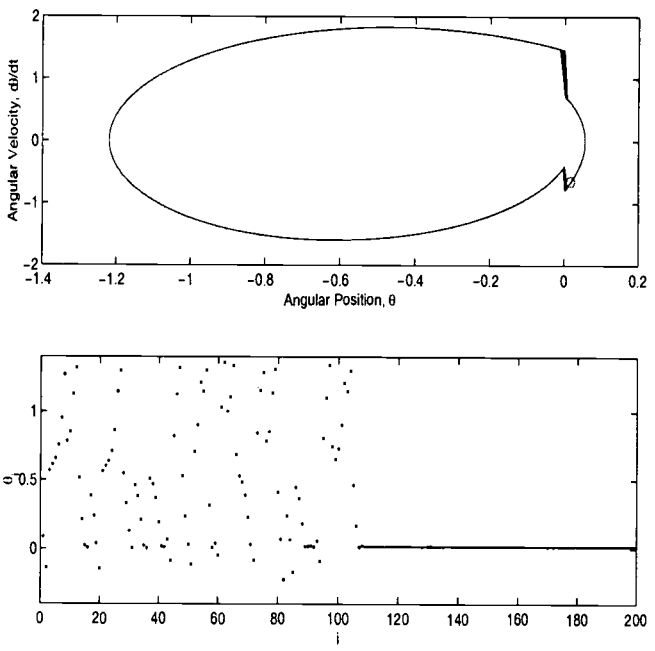

Figure 6 - Control of a secondary period-1 oscillation for the a) phase space portrait and b) the Poincaré points plotted as a function of time.

3.6.3 Period-9 Oscillation

A period-9 oscillation was found at Z^*=[0.0457, 0.0550]. Again, by the nature of the position of this point on the chaotic attractor, the control law can be defined to be diagonal, hence the two states can be decoupled as before. The control matrix used for this example is

$$A - bK^T = \begin{bmatrix} 1.00 & 0 \\ 0 & 0.25 \end{bmatrix} \tag{20}$$

Fig.7 plots the results of this simulation. As before, the system is allowed to oscillate until the trajectory enters the control region. Then, the controller is turned on and the system is locked into the desired oscillatory mode.

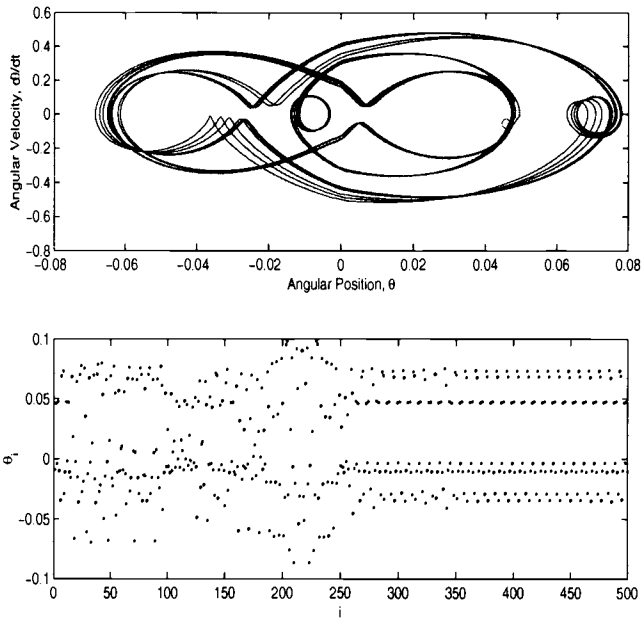

Figure 7 - Control of a period-9 oscillation for a) the phase space portrait and b) the Poincaré points plotted as a function of time.

3.6.4 Period-13 Oscillation

As a final example, another higher order oscillatory state is used to exhibit the effectiveness of the method to control the chaotic system to arbitrary unstable periodic orbits. Figure 8 shows the results for this case. Here, a period-13 orbit was identified at $Z^* = [0.0105, -0.193]$. In this case, however, the modes cannot be decoupled and the control matrix is given by

$$A - bK^T = \begin{bmatrix} -0.45679 & -0.01421 \\ 0.36295 & 0.90379 \end{bmatrix} \tag{21}$$

Fig.8a is the phase space portrait while Fig.8b the Poincaré points corresponding to the controlled motions. The last two examples show that, higher order trajectories can be maintained with relatively little extra work.

3.7 Relative Energy to Maintain Control

As is evident from Figure 9, the distance that the controller is required to move a trajectory on the control plane is small in comparison with the amplitude of oscillation. Hence, the relative energy exerted in order to maintain control with this methodology is small in comparison to the excitation moment. Recall that on a given control plane, the controller is only required to be operational when a trajectory intersects a Poincaré plane and only within the ball of radius ε. The maximum distance that a trajectory can be moved on that ball is given by ε/2, where ε is the chosen error tolerance for the given problem (for all

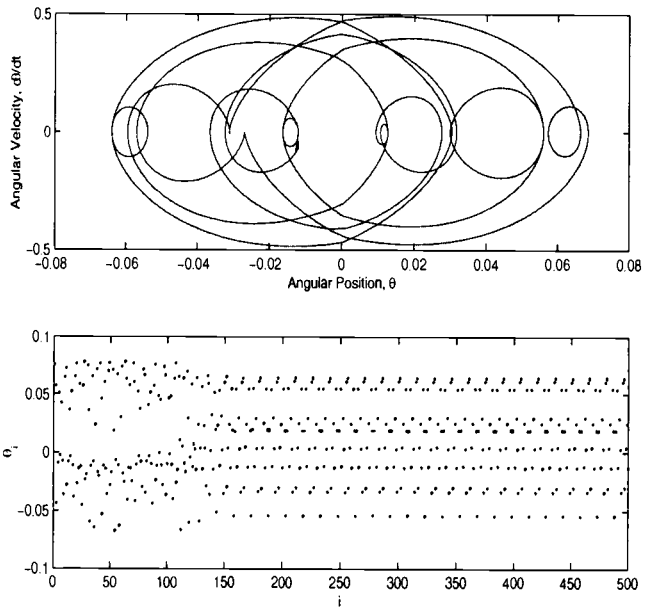

Figure 8 - Control of a period-13 oscillation showing a) the phase space portrait and b) the Poincaré points as a function of time.

examples above, it was chosen as ε=0.05). Meanwhile, the interval of time for which control can be instigated is determined by the sampling period of the system (here T_s=0.01), the control action must be complete within this interval.

The moment required to maintain this control can be calculated as follows: Recall that the feedback control rule has the form $y = -K^T x$ where x is the distance between a trajectory on the Poincaré plane and the UPO, $x = Z_i - Z^*$. Then,

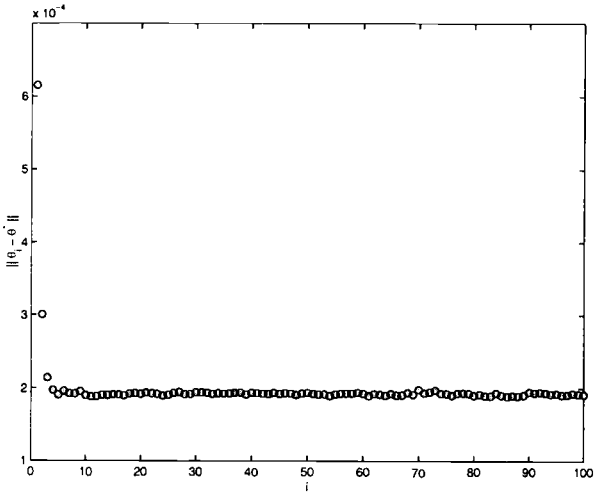

Figure 9 - Controller action on the Rocking Block System indicating the distance a trajectory must be moved in order to maintain control.

$$\begin{aligned} | y_{\max} | &= \max\{| -K^T (Z_i - Z^*) |\} \\ &\le \max\{| K^T | \varepsilon\} \\ &= \varepsilon\sqrt{(k_1^2 + k_2^2)} \end{aligned} \tag{22}$$

So, the corresponding mean force is obtained by integrating this over a period, where the integral is given as

$$< F >= \int_0^T \frac{| u_{\max} |}{H} \delta(\tau - t) dt \qquad (23)$$

where $\delta(\tau)$ is the Dirac delta function with unit area and H is the height of the rigid object. If these equations are applied to the system for the primary resonance case, the ratio of the mean force, $<F>$, required to maintain the necessary stable motions to the force applied by the external forcing is $<F>/<Ma_{gx}> = 2.13 \times 10^{-4}$. This indicates that the force necessary to achieve and maintain control of the systems unstable oscillations, even in the event of noise, is small in comparison to the force exerted by the external excitation.

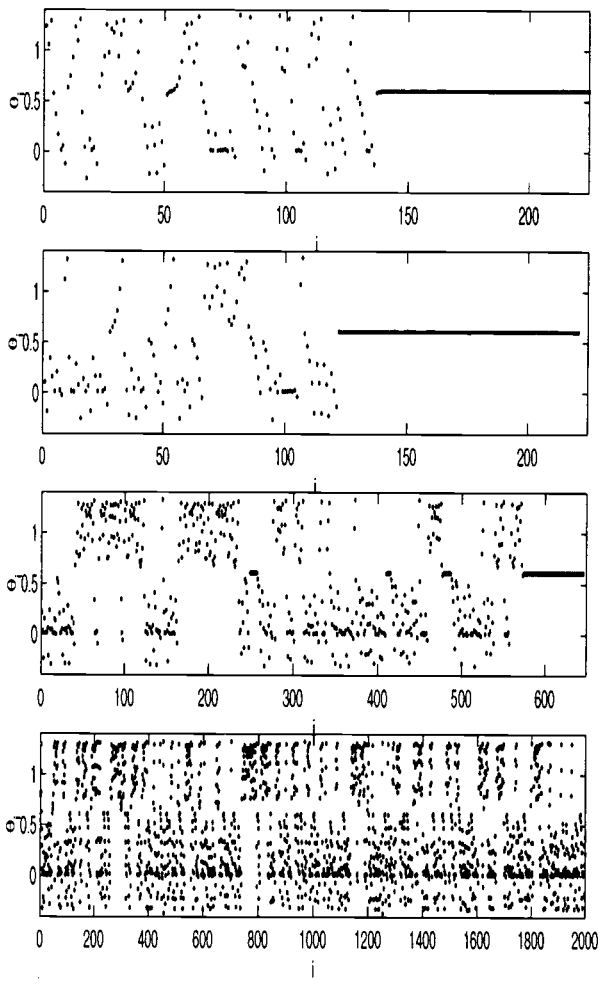

Figure 10 - Effects of band limited white noise to the control system for period-1 control as seen in the Poincaré points. Here, the signal to noise ratio is decreased from a) SNR=27.75, b) SNR=6.93, c) SNR=5.54 and d) SNR=4.29 where the controller is

3.8 Control Under Noisy Excitation

The benefit of using small perturbations to control a deterministic nonlinear dynamical system within the chaotic operating regime has been presented above. However, for a typical real physical system such as the rocking of a rigid block, there will be noise added to the system through a random component to the excitation as well as measurement errors. Additive noise has the effect of destabilizing the chaotic attractor.

Figure 10 plots the effects of noise on the controller for one of the primary resonance cases presented. Notice that for small amounts of noise, the controller appears to behave normally. However, as the noise intensity is increased, the controller looses the ability to maintain achieve control, and even then there may be periods where control is achieved in between periods where control can not be maintained. Finally, with even slight amounts of noise, the system completely looses the ability to track an unstable periodic orbit and all control is lost. This happens in this case, even though the system has not yet toppled. Part II of this study will address means of increasing the controllability under increasing noise intensities.

3.9 Concluding Remarks

This paper outlines a method of controlling the potentially catastrophic, unstable, highly nonlinear oscillations of free-standing equipment or structures placed in offshore and seismic environments. The proposed method is designed to avoid such dangerous situations and is developed through a modification of the OGY method in which a system parameter must be available for adjustment in order to change the dynamics of the system. Here, a physical device is placed on the system which applies a moment to the nonlinear system in order to perturb the system trajectory towards a stable eigenvector of the linearized first return map. In effect, this modification adjusts an observable of the system, the angular position or angular velocity, in order to maintain control.

The method utilizes the unstable characteristics of the chaotic attractor to an advantage. By observing the fact that there exists a multitude of unstable, periodic orbits, one can utilize the locally linear dynamics to build a feedback control law capable of rendering the nonlinear oscillations periodic. An outline of the methodology is presented with several examples pertaining to the rigid rocking block system. These examples clearly demonstrated the successful control of the highly nonlinear complex responses and the robustness of the methodology, reducing the complex motions to selected desirable periodic motions through the

use of a simple standard control technique (pole placement). The force required to maintain control is also investigated. It is found that through the discrete application of the controller, the ratio of the force applied by the controller to the force of the external excitation is small.

In a real ocean or seismic environment, noise will exist in the system, whether through a random component of the excitation or through measurement error. It is expected that this may cause problems with the controller. Methods of decreasing the effects of the noise are available. These methods include filtering and stochastic projection, both of which try to reconstruct the deterministic nonlinear dynamics from the noisy data. However, in the case that the noise level is relatively small compared to the forcing amplitude, it is expected that the proposed control methodology will be sufficiently robust against these disturbances. In Part II, a simple modification to the controller is developed in order to increase the effectiveness of the control in the presence of a decreasing signal to noise ratio (increasing noise intensity). It is shown that this modification is acceptable for low noise intensities. In order to increase the controllability, stochastic filtering techniques are investigated in Part II as well.

Finally, although the proposed methodology utilizes linear control theory, highly complex, nonlinear oscillations can be controlled in these systems. This is true because the method utilizes the systems sensitivity and topological transitivity to an advantage. Because a chaotic attractor has a multitude of unstable, periodic

cycles, any particular cycle can be used for control. Since the controller applies small perturbations to the system trajectory, on the scale of several orders of magnitude less then the forcing amplitude, little energy is required in the implementation. More advance control techniques, such as optimal control, etc., can be applied to achieve gains in cost or energy saving. Moreover, the methodology is equally applicable to many offshore and land-based structural systems where there is a potential for highly nonlinear and possibly chaotic responses.

3.10 Acknowledgment

The authors wish to acknowledge the financial support of the United States Office of Naval Research (Grant No. N0001-92-J-1221 and N00014-04-10008) and the U.S. Department of Energy.

3.11 References

Abarbanel, H. D. I., Korzinov, L., Mees, A. I., and Starobinets, I. M. (1997). "Optimal control of nonlinear systems to given orbits." *Systems & Control Letters*, **31**, 263-76.

Auerbach, D., Cvitanovic, P., Eckmann, J.-P.,Gunaratne, G., and Procaccia, I. (1987). "Exploring chaotic motion through periodic orbits." *Phys. Rev. Lett.*, **58**(23), 2387-2389.

Bergé, P., Pomeau, Y., and Vidal, C. (1984). *Order within chaos, towards a deterministic approach to turbulence*, John Wiley & Sons, New York.

DeCarlo, R., A. (1989). *Linear systems, a state variable approach with numerical implementation,* Prentice Hall, New Jersey.

Devaney, R. (1987). *An introduction to chaotic dynamical systems*, Addison-Wesley, New York.

Fowler, T. B. (1988). "Stochastic control techniques applied to chaotic nonlinear systems." *Proc. 1988 International Symposium on Circuits and Systems*, Vol. 1, Helsinki Univ. Tech., Espoo, Finland, June 7-9, 5-9

Franklin, G. F., Powell, J. D., and Emami-Naeimi, A. (1991). *Feedback control of dynamic systems,* 2nd ed., Addison-Weseley, New York.

Gottlieb, O., and Yim, S. C. S. (1990). "Onset of chaos in a multi-point mooring system." *Proc. First (1990) European Offshore Mechanics Symposium*, Trondheim, Norway, Aug. 20-22, 6-12.

Hammad, A., Jonckheere, E., Cheng, C.-Y., Bhajekar, S., and Chien, C.-C. (1996). "Stabilization of chaotic dynamics: A modern control approach." *Int. J. Control*, **64**(4), 663-677.

Hogan, S. J. (1990). "The many steady state responses of a rigid block under harmonic forcing." *Earthquake Engrg. and Struct. Dynam.*, **19**, 1057-1071.

Iyengar, R. N. and Roy, D. (1996). "Nonlinear Dynamics of a Rigid Block on a Rigid Base," *ASME J. Appl. Mech.*, Vol. 63, 55-61.

Jeong, M.Y., Suzuki, K. and Yim, S.C.S. (2003). "Chaotic Rocking Behavior of Freestanding Objects with Sliding Motion," *Int. J. Sound and Vibration*, **262**(5), 1091-1112.

Lathrop, D. P. and Kostelich, E. J. (1989). "Characterization of an experimental strange attractor by periodic orbits." *Phys. Rev. A*, **40**(7), 4028-4031.

Lenci, S. and Rega, G. (2005). "A dynamical systems approach to the overturning of rocking blocks," *Chaos, Sol. & Fract.*, in press.

Lin, H. and Yim, S. C. S. (1996a). "Nonlinear rocking motions. I: Chaos under noisy periodic excitations." *J. Engrg Mech.*, ASME, **122**(8), 719-727.

Lin, H. and Yim, S. C. S. (1996b). "Nonlinear rocking motions. II: Overturning under random excitations." *J. Engrg Mech.*, ASME, **122**(8), 728-735.

Grebogi, C., Ott, E., and Yorke, J. A. (1988). "Unstable periodic orbits and the dimensions of multi-fractal chaotic attractors." *Phys. Rev. A*, **37**(5), 1711-1124.

Nitsche, G., and Dressler, U. (1992). "Controlling chaotic dynamical systems using time delay coordinates." *Physica D*, **58**, 153-164.

Ott, E., Grebogi, C., and Yorke, J. A. (1990). "Controlling chaos." *Phys. Rev. Lett.*, **64**(11), 1196-1199.

Pompei, A., Scalia, A., and Sumbatyan, M. A. (1998). "Dynamics of rigid block due to horizontal ground motion." *J. Engrg Mech.*, ASCE **124**(7), 713-717.

Romeiras, F., J., Grebogi, C., Ott, E., and Dayawansa, W., P. (1992). "Controlling chaotic dynamical systems." *Physica D*, **58**, 165-192.

Thompson, J. M. T. (1983). "Complex dynamics of compliant off-shore structures." *Proc. R. Soc. Lond. A*, **387**, 407-427.

Thompson, J. M. T., Bokaian, A. R., and Ghaffari, R. (1984). "Subharmonic and chaotic motions of compliant offshore structures and articulated mooring towers." *ASME J. Energy Resources Tech.*, **106**, 191-198.

Yim, C. S., Chopra, A. K., and Penzien, J. (1980). "Rocking response of rigid blocks subject to earthquakes", *Earthquake Eng. and Structural Dynam.*, **8**(6), 565-587.

Yim, S. C. S. and Lin, H. (1991a). "Nonlinear impact and chaotic response of slender rocking objects." *J. Engrg Mech.*, **117**(9), 2079-2100.

Yim, S. C. S. and Lin, H. (1991b). "Chaotic behavior and stability of free-standing offshore equipment." *Ocean Engrg.*, **18**(3), 225-250.

Stochastic Control of Sensitive Nonlinear Motions of an Ocean Mooring System

Paul E. King

Solomon C. Yim

submitted to

Offshore Mechanics and Arctic Engineering

ASME Publication

Manuscript Number OMAE-05-1071

4.1 Abstract

Complex sensitive motions have been observed in ocean mooring systems consisting of nonlinear mooring geometries. These physical systems can be modeled as a system of first order nonlinear ordinary differential equations, taking into account geometric nonlinearities in the restoring force, quadratic viscous drag and harmonic excitation. This study examines the controllability of these systems utilizing an embedded approach to noise filtering and online controllers. The system is controlled using small perturbations about a selected unstable cycle and control is instigated for periodic cycles of varying periodicities. The controller, when applied to the system with additive random noise in the excitation has marginal success. However, the addition of an Iterated Kalman Filter applied to the system increases the regime under which the controller behaves under the influence of noise. Because the Kalman Filter is applied about locally linear trajectories, the feedback of the nonlinearities through the filter has little effect on the overall filtering system.

4.2 Introduction

Sensitive nonlinear responses, including chaotic motions, have been predicted in a mass moored in a fluid medium subject to wave excitations and which is characterized by a large geometric nonlinearity in the restoring force and viscous drag excitation. These systems include sonars, remote sensors and data collection devices deployed in the ocean environment and which are of interest to the U. S. Navy and the U. S. Department of Energy. This class of fluid-structure interaction problems contain highly nonlinear drag and mooring effects. The overall effects of the nonlinear fluid loads on the structure can be approximated in terms of an added inertia and a nonlinear coupling of the Morison form.[1,2] The nonlinear mooring resistance force can be approximated by a low order polynomial and hence the resulting mathematical models of these systems are reducible to a low degree system of ordinary differential equations. This order of

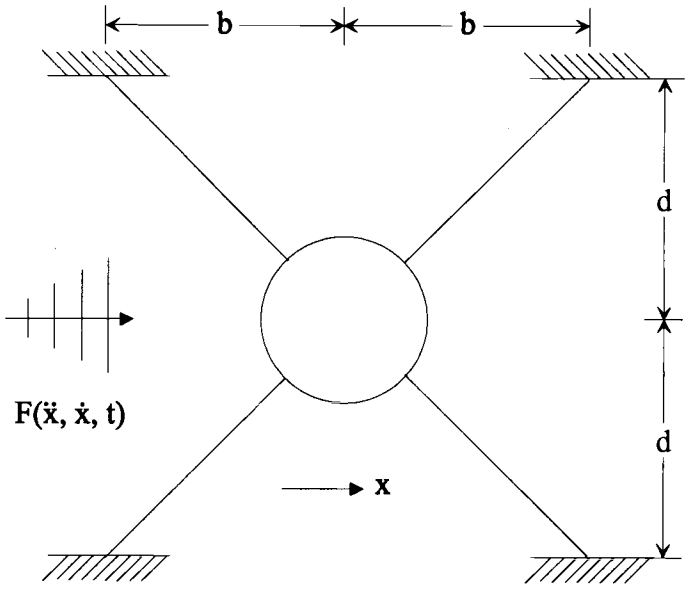

Figure 1 - Schematic of a moored structure subject to current and wave excitation

approximation is often acceptable for preliminary analysis and design of the types of fluid-structure systems considered.

Preliminary analysis of experimental data from such a system as modeled here has demonstrated the likely presence of sensitive and chaotic motions in noisy environments.[3] These sensitive motions are not considered in the fluid-structure system design. Should the unpredictability of the sensitive behavior observed in these systems be deemed undesirable, methods of analyzing the system response to harmonic and noisy excitations and subsequent control of the systems are needed. By representing the desirable states of motion of the nonlinear response of the system with unstable periodic orbits (UPO's), a consistent means of characterizing the strange attractors can be obtained.[4] Thus, the system can be characterized by such topological invariants as the entropy or the Lyapunov spectrum.[5] The analysis and control procedure presented in this study utilizes this representation of the sensitive response to its advantage.

Figure 1 is a schematic of a system moored by cables in a fluid medium. The fluid itself is undergoing motion and an associated excitation force is induced which can be described by a forcing function of the form $F(\dot{x},\ddot{x},t)$, where $\dot{x} = dx/dt$ and $\ddot{x} = d\dot{x}/dt$. With restraints for vertical and rotational motion, this system is modeled as a single-degree-of-freedom (SDOF) system for the surge, x.[1] The nonlinear, second order,

ordinary differential equation of motion is derived by using the fact that the system is hydrodynamically damped with external forcing. The forcing excitation is modeled as the sum of a constant current and an oscillatory wave term. Because the cables are thin and the dimension of the mass is small compared to the orbital motions of the wave particles, the fluid-structure interaction can be modeled accurately by use of the small-body theory which assumes that the presence of the structure does not influence the wave field. This implies that the waves flowing past the structure are not affected by the interaction with the structure.

The mooring angle produces a geometric nonlinearity in the restoring force that can become highly nonlinear for $b = 0$, a two-point system, or nearly linear for $b \gg d$ for the four-point system. The equations of motion are taken from the prototypical form for second order nonlinear differentials:

$$m\,\ddot{X} + c\,\dot{X} + R(X) = F(\dot{X},\ddot{X},t) \qquad (1)$$

where the nonlinearities are contained in the restoring force $R(X)$ and the excitation force $F(\dot{X},\ddot{X},t)$. The restoring force describes the geometric configuration of the mooring lines and assumes linear elastic behavior so that the nonlinearity is strictly due to the geometric configuration of the system. The restoring force has the form

$$R(X) = k\,(X + b\,sgn(X)) * \left[1 - \sqrt{\frac{d^2 + b^2}{d^2 + (X + b\,sgn\,(X))^2}}\right] \tag{2}$$

and where sgn(X) is the signum function defined by

$$\text{sgn}\,(X) = \begin{cases} +1 \text{ for } X > 0 \\ 0 \text{ for } X = 0 \\ -1 \text{ for } X < 0 \end{cases} \tag{3}$$

The excitation force is a combination of viscous drag and inertial components based upon the interactions between the moored structure and the fluid medium. This type of excitation force is found to be modeled by

$$F(\dot{X},\ddot{X},t) = \lambda(u - \dot{X})\,|u - \dot{X}| + \mu(\dot{u} - \ddot{X}) + \rho\bar{V}\dot{u} \tag{4}$$

which couples the fluid motion and the structure motion through the inertial interaction between the two constituents in motion, the moored structure and the fluid medium. The system parameters are identified as the system mass m, damping c, and line stiffness $k = 2EA/\sqrt{(d^2+b^2)}$ and where EA is the elastic cable force. The line lengths b and d are observed in Figure 1 while λ and μ are the hydrodynamic viscous drag and added mass, ρ is the fluid density and $\bar{V}$ is the displaced volume of fluid. $u = u(t)$ is the fluid particle velocity under current and wave excitation and is given by $u(t) = u_0 + u_1 \sin(\omega t)$ and $u_1 = u_1(a,\omega)$, where a and ω are the wave amplitude and frequency

respectively.

Assuming that the structure does not alter the fluid flow, that is, that the wave field does not change due to the motions of the moored structure, employing the small body theory, and then employing an equivalent linearization process on the quadratic drag force and finally normalizing, then, an autonomous set of first order nonlinear differential equations are obtained which are given by:

$$\begin{aligned} \dot{x} &= y \\ \dot{y} &= -R(x) - \gamma\, y + F(x,y,\theta) \\ \dot{\theta} &= \omega \end{aligned} \tag{5}$$

where x = X/d.

Under the equivalent linearization, the nonlinearity is seen to be strictly due to the geometric configuration of the system which is manifested in the restoring force. Hence, the restoring force describes the geometric configuration of the mooring lines, assuming linear elastic behavior of the mooring lines. The restoring force has the form

$$R(x) = \psi\,(x + \beta\, sgn(x)) * \left[\frac{1}{\sqrt{1 + \beta^2}} - \frac{1}{\sqrt{1 + (x + \beta\, sgn(x))^2}}\right] \tag{6}$$

Although the excitation force is a combination of viscous drag and inertial components based upon the interactions between the moored structure and the fluid medium, through the normalization process, the excitation force is found to have the form:

$$F(x,y,\theta) = f_0 - f_1 \sin(\theta) \tag{7}$$

where the viscous drag and inertial components are combined into the current and amplitude parameters. The appropriate dimensionless constants are defined by

$$\psi = \frac{k}{m + \mu} \; ; \; \beta = \frac{b}{d} \; ; \; \gamma = \frac{c + \lambda}{m + \mu} \tag{8}$$

The constants f_0 and f_1 depend upon the hydrodynamic characteristics of the system and are given by

$$f_0 = \frac{\lambda u_0}{m + \mu} \; ; \; f_1 = \frac{\rho \bar{V} u_1}{m + \mu} \sqrt{\omega^2 (1 + C_a)^2 \frac{1}{4} C_{dl}^2 (\frac{\bar{V}}{S})^2} \tag{9}$$

where C_a and C_{dl} are the inertial drag coefficient and the linearized drag coefficients, S is the projected drag area, and ρ is the water mass density. The associated wave frequency is obtained through the relation $\theta = \omega t$ where t is time.

Although at first glance this system appears to be significantly more complex than the simple nonlinear systems presented in standard texts it turns out that the fluid-structure system possesses nonlinear response properties very similar to those found in classic nonlinear systems such as the Duffing system.[6]

4.3 Mooring System Response

As has been mentioned, a complete analysis of this system appears in the literature[1-2,7-8] and hence only some of the important results for the purposes of this paper are repeated. This system includes at least three types of dynamic response based upon wave and current excitation, these being periodic, quasi-periodic and chaotic responses. A fourth state exists, when no motion is observed. This implies that the wave and current excitations are not of a significant magnitude to transfer enough energy to the mooring system in order to instigate motion. The no-motion state is uninteresting and won't be studied further. In fact, for this discussion, only the chaotic response of the system is of importance and therefore the other states will not be included.

Highly nonlinear (chaotic) oscillations are those deterministic oscillations which are characterized by a random-like, unpredictable response and yet includes underlying order and structure. The unpredictability stems from the sensitivity to initial conditions. That is, two nearly identical initial conditions give rise to vastly different outcomes, they become macroscopically separated after a finite amount of time.[9] However, this alone is not enough to define sensitive (chaotic) response. A sensitive system must also possess an element of regularity as well as it must be indecomposable. The regularity usually stems from the so-called unstable periodic orbits. That is, two infinitesimally close points will come arbitrarily close to one another after a predefined period of time.[4] However, because they are unstable, the

periodicity is lost under integration. The third element is the notion of indecomposability. Most easily thought of as the fact that a point within the chaotic system will enter within an arbitrarily small neighborhood of any other point at some time under the integration.[9] Putting these three conditions together, one can see that chaos posses an element of unpredictability (sensitivity to initial conditions), regularity (unstable periodic points) and the fact that it is the smallest set which contains these necessary conditions (indecomposability).[9] Notice that these chaotic attractors are stable in the sense that as $t \to \infty$, all trajectories of the system tend towards them.

Figure 2 plots one of the many possible highly nonlinear (chaotic) responses of the mooring system shown. This example is given for the system parameter values ω = 0.335, γ = 0.01, ψ = 4.0, β = 0.0, f_0 = 0.0, and f_1 = 2.0. Figures 2a -d plot the a) Poincaré section, b) phase space portrait, c) frequency spectrum and d) a typical time series, respectively, of the chaotic response. Notice that through only small changes in the system parameters, change fundamentally different response characteristics are obtained, whether it leads to afrom periodic to chaotic dynamics or from one strange attractor to another. The presence of an abundance of these complex harmonic responses predicted by associated analytical techniques and verified by numerical results indicate that their influence on extreme and fatigue designs of the fluid-structure interaction systems may need to be considered in the future.

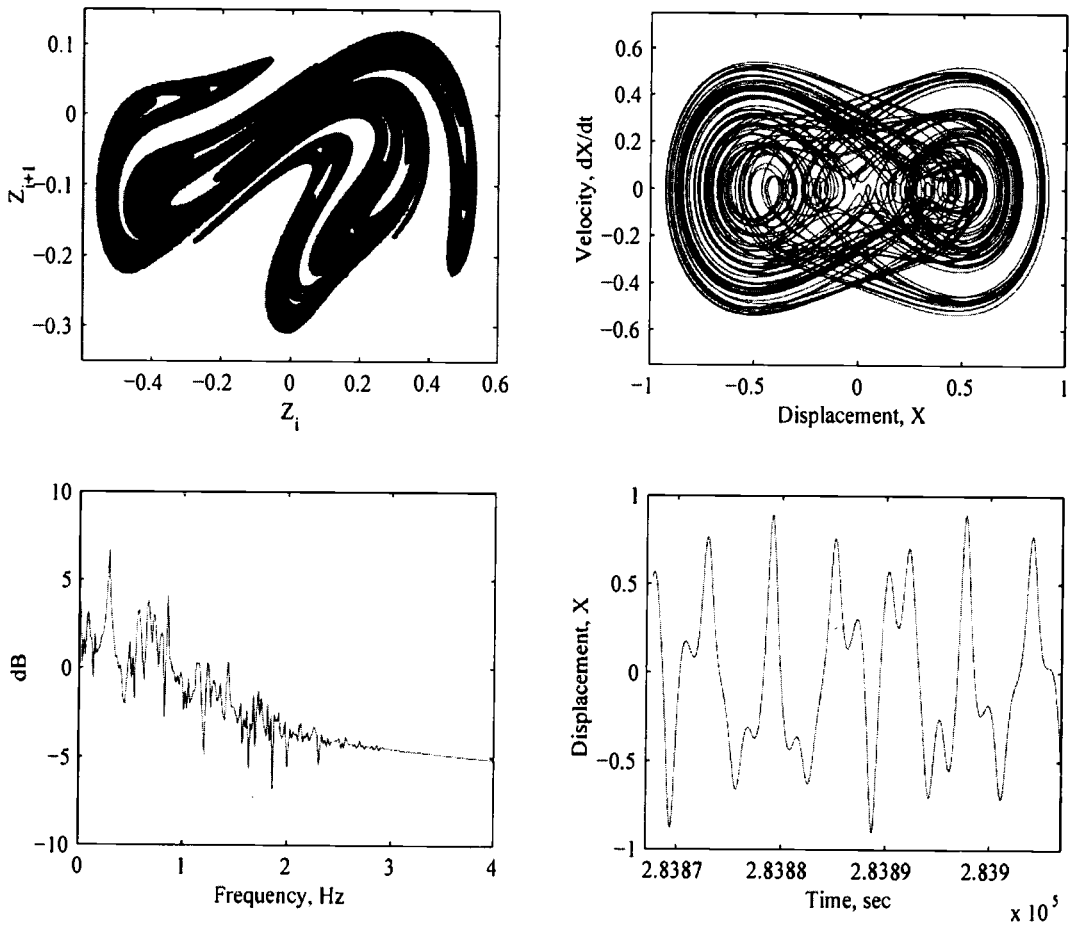

Figure 2 - Chaotic response of the mooring system showing a) the phase space portrait, b) the period 3 Poincaré section, c) the frequency spectrum and d) a time series plot.

4.4 Feedback Control of Chaotic Systems

This section introduces the notion of feedback control as applied to sensitive nonlinear systems. Control of chaos has been a topic of wide research since Ott, Grebogi and Yorke[10] introduced a method, now called OGY control, in 1990. This method utilizes periodic pulses to direct a trajectory towards the stable eigenvector of

a linearized model of the chaotic system.

Figure 3 is a schematic of a general feedback controller. The input is the system

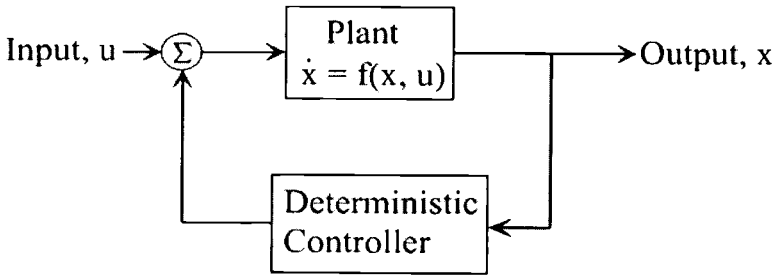

Figure 3 - Schematic of feedback control of a general plant represented as a set of differential equations

excitation, variables or parameters which define the system and set it into oscillation. The output is the result of the plant dynamics and any external adjustments that can be made. These external adjustments can be via control or through some random component. For now, we will consider only the purely deterministic case. The plant is a set of relations, usually differential equations, which relate the output to the input. The feedback box is a set of relations which tell how the system should be adjusted in order to maintain a certain operational state of the plant based upon known measurements.

The goal of the feedback control is to render the system dynamics into a known, stable operating mode. This can be accomplished by any of a number of methods and control theory is a rich field of study. Here, the pole placement algorithm is considered in order to place the unstable eigenvalues (poles) of the uncontrolled system within the unit circle on the complex plane, ensuring that the eigenvalues of the controlled system are stable and hence the dynamics are well behaved. This technique was devised for linear systems, however. But, because of the nature of the sensitive

systems considered, there are instances under which this methodology is useful. Recall that there is a set of unstable periodic orbits embedded within any given strange attractor. These unstable periodic orbits can, in fact, be modeled by a linear set of equations and hence the linear pole placement method is applicable under these conditions.

In order to describe the nonlinear dynamics by a linear set of equations, a useful tool called Poincaré Sections must be introduced. Poincaré Sections are obtained by stroboscopically sampling the time series at regular intervals and then plotting one point against the previous. This has the effect of decreasing the dimension of the problem by one dimension. Moreover, it has the effect of rendering the continuous time dynamical system into a discrete time one, a feature that becomes useful for the application of control. Yet, all of the nonlinear dynamics are maintained in the reduced system. From this, the unstable periodic orbits of all orders can be identified. A linear map of a given unstable periodic orbit is constructed and this map used as the basis for the control algorithm. Because the map is unstable, it will have at least one eigenvalue greater than unity.

Once a suitable set of linear equations have been obtained, the Pole Placement technique can then be employed in order to render the unstable system stable.[11] Equation10 is the feedback control law on a Poincaré Section where Z^* is the centroid of the points under consideration on the Poincaré Section, A is the linear map created about Z^* and K^T is the feedback law obtained through Pole Placement:

$$Z_{i+1}=(A - bK^T)(Z_i - Z^*) + Z^* \quad (10)$$

4.5 Applications of Feedback Control

The algorithm to control the chaotic dynamics of the systems is to first obtain enough Poincaré points to be able to characterize an unstable periodic orbit, typically a minimum of 20 points. Once the unstable orbit is identified, a linear map is obtained by a least-squares minimization of the matrix equation involving the points near the UPO and their iterates. Given this map, a feedback law is postulated that places the control poles in a stable operating regime. Finally, the system is allowed to oscillate until the trajectory enters within η of the UPO. At this time, control is applied to produce the desired periodic orbit.

This algorithm is successful in maintaining stable, harmonic oscillations of the mooring system under deterministic situations. The next section presents the results of the application of this control algorithm to the mooring system for primary resonance aswell as a number of sub-harmonic resonance cases. The following section calculates a bound on the amount of energy required to achieve and maintain this control.

In the physical environment, there will be noise added to the system. Whether this noise is a random component to the excitation or strictly through measurement error, the state of the system may not be well characterized. The addition of noise is expected

to present problems for the deterministic controller. The problems associated with additive noise in the mooring system are then outlined. These problems are addressed and a means to increase the controllability under the influence of a random component in the excitation is presented. Finally, the effects of the noise on the mooring system and the application of the new control methodology is presented. Estimates on the magnitude of noise under which the deterministic OGY controller is still able to function appropriately are given as well.

4.6 The Deterministic Mooring System

In this section, the controller outlined above is applied to the mooring system. Several cases are presented to indicate the wide variety of oscillatory states that are obtainable with this method. In each case, consider the chaotic oscillations of Equations (5) - (7) for the parameter values given as before (ω=0.335, γ=0.01, ψ=4.0, β=0.0, f_0=0.0, and f_1=2.0). In order to investigate the structure of the chaotic attractor, the Poincaré section (Figure 2b), the probability density of the attractor is computed to identify regions of high probability that an unstable periodic orbit (UPO) will be found. The probability density gives a starting point for the search for UPOs and also yields a measure of the stability of the chaotic attractor under the influence of noise.[11]

4.6.1 Primary Resonance Control

A search was done on the Poincaré data to obtain all points that were near a period-1 orbit. This is done by comparing all points Z_i that are close and whose next iterate Z_{i+1} are also close (where the Z_i's are taken by stroboscopically sampling the position, x). Then, a UPO of period-1 is estimated as the mean of the set of points found to correspond to this set. Utilizing this method on the system structural response data, a UPO of period-1 was found at the values $Z^* = [x, \dot{x}]^T$ where x = -0.2623 and $\dot{x}$ = -0.0677. A linear map is constructed which maps the points near the UPO Z^* toward Z^* along the direction of the stable eigenvector. In this case the linear map is given by

$$A = \begin{bmatrix} 1.4746 & -0.3997 \\ 1.4692 & -0.4450 \end{bmatrix} \tag{11}$$

which has a practically neutrally stable eigenvalue $\lambda_u = 0.9970$ and a stable eigenvalue $\lambda_s = -0.1906$. If the feedback control is applied only to the position x, this gives

$$b^T = [1 \quad 0] \tag{12}$$

Choosing the gain vector $K^T = [\lambda_u, -\lambda_u\lambda_s]$ yields the control poles at $p_{1,2} = [-0.2951, 0.1044]$. Thus, each time the system trajectory crosses the Poincaré section near Z^* the controller affects this point by applying the control law, Equation (10), ensuring that the trajectory returns near the point Z^* on the next return to the Poincaré section. The

results of this application are shown in Figure 4. Figure 4a is a plot of the Poincaré points versus time exhibiting the controlled periodic oscillation after an arbitrary duration of chaotic oscillations while Figure 4b is the corresponding oscillatory state in phase space.

The average transient length expected before being able to apply the controller is computed to be $<\tau>$ ~ 48 iterates (returns to the Poincaré map) for the case outlined.[11] Observe that, despite the complexity of the dynamics between points in time where control is applied, the method produces a desired periodic motion through small adjustments.

4.6.2 ½ Sub-Harmonic Control

Again, a search was done on the Poincaré data to obtain all points that were near a period-2 orbit. A UPO of period-2 was found at the values $Z^* = [x, \dot{x}]^T$ where $x = 0.3301$ and $\dot{x} = -0.1884$. A linear map is constructed as outlined and, in this case is given by

$$A = \begin{bmatrix} 0.8793 & 0.2766 \\ 0.4553 & -0.0729 \end{bmatrix} \tag{13}$$

which has an unstable eigenvalue $\lambda_u = 1.0927$ and a stable eigenvalue $\lambda_s = -0.0631$. If the feedback control is applied to the position as in the previous case, and choosing the gain vector $K^T = [\lambda_u, -\lambda_u\lambda_s]$ yields the regulator poles at $p_{1,2}$= [-0.0316+0.7194 i,

-0.0316-0.7194 i], which have magnitude 0.5186. Each time the system trajectory crosses the Poincaré section near Z^* the controller, Equation (10) is applied ensuring that the trajectory returns near the point Z^* on the next return to the Poincaré section. The results of this simulation are shown in Figure 4. Figure 4c is a plot of the Poincaré points versus time and Figure 4d the corresponding phase space portrait of the controlled system.

4.6.3 1/3 Sub-Harmonic Control

To further demonstrate the effectiveness of this strategy, a higher order periodicity is identified and the controller is again applied, in this case a period-3 orbit. A period-3 orbit was identified at the point $Z^* = [x, \dot{x}]^T$ for $x = -0.3609$ and $\dot{x} = 0.0359$. The linear map obtained for this case is given by

$$A = \begin{bmatrix} 0.9904 & -0.113 \\ -0.097 & -0.145 \end{bmatrix} \tag{14}$$

which has a neutrally stable and a stable eigenvalues $\lambda_u = 1.000$ and $\lambda_s = -0.1544$, respectively. The controller poles are placed at $p_{1,2} = [-0.6177, 0.2068]$ and the controller is again applied to initiate control each time the system trajectory intersects the Poincaré section near the UPO at Z^* with period 3. Figure 4e-f plots the results of the period-3 control.

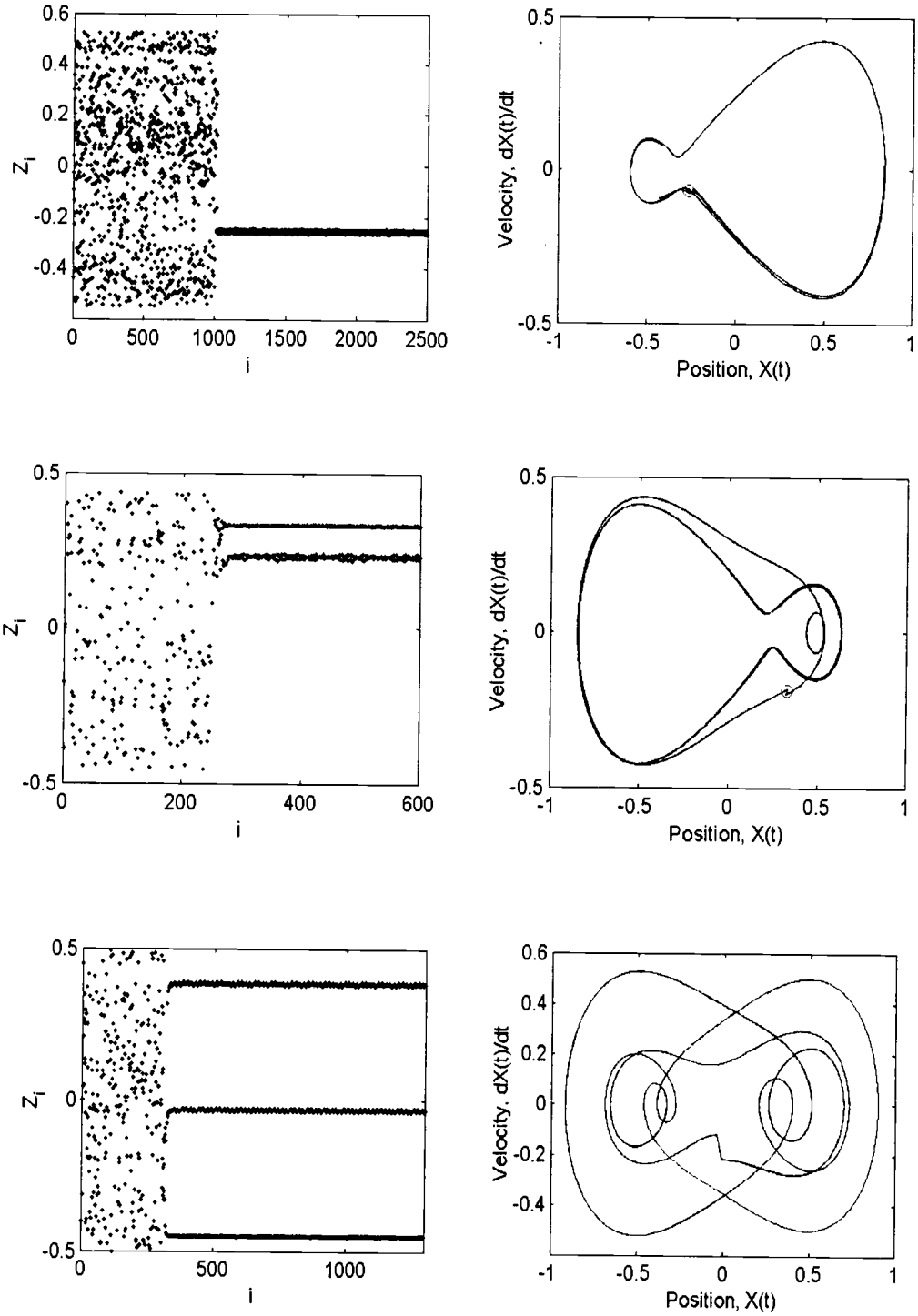

Figure 4 - Control of the ocean mooring system, a-b) primary resonance, c-d) ½ sub-harmonic and e-f) 1/3 sub-harmonic.

4.7 Relative Energy to Maintain Control

The magnitude of the instantaneous displacement a trajectory undergoes under the action of the controller is small by construction of the algorithm, as it is for the instantaneous change in the velocity as well. Therefore, the relative energy exerted in order to maintain control with this methodology is small in comparison to the excitation force. Recall that on a given control plane, the controller is only required to be operational when a trajectory intersects a Poincaré plane and only within the ball of radius η. The maximum distance that a trajectory can be moved on that ball is given by $\eta/2$, where η is the chosen error tolerance for the given problem (for all examples above, it was chosen as $\eta = 0.05$). Meanwhile, the interval of time for which control can be instigated is determined by the sampling period of the system, the control action must be completed within this interval.

The energy imparted to the system by the controller during a Poincaré "interval" in moving the trajectory towards the stable eigenvector from it's current position is obtained through an investigation of the equilibrium equations of motion during the change in position and velocity. The (work) energy imparted to the system to change the system position is given by $u\,\Delta x$, where u is the control input and Δx is the change in position. Recall that the equilibrium equations can be written as

$$\ddot{x} + \gamma\dot{x} + R(x) - F(\theta) = \delta(t-T_s)\, u(t) \tag{15}$$

where $\delta(t\text{-}T_s)$ indicates that $u(t)$ is applied only on the Poincaré plane. Then, substituting the instantaneous change Δx, into Equation (15) and rearranging and collecting terms the following term is obtained:

$$u(T_s) = \frac{\Delta\dot{x}}{\Delta t}(1 + \gamma\Delta t) + \Delta R(x) - \Delta F(\theta) \tag{16}$$

where the approximation $\Delta\ddot{x} \approx \Delta\dot{x}/\Delta t$ is used. Here, Δx, $\Delta\dot{x}$ and Δt are all known values as well as the system parameters. So, the power required to instigate a movement of Δx is obtained by

$$Pwr = \left| \frac{\Delta w}{\Delta t} \right| = \left| \frac{\Delta x\, u(T_s)}{\Delta t} \right| \tag{17}$$

Similarly, the energy imparted to adjust the momentum is given by $M\,\Delta x^2$ where $M = m + \mu$ for m the system mass and μ the added mass (the mass of the displaced volume of fluid). In this case, the normalized equations of motion indicate that $M = 1$ and we have the total power required to instigate a motion in position and velocity to obtain control on a Poincaré plane as

$$Pwr = \left| \frac{\Delta x \; u(T_s)}{\Delta t} \right| + \left| \frac{\Delta \dot{x}^2}{\Delta t} \right| \tag{18}$$

For the period-1 case, the power required to maintain instantaneous control of the system on the Poincaré plane is $Pwr_{\text{period-1}} = 0.0025$ per cycle in dimensionless units. The mean power input to the system in order to instigate the nonlinear motions in the first place is give by

$$Pwr_{sys} = \frac{1}{T}\int_0^T F(\theta) \; \frac{d\dot{x}}{dt} \; dt \tag{19}$$

and is calculated to be $Pwr_{\text{sys}} = 1.0739$ per cycle. This argument indicates that the power input required by the controller is several orders of magnitude less then the power required to drive the system, indicating that control can be achieved with little overhead to the overall design of the system.

4.8 Effects of Additive Noise

The benefit of using small perturbations to control a deterministic nonlinear dynamical system within the chaotic operating regime has been presented above. However, for a typical, real physical system such as a moored fluid-structure system, there will be noise added to the system through measurement errors as well as a random component in the excitation. Additive noise has the effect of destabilizing the

chaotic attractor.

Here, the noise energy content is characterized by the signal-to-noise ratio (SNR) defined as $\log_{10}(P_s/P_n)$ where P_s is the power of the noise free signal and P_n is the power of the noise and where the power is defined by

$$P = \frac{1}{T}\int_0^T x(t)^2\, dt \tag{20}$$

A simple modification to the control scheme can dramatically increase the controllability of the system. A series of Poincaré sections about the chaotic attractor can be constructed by stroboscopically sampling every $2\pi/r\Gamma$, where r is the number of sections desired. This yields r separate controllers evenly distributed throughout the cycle as exhibited by Figure 5, thus decreasing the long term effects of the noise with respect to an individual controller.[12] By applying the above control scheme on each Poincaré section, the UPO can be targeted from one section to the next. If these sections are selected appropriately, then the effects of the noise can be minimized.

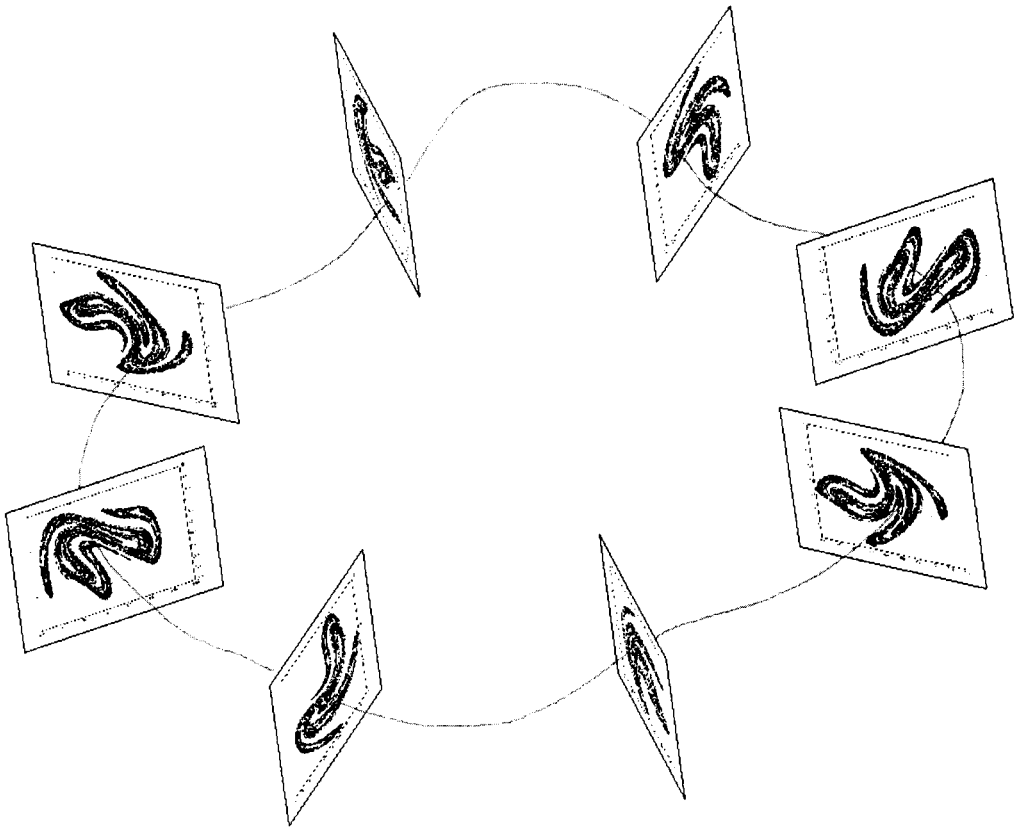

Figure 5 - Multi-plane control is achieved by constructing r separate control planes distributed evenly throughout phase space as exhibited here for r = 8 for the Mooring System.

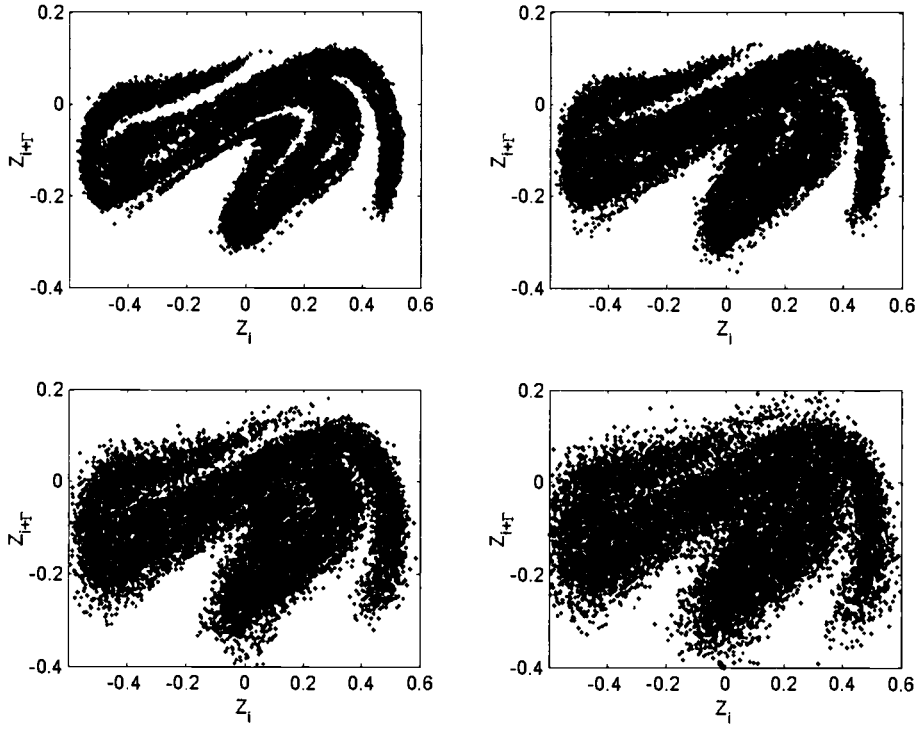

Figure 6 - Effects of noise on the chaotic mooring system attractor as seen through the Poincaré section of the mooring system for a SNR of (a) 2.42, (b) 2.07, (c) 1.81 and (d) 1.48.

4.9 The Stochastic Mooring System

Figure 6 shows the Poincaré map of the noisy chaotic response obtained by adding (band-limited) white noise of finite variance to the excitation term in the deterministic case as the noise intensity increases (hence the SNR decreases) from a SNR of 2.42 (Figure 6a) to 1.48 (Figure 6d). An examination of the corresponding probability density for this case indicates that destablization of the sensitive dynamics manifests

itself as an overall increase in the number of orbits which appear to be UPOs, but in fact are not.[11]

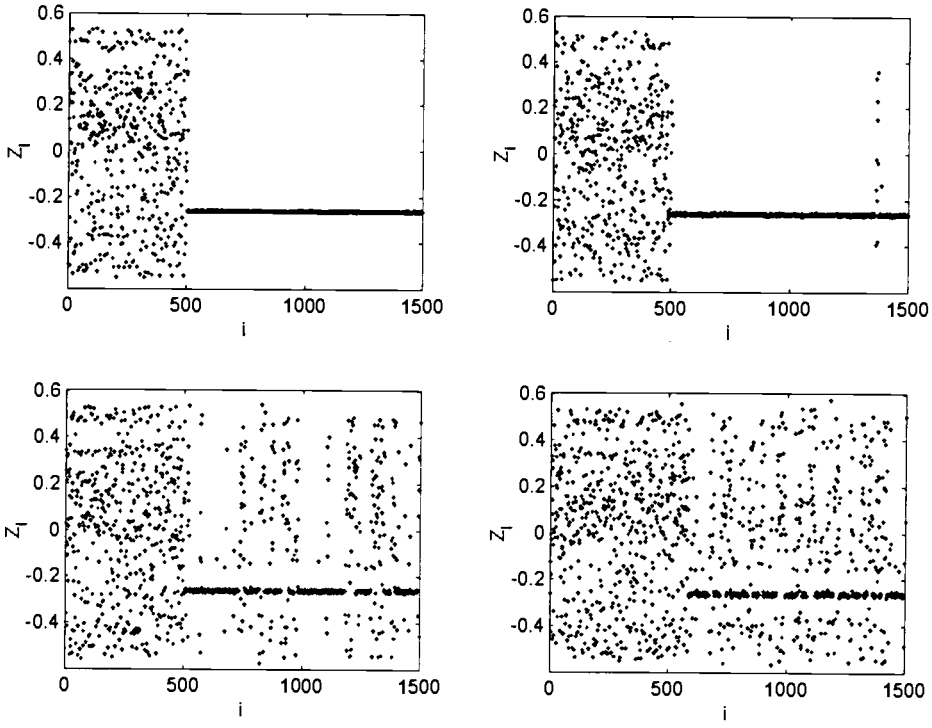

Figure 7- Effects of additive noise on mooring system control for the period-1 cycle and for the SNR of (a) 2.42, (b) 2.07, (c) 1.81 and (d) 1.48.

Figure 7 plots results of the addition of the noise to the period-1 controlled system (Figure 4a-b). As the noise intensity is increased and the corresponding SNR decreases from 2.42 to 1.48 there is a corresponding destablization of the system dynamics as well as the controller and a loss of control is realized. Observe that, as the noise level is increased, the system goes from being completely controlled, to a mode where the controller appears to be effective only for limited durations finally to the point where

the effects of noise overpowers the influence of the controller.

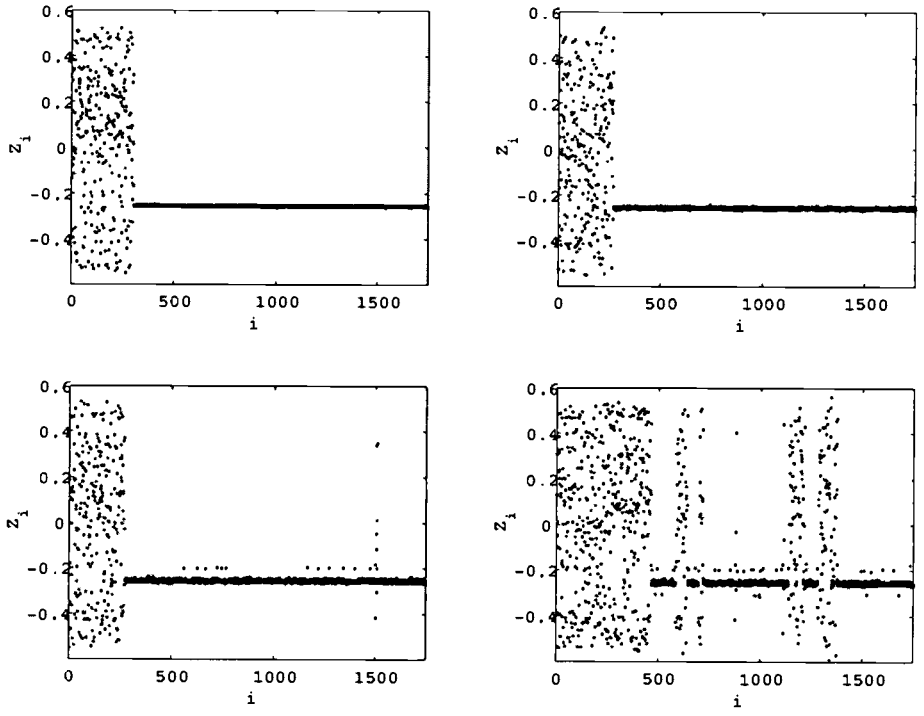

Figure 8 - Application of the multi-plane control on the Mooring System for the period-1 case and for a SNR of (a) 2.42, (b) 2.07, ©) 1.81 and (d) 1.48.

If the controller is modified to operate on multiple planes per cycle, it is expected that control will be maintained for an increasing intensity of noise. Figure 8 shows the results of the period-1 example with noise and operating under control on 8 sections, where each section has an associated linear reconstruction and controller created as outlined.

The number of control sections verses the amount of noise that the system controller is able to handle for this case is shown in Figure 9. Here, two levels of

control influence, i.e. two different values of η (0.05 and 0.1), are reported. It is assumed that the system is fully controlled if it can be controlled for 100 Poincaré points (or about 85,000 time series data points). This analysis indicates an approximately linear relationship between the controllable level of the energy of the noise versus the number of sections required for complete control for this system.

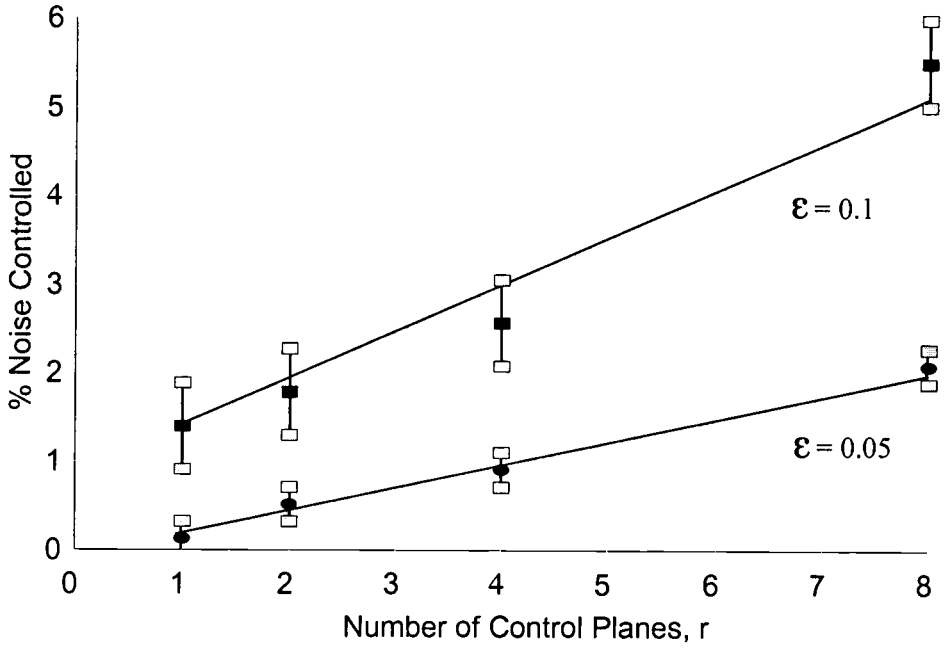

Figure 9 - Effects of the number of control planes used versus the noise level for the mooring system.

4.10 Estimation and Stochastic Filtering

The previous sections introduced the idea of controlling a nonlinear, chaotic system and applied this technique to the mooring system. The control system was then tested and consequently modified in the case where additive noise is present. The extension of the control algorithm was based on the rate at which reconstructed Poincaré Planes were constructed and then a linear controller was built on each of these planes. In this way, moderate amounts of noise can be handled. In order to increase the effectiveness of the control system in the presence of other then moderate levels of noise, the Kalman-Bucy Filter is considered. This section gives a brief introduction to the Kalman-Bucy Filter and several variants as they apply to nonlinear systems.

4.11 The Kalman-Bucy Filter

The Kalman Filter addresses the general problem of estimating the state of a first order, discrete time system that can be represented as a system of linear difference equations. (For the purposes here, it suffices to consider only the discrete time Kalman Filter.) Consider the system of equations

$$x_{k+1} = Ax_k + Bu_k + w_k \tag{21}$$

with the measurement equation

$$z_k = H x_k + v_k \tag{22}$$

where $x_k \in \Re^n$ is the state variable, A is an $n \times n$ matrix of state coefficients relating the state at time k to the state at time k+1 in the absence of either a driving force or process noise. $u_k \in \Re^n$ is the vector of control inputs while B is an $n \times l$ matrix that relates the control inputs to the state. w_k represents the process noise. Similarly, $z_k \in \Re^m$ is the measurement, H is an m x n measurement matrix which relates the state to the measurement and v_k is the measurement noise.

The process and measurement noise are assumed to be white noise with normal probability distributions given by

$$p(w) = N(0,Q) \tag{23}$$

$$p(v) = N(0,R) \tag{24}$$

and are assumed to be independent of one another. In practice, the noise covariance Q is either determined on some basis of intuition, or it us guessed. Similarly, the measurement covariance, R, is provided by a signal processing algorithm or is again guessed. And, in general, the noise levels are determined independently, hence there are no correlations between the two noise processes. The details of the development of the Kalman Filter and the Iterated Kalman Filter as used here can be found in King.[11]

4.12 Stochastic Control of Chaotic Systems

The Kalman Filter data processing algorithm and it's variants for nonlinear systems, the Extended Kalman Filter and the Iterated Kalman Filter, have been

successfully applied to an assortment of nonlinear and chaotic systems, both for filtering as well as control purposes.[13] The Kalman Filter has also been applied in order to obtain a reference trajectory for control purposes, in this case, the Extended Kalman Filter was exploited.[14]

For the purposes here, we apply the Kalman Filter for noise reduction and then utilize the previous control method previously defined in order to bring the response of the system to a stable, periodic orbit. Of interest is the extent to which the Kalman Filter can be applied under the presence of increasing noise levels while still being able to maintain system dynamics and control. That is, it is expected that the Kalman Filter will successfully reduce noise levels in the systems as exhibited by the previous work, however, as the noise intensity increases, how well does the Kalman Filter perform? The Iterated Kalman Filter is utilized since it is generally believed that the standard Kalman Filter cannot successfully filter the data except under special circumstances.[11] Because of it's increased potential for convergence and robustness, the IKF becomes the ideal method of ensuring stable filtering to the fiduciary trajectory, which is then used for control purposes.

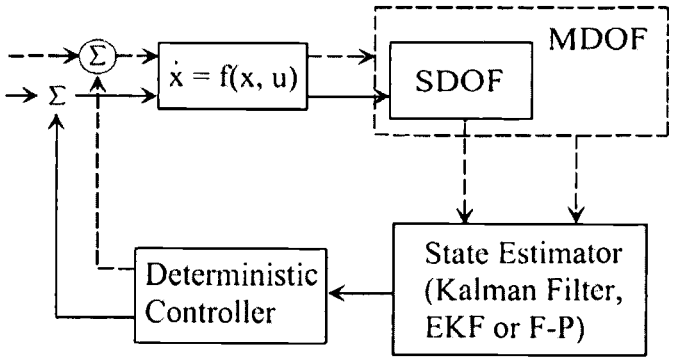

Figure 10 - Kalman Filter approach to controller the discrete time nonlinear system.

Figure 10 is a

diagram of the filtering and control process. The nonlinear system output at each time step is put through the Kalman Filter. The estimate of the state is then used in the control algorithm to maintain stability. Recall that the system is allowed to oscillate until the trajectory enters within the ε-ball at which time the control is applied. Also recall that this is performed on a Poincaré plane and hence, the time step indicated is that discrete time between planes. However, this can be relaxed so that the Kalman Filter is applied at each numerical integration time step and the control applied only on a Poincaré plane.

Recall the nonlinear ordinary differential equations governing the evolution of the system response of the mooring system, Eqs. (5)-(7) and, where $w_1(t)$ and $w_2(t)$ are noise components added to the position and velocity respectively. It is assumed that the frequency of excitation is known and that the noise is additive to the position and velocity alone. By "discrete mooring system," it is meant that all control actions are taken on the Poincaré plane. However, as previously indicated, the IKF is applied at each numerical integration. Thus, the linearization procedure inherent in the IKF is applied locally at each step and the system trajectory smoothed, bringing the state back to the intended fiducial trajectory.

Using the same paramaters as before, the chaotic (noise free) system response for these parameter values is seen in Figure 2a-2d. Meanwhile, the noisy chaotic response is exhibited in Figure 8, where the Poincaré section becomes "cloudy" under the addition of noise. As is evident in Figure 9, the addition of increased noise renders the

system uncontrollable with only small amounts of noise, even as the number of control planes is increased. For this reason, the Kalman Filter is applied in order to investigate the ability for the filter to reduce the effects of the noise, stochastically, for increased prediction of the current state and consequently to produce a stable, robust controller.

The implementation of the IKF introduces several parameters for which there is some control over. First, the number of Gauss-Newton iterations is predetermined. The implementation here applies a set number of iterations for the IKF update scheme as opposed to monitoring the difference between succeeding filtered points. Let M be the number of Gauss-Newton iterations. It should be apparent that if $M = 0$, then the IKF reduces to the Extended Kalman Filter. The number, N, of measurement points used in the calculations can be set as well. This is the number of time measurements that will be used in the smoothing operation.

For the Mooring System, the following equations define the filter inputs:

$$\begin{aligned} f_1(x_1, x_2, x_3) &= x_2 \\ f_2(x_1, x_2, x_3) &= -\alpha x_1\left(1-\frac{1}{\sqrt{1+x_1^2}}\right)-\gamma x_2-f_1 \sin(x_3) \\ f_3(x_1, x_2, x_3) &= \omega \end{aligned} \tag{25}$$

where the Jacobian is given by (where i,j=1,2,3)

$$\frac{\partial f_i}{\partial x_j} = \begin{bmatrix} 0 & 1 & 0 \\ -\alpha\left(1-\frac{1}{\left(1+x_1^2\right)^{3/2}}\right) & -\gamma & -f_1\cos(x_3) \\ 0 & 0 & 1 \end{bmatrix} \tag{26}$$

The measurement function, h, is given by

$$h(x) = H\,x = \begin{bmatrix} 1 & 0 & 0 \\ 0 & 1 & 0 \end{bmatrix} \begin{bmatrix} x \\ y \end{bmatrix} \tag{27}$$

where, again, $v_1(t)$ and $v_2(t)$ are white, Gaussian, uncorrelated measurement noise variables. For the application here, it is sufficient to define the measurement functions as linear functions of the state variables. That is, we allow

$$h_1(x, y, t) = x \tag{28}$$

and

$$h_2(x, y, t) = y \tag{29}$$

so that the "linearized" measurement equations are, simply

$$\begin{bmatrix} z_1 \\ z_2 \end{bmatrix} = \begin{bmatrix} h_1(x, y, t) \\ h_2(x, y, t) \end{bmatrix} + \begin{bmatrix} v_1(t) \\ v_2(t) \end{bmatrix} \tag{30}$$

Given this representation of the state and measurement equations for the mooring system, and given the parameter values cited previously, the Iterated Kalman Filter can now be applied. Figure 11 is a plot of the Poincaré section for the noisy mooring system and the subsequent application of the Iterated Kalman Filter. Here, the noise magnitudes for the separate measurement and state noise variables are $|w_1| = 0.05$, $|w_2|$

$= 0.05$, $|\nu_1| = 0.01$, $|\nu_2| = 0.01$, and the noise magnitude for the initial conditions are 0.01 respectively. Four Gauss-Newton iterations are used while only two measurement points are utilized in the filter process. Figure 11a is the noiseless system response as seen on the Poincaré section while Figure 11b is the noisy response. Figure 11c is the result of applying the Iterated Kalman Filter to the noisy system. Figure 12 plots three of the period-1 orbits of the system and their iterates for the original dynamical system and the associated orbits when noise is applied and then filtered with the IKF. Here, the solid circles are the points associated with the unstable periodic orbit of the noise free system while the lightly colored circles are the iterates. The solid triangles represent the unstable periodic orbits after the filtering process and the lightly filled triangles are the iterates in this case.

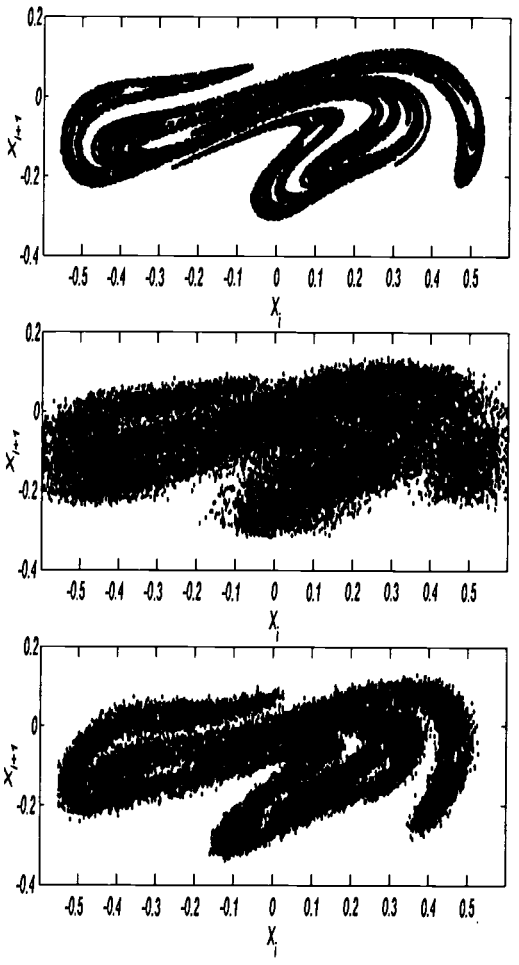

Figure 11 - Application of the IKF to the nonlinear mooring system.

Notice that the magnitude of the difference between the filtered and original

dynamical system is minimized to such an extent that it is enough to achieve the desired control objective with only a single control plane, in which case, the unstable periodic orbit (the associated dynamic invariant of interest) is maintained as previously shown.

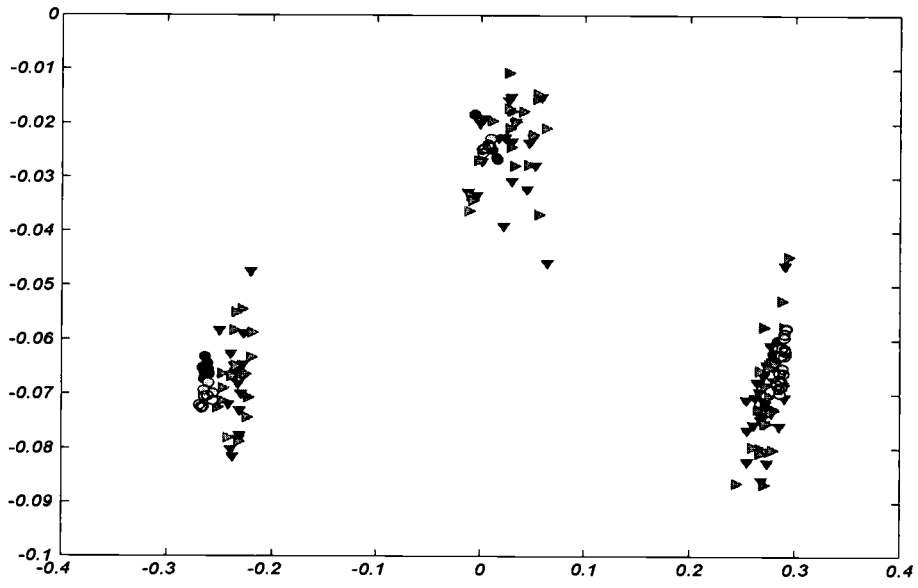

Figure 12 - Unstable periodic orbit and iterates under the influence of the IKF for three of the period-1 cycles found within the Mooring System.

As exhibited, the Iterated Kalman Filter was successful in separating the noise from the chaotic signal for moderate levels of noise and consequently the control scheme previously defined is applicable. The IKF becomes a sub-optimal estimator, in the least squares sense, for the nonlinear signal. This is accomplished by iterating the time update and the covariance matrix in order to obtain a more accurate estimate of the actual system trajectory shadowed. Notice, however, that the Iterated Kalman Filter

can be used as a predictor as well.

4.13 Concluding Remarks

This study examines control of the chaotic oscillations of a fluid-structure interaction system. The system under consideration, although of fluid origin, is modeled as a low degree of freedom system by considering cases for which the small body theory applies. The method uses a chaotic time series to categorize unstable periodic orbits. This is done by mapping the time series to a Poincaré section and then obtaining the unstable periodic orbits through an exhaustive search of the Poincaré points. A linear map is produced for which the pole placement method of feedback control can be applied. The method was first applied to the nonlinear system to verify control. Then, the method was applied to the model in the case that band-limited white noise of finite variation was added to the excitation term, indicating that (stochastic) control of moored systems is possible. An extension of this methodology was investigated by obtaining a series of Poincaré sections, stroboscopically sampling every $2\pi/r\Gamma$, where r is the number of sections desired, and building a corresponding controller on each section. This yields r separate controllers evenly distributed, thus decreasing the long term effects of the noise with respect to an individual controller. Finally, under increasing levels of noise, an Iterated Kalman Filter was succesfully applied in order to filter this noise.

Finally, should the responses of the prototypes corresponding to the model tests mentioned in the beginning of this study confirm the existence of chaotic motions in the (noisy) field environments, the analysis and control method presented in this study can be applied to suppress these motions if desired. Extensions of this study to the multi-degree-of-freedom physical models and subsequent design of practical controllers for experimental tests are being examined.

4.14 Acknowledgments

The authors wish to acknowledge the financial support of the U. S. Bureau of Mines process control-program (AL-92-A-001) and the United States Office of Naval Research (Grant No. N0001-92-J-1221 and N00014-04-10008).

4.15 References

1. Gottlieb, O., and Yim, S. C. S., "Onset of Chaos in a Multi-Point Mooring System", Proc. First (1990) European Offshore Mechanics Symposium, Trondheim, Norway, Aug. 20-22, 1990, pp. 6-12.

2. Gottlieb, O., and Yim, S. C. S., "Deterministic Motions of Nonlinear Mooring Systems Part I: Analysis and Predictions", Ocean Engineering Report No. OE-93-02, Oregon State University, Corvallis, OR, 1993.

3. Yim, S. C. S., Myrum, M. A., Gottlieb, O., Lin, H., and Shih, I. M., "Summary and

Preliminary Analysis of Nonlinear Oscillations in a Submerged Mooring System Experiment", Ocean Engineering Report No. OE-93-03, Oregon State University, Corvallis, OR, 1993.

4. Lathrop, D. P. and Kostelich, E. J., "Characterization of an Experimental Strange Attractor by Periodic Orbits.', Phys. Rev. A, Vol. 40, No. 7, pp 4028-31, Oct. 1989.

5. Sano, M., and Sawada, Y., "Measurement of the Lyapunov Spectrum from a Chaotic Time Series", Phys. Rev. Lett., Vol. 55, No. 10, Sept., 1985, pp. 1082-85.

6. Jordan, D. W. and Smith, P. (1999). *Nonlinear Ordinary Differential Equations, 3rd Ed.*, Clarendon Press, Oxford, 560 pps.

7. Gottlieb, O., Feldman, M., and Yim, S. C. S. (1996). "Parameter Identification of Nonlinear Ocean Mooring Systems Using the Hilbert Transform," *ASME Journal of Offshore Mechanics and Arctic Engineering*, 118, No. 1, 29-36.

8. Gottlieb, O., Yim, S. C. S., and Lin, H. (1997). "Analysis of Bifurcation Superstructure of Nonlinear Ocean System," *ASCE Journal of Engineering Mechanics*, 123, No. 11, 1180-87.

9. Guckenheimer, J. and Holmes, P. (1983). *Nonlinear Oscillations, Dynamical Systems, and Bifurcations of Vector Fields,* Springer-Verlag, New York, 453 pps.

10. Ott, E., Grebogi, C., and Yorke, J. A. (1990), "Controlling Chaotic Dynamical Systems", in *CHAOS/XAOS, Soviet-American Perspective on Nonlinear Science*, Ed. By D. Campbell, Am. Inst. Phys., New York.

11. King, P. E. (2005). *Deterministic and Stochastic Control of Nonlinear*

Oscillations in Ocean Structural Systems. PhD Dissertation, Oregon State University, Corvallis, OR, 97331.

12. King, P. E. and Yim, S. C. S (1997). Control of Noisy Chaotic Motion in a System with Nonlinear Excitation and Restoring Forces," *Chaos*, Vol. 7, No. 2, 290-300.

13. Fowler, T. B. (1989). "Application of Stochastic Control Techniques to *J. Basic Eng., Trans. ASME*, Series D, Vol. 82, No. 1, 35-45. Chaotic Nonlinear Systems," *IEEE Trans. Automatic Control*, Vol 34, No. 2, 201-205.

14. B. Cazelles, G. Boudjema, and N. P. Chau, "Adaptive control of chaotic systems in a noisy environment," Phys. Lett. A, 196, pp. 326-330, 1995.

Nonlinear Rocking Responses of Free Standing Rigid Blocks, Part II - Stochastic Filtering and Control

Paul E. King[1]

Solomon S. C. Yim[2]

Submitted to

Journal of Engineering Mechanics

ASCE Publications

Manuscript Number EM/2005/024247

5.1 Abstract

An understanding of the rocking response and overturning stability of rigid blocks is of importance to the preservation of free-standing equipment and structures placed in the ocean and seismic environments. Previous studies have indicated a wide spectrum of possible responses under support excitation including periodic, quasi-periodic and chaotic motions, which may lead to overturning. To avoid potentially catastrophic responses, a means of actively controlling the nonlinear oscillations is presented. In Part I of this report, responses to purely deterministic excitations were investigated. It was shown that the controller designed was able to maintain stable system response under the conditions outlined. The control methodology introduced applied a small force to induce small perturbations about a nonlinear system trajectory at prescribed times in order to guide the system towards the stable operating state. This was accomplished by creating a locally linear map about the desired system trajectory. A feedback controller was designed based upon this linear reconstruction in order to guide the system trajectory towards the associated stable eigenvector of the linearized system, ensuring that the trajectory is maintained in a neighborhood of the desired periodic motion during the interval between sampling. In Part II, the methodology is tested against increasing levels of noise. It is expected that as the noise level increases, the controller will loose its ability to maintain a stable operating condition. In order to combat this, the Iterated Kalman Filter is employed in order to filter the data. It

is known that Kalman Filtering will not work in the general nonlinear case. However, this methodology produces a locally linear map where the Kalman Filter is effective. This paper outlines the proposed method defined it Part I. Then, the Iterated Kalman Filter is utilized to study the varying effects due to an increase in noise intensity. From this, an estimate of the amount of noise that is able to be handle before catastrophic toppling of the system is guaranteed, at which time control is no longer effective.

[1]Research Program Leader, U. S. Department of Energy, Albany Research Center, Albany, OR 97321
[2]Professor, Civil, Construction and Environmental Engineering Dept., Oregon State University, Corvallis, OR 97331.

5.2 Introduction

In Part I of this two-part study, the nonlinear responses of the rigid rocking of free standing equipment subject to base excitation was investigated. This type of system may include models of engineering systems in the offshore and seismic environments as reported. In this study, it is assumed that the supporting base of the rigid blocks is either under going periodic oscillations or is periodic with low amplitude, band limited white noise component (Yim and Lin 1996a). As was exhibited in Part I, even though these complex oscillations may appear to be problematic, control of the deterministic motions can be achieved. This was accomplished by applying small moments to the system at strategic times in order to achieve control. However, this control technique may not be robust under the presence of increasing levels of low amplitude, band limited what noise. The addition of an increasing intensity of random noise, such as may be encountered in an ocean or seismic environment, may impose a significant problem for the control scheme. Part II investigates the controllability of the rocking system under increasing noise intensities. First, a simple modification of the control algorithm is investigated. It is seen that this modification increases the regime that the control algorithm is applicable for the rocking system. To continue to increase this regime and to address the issue of measurement error, the Kalman Filter and several if its variants are investigated to the point where the stable motions are unachievable and over turning becomes imminent.

5.3 Control Under Noisy Excitation

The benefit of using small perturbations to control a deterministic nonlinear dynamical system within the chaotic operating regime was presented in Part I. However, for a typical real physical system such as the rocking of a rigid block in seismic or ocean environments, there will be noise added to the system through a random component to the excitation or measurement errors. A means of characterizing the influence of the noise on the rocking system is given by the signal-to-noise ratio (SNR) defined as the power of the noise free signal divided by the power of the noise, where the power is given by

$$P_S = \frac{1}{T}\int_0^T \theta(t)^2\, dt \tag{1}$$

where T is the period of the system.

Figure 10 in Part I plotted the results of adding (band limited) white noise to the excitation term a primary resonance example. In this example, the signal to noise ratio was decreased from 27.75 (the nearly noise-free case) to 4.29 in order to exhibit the effects of the noise on the controller without making any modifications to the control scheme. Observe that, as the noise intensity increases, the system goes from being completely controlled, to a mode where it takes a much longer transient period before the controller latches onto the desired system trajectory and obtains the necessary control,

and finally to the point where the effects of noise overpowers the influence of the controller and the controller fails altogether.

A controller can still be designed in order to handle the noisy system by utilizing a simple extension of the preceding algorithms. A series of Poincaré sections about the chaotic attractor can be constructed by stroboscopically sampling the time series at intervals of $2\pi/r\Gamma$, where r is the

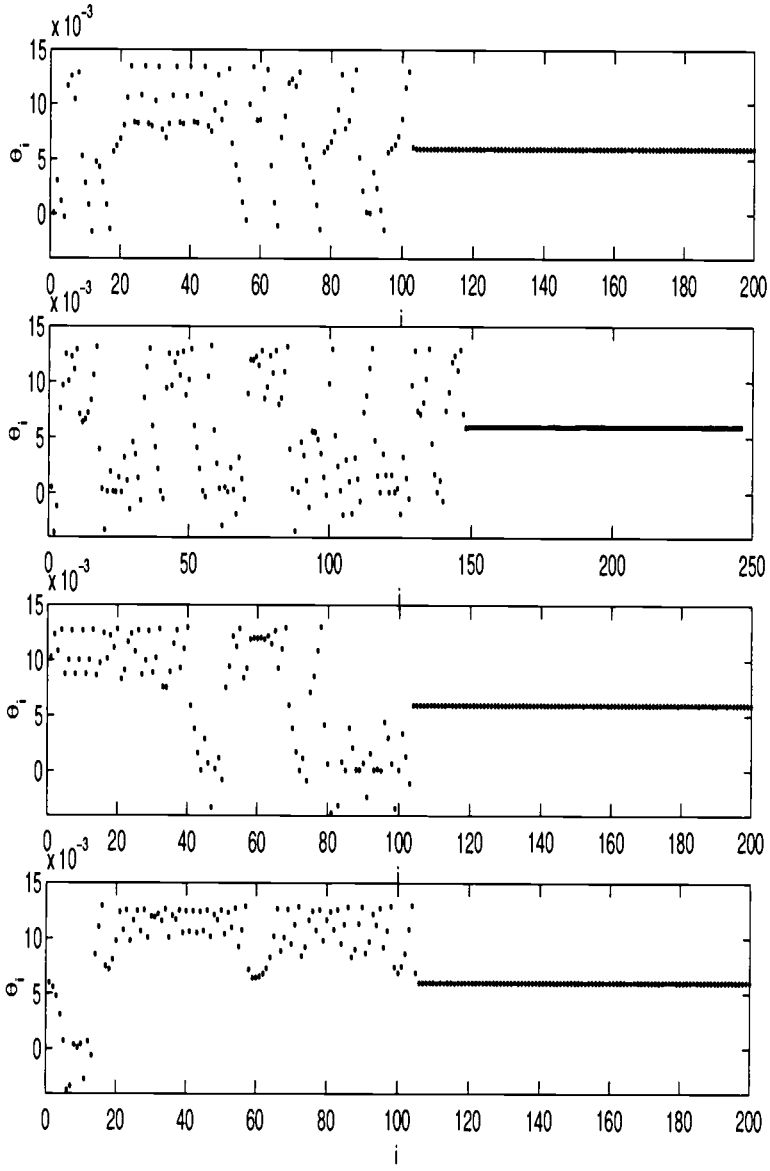

Figure 1 - Effects of multiple control planes on the period-1 controller exhibited in Fig. 9 for the signal to noise ratio of a) SNR=27.75, b) SNR=5.54, c) SNR=3.08 and d) SNR=2.80 control section.

number of sections desired (King and Yim 1996). This yields r separate controllers evenly distributed throughout the cycle, thus decreasing the long term effects of the noise with respect to an individual controller. By applying the above control scheme on each

Poincaré section, the desired UPO can be targeted from one section to the next. If these sections are selected appropriately, then the effects of noise can be minimized.

This modification to the overall control scheme outlined can significantly increase the controllability of the system. For the rocking block system, by taking several Poincaré sections along a single cycle, and then building a feedback controller on each section, the effects of the noise are reduced with respect to the number of sections the controller is applied per cycle. Figure 1 shows the results of the previous example (Part I) with 4 control planes.

Each of the 4 sections has been created by sampling the same time series data set at 4 times the rate of that in Figure 10 of Part I (r = 4). Then, using the scheme outlined previously, a linear map on each section is constructed, finally, each time a trajectory crosses a section within the control tolerance, Eq.(15) from Part I is applied for that section. The SNR is decreased from

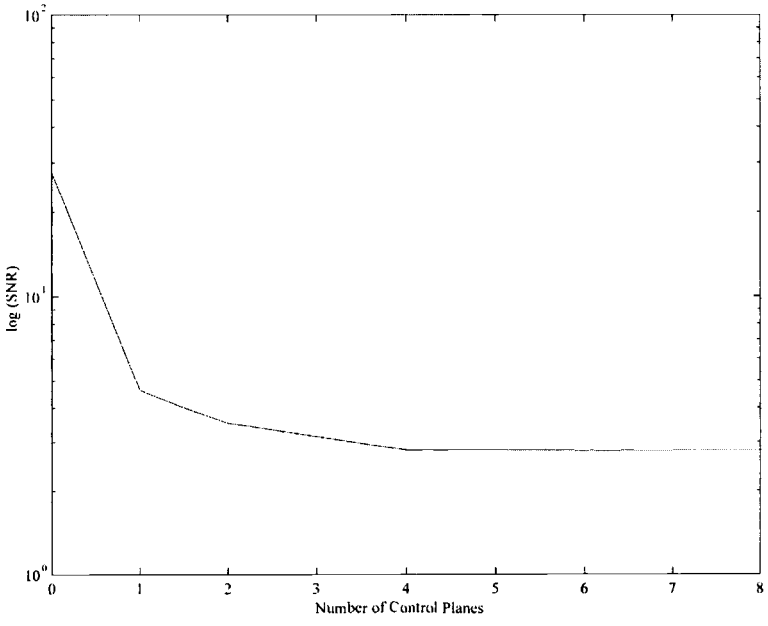

Figure 2 - The number of control planes required to control the system versus the signal to noise ratio.

27.75 in Fig.1a to 2.80 in Fig.1d. After this point, further additions of noise cause the system to overturn and further control is not possible for this case.

The number of control sections versus the noise intensity that the system controller can handle is shown in Figure 2. This analysis indicates an approximately logarithmic relationship between the controllable level of noise versus the number of sections required to maintain control. This is due to the inherent instability leading to overturning of this particular system and it is evident that the addition of more control planes only makes marginal increases in the controllability of the system in the presence of increasing noise levels. The noise level will reach an intensity under which this control scheme will no longer

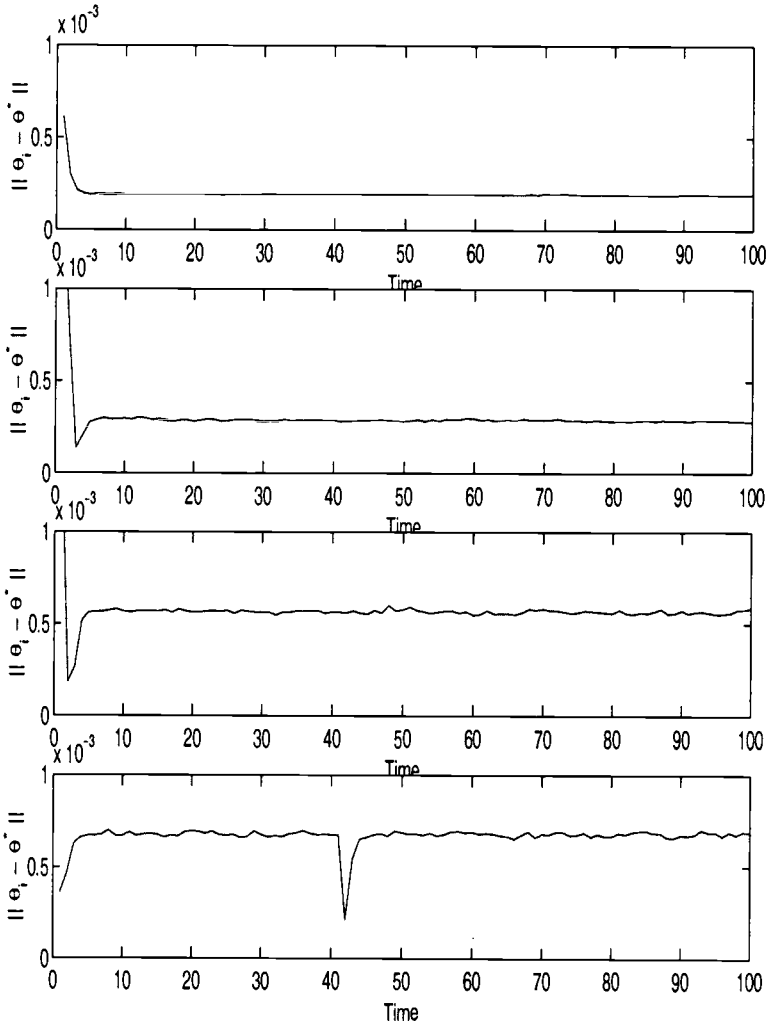

Figure 3 – Controller action on a single control plane indicating the distance a trajectory must be moved in order to maintain control under increasing noise intensities.

work and continuous control methodologies, requiring substantially more energy, are required.

Figure 3 plots the controller action as a function of time for different noise levels. As is evident from the Figure, the distance that the controller is required to move a trajectory on the control plane is small in comparison with the amplitude of oscillation. Hence, the relative energy exerted in order to maintain control with this methodology is small in comparison to the excitation moment. Recall that on a given control plane, the controller is only required to be operational when a trajectory intersects a Poincaré plane and only within the ball of radius ε.

5.4 Kalman Filtering

In an effort to increase the regime where control is achievable, the Kalman Filter and its derivatives are investigated. The extension of the control algorithm was based on the rate at which reconstructed Poincaré Planes were constructed, then, a linear controller was built on each of these planes. In this way, moderate amounts of noise could be handled. In order to increase the effectiveness of the control system in the presence of other then moderate levels of noise or measurement error, the Kalman-Bucy Filter is considered. The Kalman Filter data processing algorithm and it's variants for nonlinear systems, the Extended Kalman Filter and the Iterated Kalman Filter, have been successfully applied to an assortment of nonlinear and chaotic systems, both for filtering

as well as control purposes (Fowler 1989, Julier *et al* 1997, Wallker and Mees 1997, 1998). The Kalman Filter has also been applied in order to obtain a reference trajectory (for control purposes), in this case, the Extended Kalman Filter was exploited (Cazelles *et al* 1995).

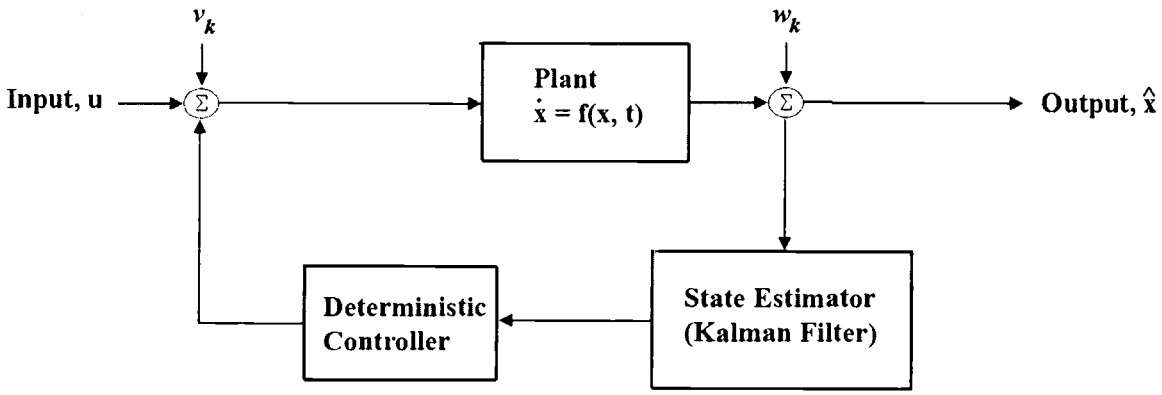

Figure 4 – Stochastic Filtering and control of the nonlinear dynamical system.

The apparent universality of the Kalman Filter has spurned much interest across a wide platform of applications. Since the Kalman Filter is a second order estimator, it has proven to have wide ranging applicability with robust results, in general. For the case of the systems considered, it appears that the important sensitive nonlinear characteristics are retained while under the influence of the estimation procedure (Fowler 1988, 1989). However, because the Kalman Filter is defined for linear (possibly time-varying or of arbitrary observation intervals, which could be extremely complex) it is expected that the filter in general will not be robust against the nonlinear systems studied here. Extensions to the Kalman Filter have been introduced, namely the Extended Kalman Filter

(Anderson and Moore 1979) and the Iterated Kalman Filter (Maybeck 1982, Walker 1998, Walker *et al* 1998). Both of these extensions to the Kalman Filter increase the robustness of the Kalman Filter for nonlinear systems. As will be seen, the Extended Kalman Filter (EKF) is a special case of the Iterated Kalman Filter (IKF).

The idea in the use of the Kalman Filter is to produce an estimate of the state of the system at each time step or, alternatively, on each Poincarè Plane. This state estimate is based upon the known dynamics and incorporates an unknown system error or an unknown measurement error in such a manner as to render the cost of that error at a minimum (Figure 4). Then, with this estimate of the state, system control on the estimated state can be instigated. The aim is to produce a state estimator that does the best job possible. This estimate is the Iterated Kalman Filter as applied to the nonlinear system dynamics of the rocking response of the rigid block.

Recall that the derivation of the Kalman Filter was based on linear systems. Fowler (1986) in his PhD dissertation showed that the Kalman Filter can be used with some success on certain nonlinear systems. He showed that a control system based upon the Kalman Filter estimator yields significant improvement with respect to covariance over other control systems. He also showed that for nondissipative systems, the improved performance translated to improved stability (Fowler 1988 and 1989). However, in general, the covariance matrix will grow, particularly with respect to prediction, as the nonlinearities take effect. That is, while filtering in a linearized portion of phase space,

the optimal filter performs well. As a trajectory strays from this linearized field, the performance of the filter will degrade.

In order to obtain further improvement under this more general case, the Extended Kalman Filter (EKF) and the Iterated Kalman Filter are investigated. The EKF is an extension of the Kalman Filter where the filter is continually updated by creating a linearization around the previous state estimate, starting with the given initial guess. A first order Taylor series approximation of the system dynamics is calculated at the previous state estimate as well as the measurement function at the corresponding predicted state. Consider the nonlinear difference equations

$$\tilde{x}_{k+1} = f(x_k, u_k, w_k) \tag{2}$$

with measurement update

$$\tilde{z}_k = h(x_k, v_k) \tag{3}$$

where w_k and v_k represent the process and measurement noise respectively. To estimate the process with these nonlinear state and measurements, we perform a linearization about the previous estimate. This is done by investigating the linearized versions of Eqs.(2) and (3), which are seen to be given by

$$x_{k+1} = \tilde{x}_{k+1} + A(x_k - \hat{x}_k) + Ww_k \tag{4}$$

and

$$z_k = \tilde{z}_k + H(x_k - \hat{x}_k) + Vv_k \tag{5}$$

where A is the Jacobian matrix given by

$$A_{ij} = \frac{\partial f_i}{\partial x_j}(x_k, u_k, 0) \tag{6}$$

W is the Jacobian matrix given by

$$W_{ij} = \frac{\partial f_i}{\partial w_j}(x_k, u_k, 0) \tag{7}$$

H is the Jacobian given by

$$H_{ij} = \frac{\partial h_i}{\partial x_j}(x_k, 0) \tag{8}$$

and V is the Jacobian given by

$$V_{ij} = \frac{\partial f_i}{\partial v_j}(x_k, 0) \tag{9}$$

Now, define the notation for the prediction error to be

$$\tilde{e}_{x_k} = x_k - \tilde{x}_k \tag{10}$$

and the measurement error to be

$$\tilde{e}_{z_k} = z_k - \tilde{z}_k \tag{11}$$

Substituting Equation (10) and (11) into Equation (4) and (5) yields

$$\tilde{e}_{x_k} \approx A(x_k - \hat{x}_k) + \varepsilon_k \tag{12}$$

and

$$\tilde{e}_{z_k} \approx H\tilde{e}_{x_k} + \eta_k \tag{13}$$

where ε_k and η_k are ensembles of independent random variables with zero mean and covariance matrices WQW^T and VRV^T.

Notice that these last two equations closely resemble the difference equations for the discrete Kalman Filter (King 2006). This suggests that we use the measured residual, Eq.(11), and a second, hypothetical Kalman Filter to estimate the prediction error, Eq.(10). This estimate is then used to obtain the a posteriori state estimates for the nonlinear process. Suppose that the interim estimate is given as $\hat{\tilde{e}}_k$, then the a posteriori state estimate is

$$\hat{x}_k = \tilde{x}_k + \hat{\tilde{e}}_k \tag{14}$$

The random variables defined in this process have probability density functions defined by

$$\begin{aligned} p(\tilde{e}_{x_k}) &= N(0, E[\tilde{e}_{x_k}\tilde{e}_{x_k}^T]) \\ p(\varepsilon_k) &= N(0, WQ_kW^T) \\ p(\eta_k) &= N(0, VR_kV^T) \end{aligned} \tag{15}$$

Given this, the predicted value of the interim estimate, $\hat{\tilde{e}}_k$, is zero and the (hypothetical) Kalman Filter used to estimate it is simply

$$\hat{e}_k = K_k\tilde{e}_k \tag{16}$$

Substituting this back into Eq.(11) and then using the measurement residual Equation (14) we obtain

$$\hat{x}_k = \tilde{x}_k + K_k(z_k - \tilde{z}_k) \tag{17}$$

where, it is evident that we don't really need the hypothetical Kalman Filter. We can now use this for the measurement update in the Extended Kalman Filter (EKF) with $\tilde{x}_k$ and $\tilde{z}_k$ as defined in Equations (4) and (5) and the Kalman gains , K_k (Anderson and Moore 1979)

$$K_k = P_k^- H_k^T (H_k P_k^- H_k^T + R_k)^{-1} \tag{18}$$

and the appropriate substitution for the measurement error covariance. The complete EKF algorithm is shown in Figure 5 and the complete set of EKF equations are give by

$$\begin{aligned} \bar{x}_{k+1} &= f(x_k, u_k, 0) \\ \bar{P}_{k+1} &= A_k P_k A_k^T + W Q_k W^T \end{aligned} \tag{19}$$

with the measurement update given by

$$\begin{aligned} K_k &= \bar{P}_k H_k^T (H_k \bar{P}_k H_k^T + V R_k V^T)^{-1} \\ \hat{x}_k &= \hat{x}_k^- + K(z_k - h(\hat{x}_k^-, 0)) \\ P_k &= (I - K_k H_k) \bar{P}_k \end{aligned} \tag{20}$$

where, as with the discrete Kalman Filter, Eq.(20) corrects the state and covariance estimates with the measurement z_k. Notice that the Jacobian, H_k, in the equation for the Kalman gain K_k serves to correctly propagate only the relevant components of the measurement information, that is, the observable components of the state.

Now, taking this one step further, we define the Iterated Kalman Filter by noticing that an iteration technique can be applied to update the state estimate and covariance matrix, consequently improving performance. That is, within a given time step, the sequences $\{x_k^i\}$ and $\{P^i\}$ can be defined inductively as follows:

$$x_k^{i+1} = \hat{x}_k + K_k^i(z_k - h(x_k^i) - H_k^i(\hat{x} - x_k^i)$$
$$P_k^{i+1} = (I - K_k^i H_k^i)P_k^i \tag{21}$$

where

$$H_k^i = \frac{\partial h}{\partial x_k}(x_k^i) \tag{22}$$

and

$$K_k^i = P_k^i H_k^{i\,T}(H_k^i P_k^i H_k^{i\,T} + R_k)^T \tag{23}$$

are the updates for the linearized measurement matrix and the Kalman gain. The induction process begins with the initial conditions

$$x_k^0 = \hat{x}_k, \qquad P_k^0 = P_{k-1} \tag{24}$$

where the initial covariance matrix is taken to be the last one calculated in the previous step. This gives the update for the IKF as

$$\hat{x}_{k+1} = x_k^i, \qquad P_k = P_k^i \tag{25}$$

It is evident that for $i = 0$ in Eqs.(21)-(22) we obtain the EKF. Also notice that both methods reduce to the ordinary Kalman Filter in the case that the measurement function is affine.

It can be shown that the IKF is capable of providing better performance then the ordinary Kalman Filter in the presence of significant nonlinearities since the IKF introduces a reference trajectory which is incorporated into the estimates iteratively (Maybeck 1982, Bell and Cathey 1993, Bertsekas 1996). Notice that the iterations can be stopped by any number of convergence criteria such as when two consecutive values $\hat{x}_k^i$ and $\hat{x}_k^{i+1}$ differ by a pre-defined amount or after a predetermined number of iterations. Bell (1994) showed that this iteration technique becomes a Gauss-Newton process under these conditions. The trade off for this technique, of course, is computational power required to perform the iterations within each time step.

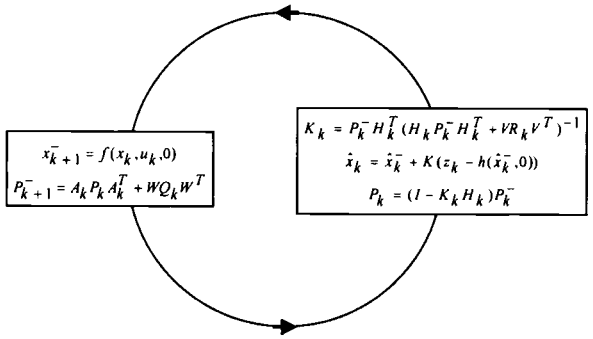

Figure 5 – The Extended Kalman Filter with time update (project ahead) and measurement update (correct for the projection).

5.5 Filtering of the Rocking Response

The Kalman Filter, therefore, addresses the general problem of estimating the state of a first order, discrete time system that can be expressed as a system of linear difference equations. Consider, then, the system give by:

$$x_{k+1} = Ax_k + Bu_k + w_k \tag{26}$$

with the associated measurement equation

$$z_k = Hx_k + v_k \tag{27}$$

where $x_k \in \Re^n$ is the state variable, A is an $n \times n$ matrix of state coefficients relating the state at time k to the state at time $k+1$ in the absence of either a driving force or a process noise. $u_k \in \Re^n$ is the vector of control inputs while B is an $n \times l$ matrix that relates the control inputs to the state. The w_k represents the process noise. Similarly, $z_k \in \Re^m$ is the measurement, H is an $m \times n$ measurement matrix which relates the state to the measurement and v_k is the measurement noise.

The process and measurement noise are assumed to be white noise with normal probability distributions given by

$$\begin{aligned} p(w) &= N(0,Q) \\ p(v) &= N(0,R) \end{aligned} \tag{28}$$

and are assumed to be independent of one another. In practice, the noise covariance Q is either determined on some basis of intuition, or an assumption is made of its structure.

Similarly, the measurement covariance, R, is provided by a signal processing algorithm or it is again, assumed. In general, the noise levels are determined independently, hence there are no correlations between the two noise processes. The details of the development of the Kalman Filter and the Iterated Kalman Filter as used here can be found in King (2006).

For the purposes here, we apply the Kalman Filter for noise reduction which then can be utilized in the control methodology previously defined in Part I in order to bring the response of the system to a stable, periodic orbit. Of interest is the extent to which the Kalman Filter can be applied under the presence of increasing noise levels while still being able to maintain system dynamics and control. That is, it is expected that the Kalman Filter will successfully reduce noise levels in the systems as exhibited by the previous work, however, as the noise intensity increases, how well does the Kalman Filter perform? The Iterated Kalman Filter is utilized since it is generally believed that the standard Kalman Filter cannot successfully filter the data except under special circumstances. Because of the increased potential for convergence and robustness, the IKF becomes the ideal method of ensuring stable filtering to the fiduciary trajectory, which is then used for control purposes.

Recall the nonlinear ordinary differential equations governing the evolution of the system response of the rocking system, Eqs.(1)-(3) in Part I. It is assumed that the frequency of excitation is known and that the noise is additive to the position and velocity alone. By "discrete rocking system," it is meant that all control actions are taken on the

Poincaré plane. However, as previously indicated, the IKF is applied at each numerical integration. Thus, the linearization procedure inherent in the IKF is applied locally at each step and the system trajectory smoothed, bringing the state back to the intended fiducial trajectory.

Recall that the nonlinearities for this system are 4-fold and are seen as firstly, the righting moment about the edges giving rise to the nonlinear restoring force as a function of angular displacement, θ. The second nonlinearity is associated with the coupled parametric excitation. The third nonlinearity is associated with the energy loss at impact and is represented as a jump discontinuity in the angular momentum while the fourth nonlinearity is due to the change in centers of rotation resulting in a transformation from one governing equation to the other.

Using the same parameters as before, the chaotic (noise free) system response for these parameter values is seen in Figure 2 in Part I. Meanwhile, the effects of noise on the chaotic response and the ensuing control are exhibited in Figure 10 of Part I. As is evident in Figure 10 (Part I), the addition of increased noise renders the system uncontrollable with only small amounts of noise, even as the number of control planes is increased. For this reason, the Kalman Filter is applied in order to investigate the ability of the filter to reduce the effects of the noise, stochastically, for increased prediction of the current state and consequently to produce a stable, robust controller.

The implementation of the IKF introduces several parameters for which there is some control over. First, the number of Gauss-Newton iterations is predetermined. The

implementation here applies a set number of iterations for the IKF update scheme as opposed to monitoring the difference between succeeding filtered points. Let M be the number of Gauss-Newton iterations. It should be apparent that if $M = 0$, then the IKF reduces to the Extended Kalman Filter. The number, N, of measurement points used in the calculations can be set as well. This is the number of time measurements that will be used in the smoothing operation.

For the rocking system, the state equations for the rocking response are given by Eqs.(1)-(3) in Part I of this study. In order to construct an appropriate Iterated Kalman Filter, the decoupled system will be investigated. For the case where the angular momentum is $\theta > 0$, a Kalman Filter can be constructed via the following:

$$\begin{aligned} f_1(x_1, x_2, t) &= x_2 \\ f_2(x_1, x_2, t) &= x_1 - 1 - a_x \cos(\omega t + \phi) \end{aligned} \tag{29}$$

and the *2 x 2* Jacobian is

$$\frac{\partial f_i}{\partial f_j} = \begin{bmatrix} 0 & 1 \\ 1 & 0 \end{bmatrix} \tag{30}$$

Similarly, for the period of time where the angular momentum is negative ($\theta < 0$), the corresponding state equations are given by

$$f_1(x_1, x_2, t) = x_2$$
$$f_2(x_1, x_2, t) = x_1 + 1 - a_x \cos(\omega t + \phi) \tag{32}$$

and, again, the *2 x 2* Jacobian is

$$\frac{\partial f_i}{\partial f_j} = \begin{bmatrix} 0 & 1 \\ 1 & 0 \end{bmatrix} \tag{33}$$

for *i, j =1,2.* The measurement function, h, is defined by

$$h(x) = Hx = \begin{bmatrix} 1000 & 2 \\ 10 & 100 \end{bmatrix} \begin{bmatrix} x_1 \\ x_2 \end{bmatrix} \tag{34}$$

For the application here, it is sufficient to define the measurement functions as linear functions of the state variables as indicated.

Figure 6 plots the noise free phase space with corresponding primary resonance points while Figure 7 plots the Iterated Kalman Filter result for the rocking response with the noise addition and including the same two primary resonance points (as defined in Part I and King 2006). In this particular case, the unfiltered noisy case toppled rather quickly (Figure 8). Comparisons of the structure of the filtered phase space with the noise free phase space show that the overall dynamic structure appears to be maintained. This is fortunate for purposes of control.

The Iterated Kalman Filter for this case utilized two measurement values and 4 Gauss-Newton iterations per time step in order to achieve the desired filtered response. Notice that these values can be adjusted as necessary to meet the needs of the filter.

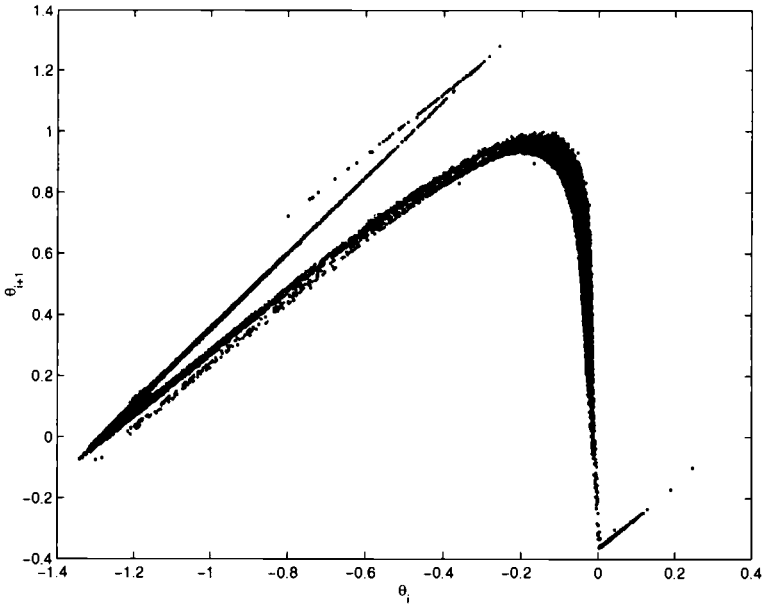

Figure 6 - The phase space of the noise free rocking response.

The questions of whether the underlying dynamics of the system are preserved is of importance for control. Because the filter itself is built upon intimate knowledge of the nonlinear dynamics, it is reasonable to expect that the important invariants are

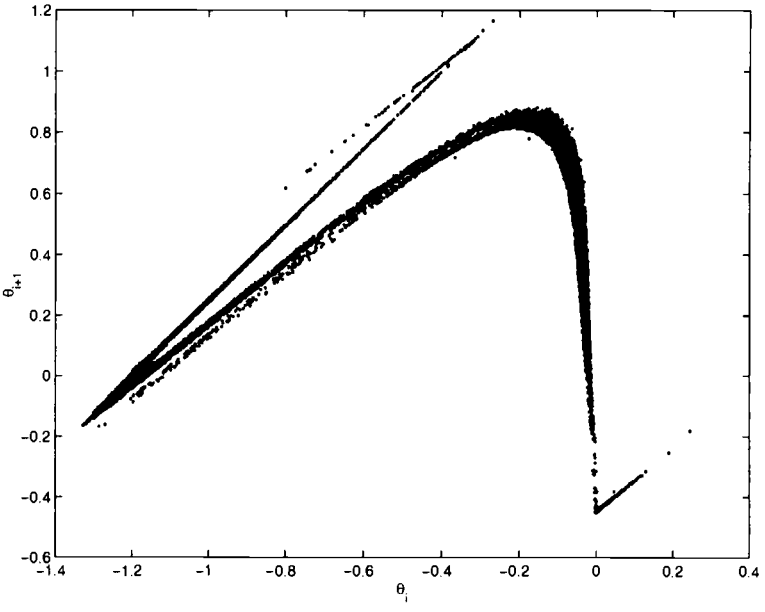

Figure 7 - The phase space representation of the filtered response of the rocking block with primary resonance points.

preserved. Figures 6 and 7 seem to indicate that at least some of invariants such as topological transitivity are preserved through the filtering technique. However, in order for the controller defined in Part I to be effective under the case of increasing noise, it is important to understand whether the structure of unstable periodic orbits are preserved under the nonlinear filtering.

Figure 9 plots the points of two of the possible primary resonance cases. Data utilized here were

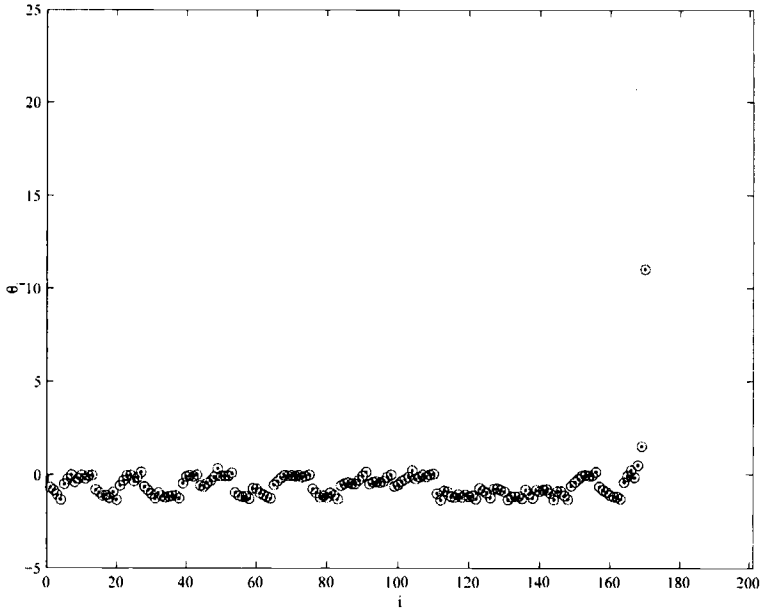

Figure 8 – Poincarè Points of the noisy rocking response exhibiting capsizing of the free standing equipment.

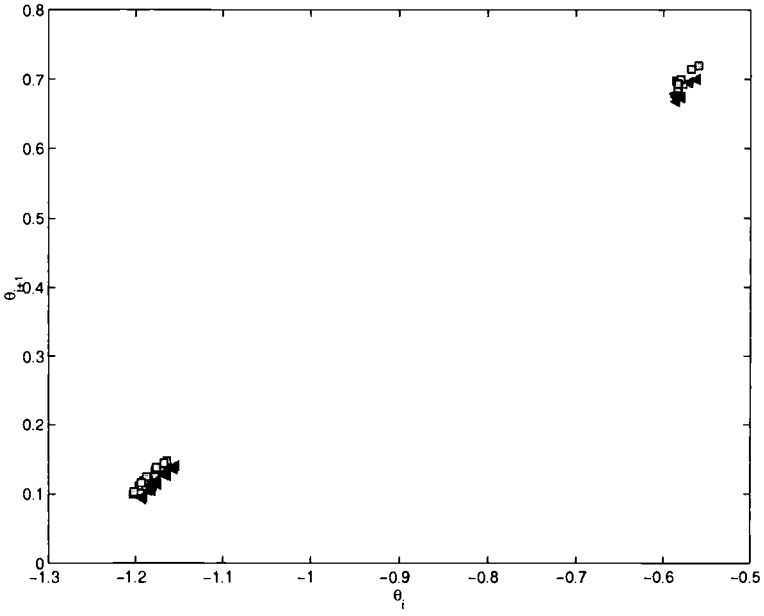

Figure 9 - Effects of nonlinear filtering on the primary resonance unstable orbits.

obtained from the data sets used to create the plots exhibited in Figures 5 and 6. From this, it appears that the primary resonance case is maintained with only a slight variation in the underlying structure of the unstable cycles. (This variation is a direct effect of the nonlinear filter itself.)

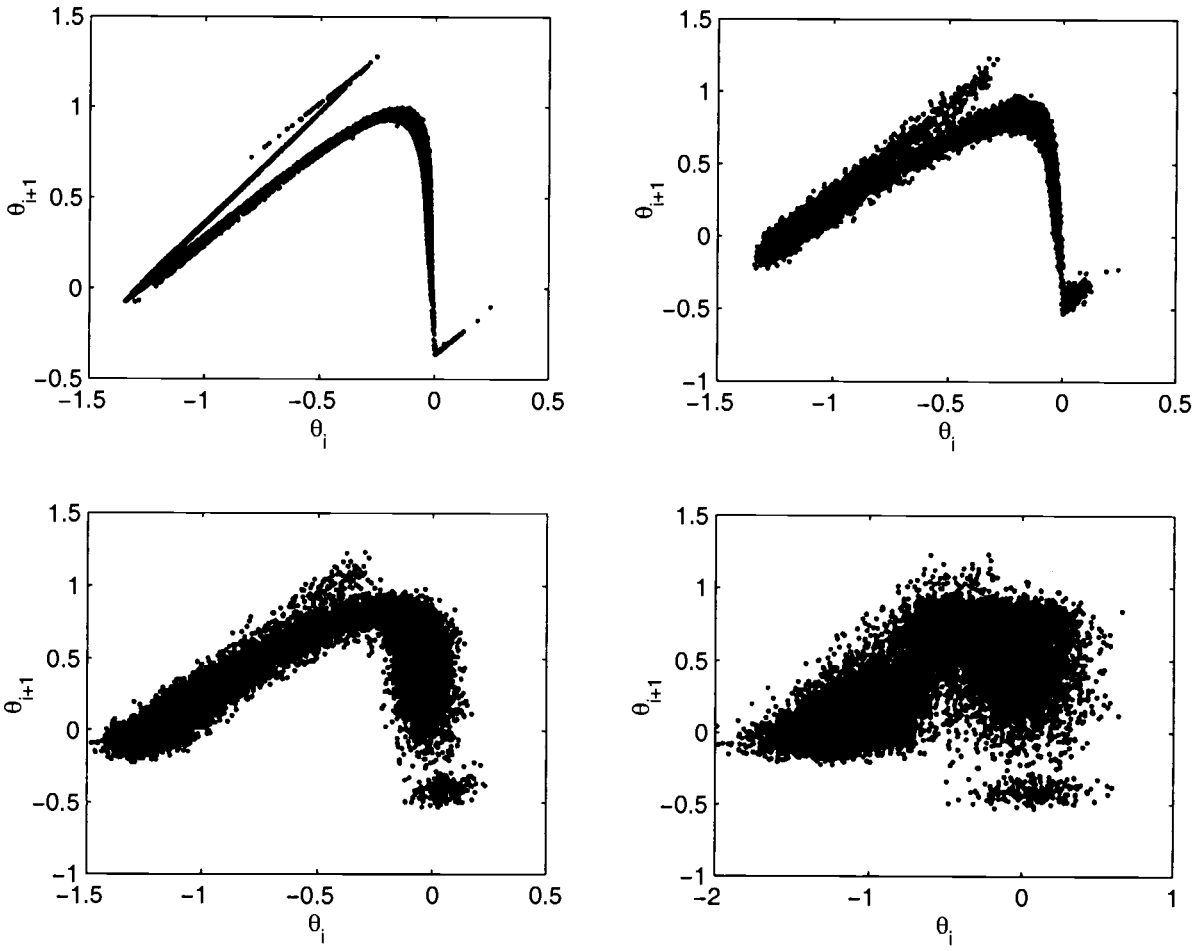

Figure 10 – Increased levels of noise on the rocking system dynamics and the structure of the invariant attractor after application of the Iterated Kalman Filter.

As indicated previously, increasing the level of noise has the effect of destabilizing the complex motions of the system. Part I detailed how this occurs while Part II indicated a means of controlling the system with moderate levels of noise. Figure 10 plots the effects of increasing the noise levels on the system phase portrait and after applying the Iterated Kalman Filter. Of interest is the maximum achievable level that can be successfully filtered and yet still maintain the necessary underlying dynamics in order to instigate control. In this case, the signal to noise ratio is decreased from the deterministic case (SNR>>0.0) to a signal to noise ratio of near unity. Figure 11 plots the corresponding effects on the points defining the primary resonance states identified earlier. Notice how the noise destabilizes the resonance cases and in particular the primary resonance case corresponding to Figure 5 in Part I is completely destabilized by the time the SNR surpasses 4.

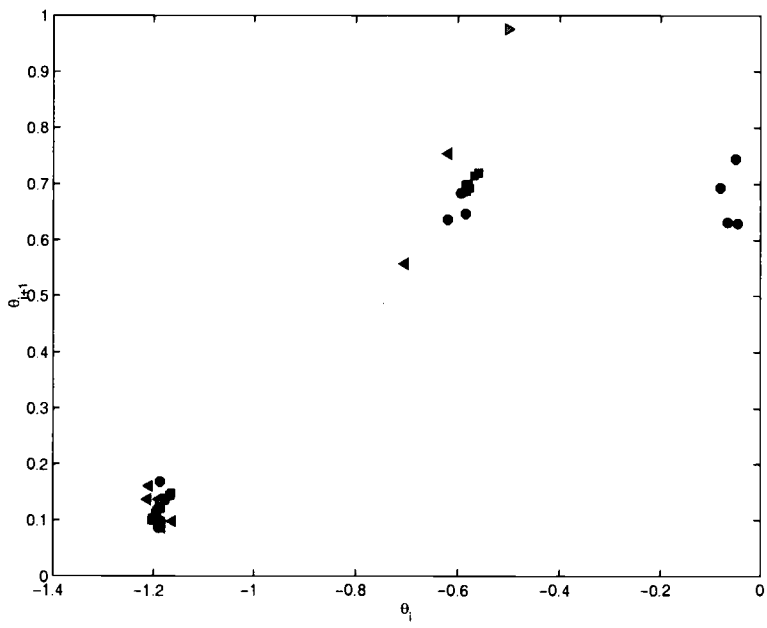

Figure 11 – Effects of increasing noise level on the two primary resonance points. Squares indicate the noise free case, circles for case b in Figure 6, left triangle for case c and right triangles for the final case.

Meanwhile, the primary resonance case corresponding to Figure 6 in Part I maintains coherence until the SNR begins to near unity at which case, the system dynamics are indistinguishable from the noise. The reason for this can be explained since for this example, the amplitude of motion is quite small and therefore the noise doesn't have as much of a relative effect. That is, since the motion has small amplitude, the noise contribution is much smaller and the system behaves better for longer. This gives an indication of where control should be maintained as well, since this also implies that smaller amounts of energy will be required to maintain control.

5.6 Concluding Remarks

These two papers outline a methodology for controlling the potentially catastrophic, unstable, highly nonlinear oscillations of free-standing equipment or structures placed in offshore and seismic environments. The proposed method is designed to avoid such dangerous situations and is developed through a modification of the OGY method in which a system parameter must be available for adjustment in order to change the dynamics of the system. Here, a physical device is placed on the system which applies a moment to the nonlinear system in order to perturb the system trajectory towards a stable eigenvector of the linearized first return map. In effect, this modification adjusts an observable of the system, the angular position or angular velocity, in order to maintain control.

The method employs the Iterated Kalman Filter in order to obtain an unstable periodic fiducial trajectory of the system which can then be utilized in an advantageous way. Since it is known that these unstable trajectories are dense within this class of nonlinear system, stable characteristics of the system can be targeted with success. That is, observing that there exists a multitude of unstable, periodic orbits, one can utilize the locally linear dynamics about these orbits to build a feedback control law capable of rendering the nonlinear oscillations periodic. An outline of the methodology was presented in Part I with several examples pertaining to the rigid rocking block system. These examples clearly demonstrated the successful control of the highly nonlinear and complex responses of the system, reducing the complex motions to selected desirable periodic motions through the use of a simple standard control technique (pole placement). The force required to maintain control was also investigated where it was shown that through the discrete application of the controller, the ratio of the force applied by the controller to the force of the external excitation is small.

Noise will naturally exist in any real seismic or ocean environment, whether introduced through a noise component in the excitation or through measurement noise. An attempt was made to exhibit that this noise component causes problems with the deterministic controller and to what extent the deterministic controller maintained a robust operating state. In the case that the noise level is relatively small compared to the forcing amplitude, it was shown that the proposed control methodology was not sufficiently robust against these disturbances. However, a simple modification to the

controller was developed in this study to increase the effectiveness of the control in the presence of a decreasing signal to noise ratio (increasing noise intensity). By stroboscopically sampling the time series at every $2\pi/r\Gamma$ intervals, where r is the number of sections desired, r separate controllers can be constructed which are evenly distributed about an unstable cycle. This modification decreases the long term effects of the noise with respect to an individual controller. This extension appears to yield a logarithmic growth in the amount of noise that the system is able to handle up to the point where the noise intensity overpowers the system controller and toppling occurs. Further research into this area is necessary.

Methods of decreasing the effects of the noise further were investigated as well. These methods include filtering and stochastic projection, both of which try to reconstruct the deterministic nonlinear dynamics from the noisy data. Continuing the effort to expand on the realm of controllability, variants of the Kalman Filter were investigated. Specifically, the Iterated Kalman Filter was implemented in order to filter the band limited noise introduced through the base excitation as well as through measurement error. This technique was successful in filtering the noise while maintaining the important dynamic invariants of interest.

Finally, although the proposed methodology utilizes linear control theory, highly complex, nonlinear oscillations can be controlled in these systems. This is true because the methodology utilizes the systems sensitivity and topological transitivity to an advantage. Moreover, since the controller applies small perturbations to the system

trajectory, on the scale of several orders of magnitude less then the forcing amplitude, little energy is required in the implementation. More advance control techniques, such as optimal control, etc., can be applied to achieve gains in cost or energy saving (Abarbanel, 1997). Note that the methodology is equally applicable to many offshore and land-based structural systems where there is a potential for highly nonlinear and possibly chaotic responses.

5.7 Acknowledgment

The authors wish to acknowledge the financial support of the United States Office of Naval Research (Grant No. N0001-92-J-1221 and N00014-04-10008) and the U.S. Department of Energy.

5.8 References

Abarbanel, H. D. I., Korzinov, L., Mees, A. I., and Starobinets, I. M. (1997). "Optimal control of nonlinear systems to given orbits." *Systems & Control Letters*, **31**, 263-76.

Anderson, B. D. O., and Moore, J., B. (1979). *Optimal Filtering,* Prentice Hall.

Bell, B. M. and Cathey, F. W. (1993). "The Iterated Kalman Filter Update as a Gauss-Newton Method," *IEEE Trans. on Automatic Control*, Vol. 38, No. 2, 294-297.

Bell, B. M. (1994). "The Iterated Kalman Smoother as a Gauss-Newton Method," *SIAM J. Optimization*, Vol. 4, No. 3, 626-636.

Bertsekas, D. P. (1996). "Incremental Least Squares Methods and the Extended Kalman Filter," *SIAM J. Optimization*, Vol. 6, 807-822.

Cazelles, B., Boudjema, G. and Chau, N. P. (1995). "Adaptive control of chaotic systems in a noisy environment," *Phys. Lett. A*, 196, pp. 326-330.

Fowler, T. B. (1986). *Stochastic Control of Chaotic Nonlinear Systems*, PhD Dissertation, George Washington University, 285 pps.

Fowler, T. B. (1988). "Stochastic Control Techniques Applied to Chaotic Nonlinear Systems," *Proc.1988 IEEE Int. Symp. on Cir. and Sys.*, Vol. 1-3, Helinki, Finland, 5-9.

Fowler, T. B. (1989). "Application of Stochastic Control Techniques to Chaotic Nonlinear Systems," *IEEE Trans. Automatic Control*, Vol. 34, No. 2, 201-205.

Julier, S. J. and Uhlmann, J. K. (1997). "A New Extension of the Kalman Filter to Nonlinear Systems," *Proc. of AeroSense: The 11th Int. Symp. on Aerospace/Defense Sensing, Simulation and Controls.*

King, P. E. and Yim, S. C. (1997). "Control of Noisy Chaotic Motion in a System with Nonlinear Excitation and Restoring Forces," *Chaos* **7**(2), 290-300.

King, P. E. (2006). *Deterministic and Stochastic Control of Nonlinear Oscillations in Ocean Structural Systems*. PhD Dissertation, Oregon State University, Corvallis, OR, 97331.

King, P. E. and Yim, S. C. (2006) "Nonlinear Rocking Responses of Free Standing Rigid Block, Part I, Deterministic Control," *J. Engrg Mech.*, ASCE, submitted.

Lin, H. and Yim, S. C. S. (1996a). "Nonlinear rocking motions. I: Chaos under noisy periodic excitations." *J. Engrg Mech.*, ASCE, Vol. 122(8), 719-727.

Maybeck, P. S.(1982). *Stochastic Models, Estimation and Control*, Volume 2, Acedimic Press, New York.

Walker, D.M. and Mees, A.I. (1997). "Noise reduction of chaotic systems by Kalman filtering and by shadowing", *International Journal of Bifurcation and Chaos*, **7**(3), pps 769-779.

Walker, D.M. (1998). "Local filtering of noisy nonlinear time series", *Physics Letters A*, **249**, pps 209-217.

Walker, D.M. and Mees, A.I. (1998). "Reconstructing nonlinear dynamics by extended Kalman filtering", *International Journal of Bifurcation and Chaos*, **8**(3), 557-569.

Walker, D.M., Allie, S.P. and Mees, A.I. (1998). "Exploiting the periodic structure of chaotic systems for noise reduction of nonlinear signals", *Physics Letters A*, **242**, pps. 63-73.

6. CONCLUSIONS

This study examines the application of small perturbations to efficiently drive the complex responses of a nonlinear system to arbitrarily selected harmonic responses. Specifically, two separate nonlinear systems were utilized in order to test the ability to control the highly sensitive oscillations found in these, and other, ocean structural systems. The first of the two nonlinear dynamical systems introduced was that of a submerged, moored structure in the ocean environment subject to wave and current excitation. An example of such a system is a moored barge or a sonar buoy tethered in a fixed location. The dynamical system is modeled as a low degree of freedom system by considering cases for which the small body theory applies. This assumes that the structure does not influence the wave field, allowing for the nonlinear fluid loads to be approximated in terms of an added inertia and a nonlinear coupling. This, together with restraints on vertical and rotational motion and, by approximating the nonlinear mooring resistance with a low order polynomial, yields the desired low order dynamics. The second system investigates equipment that is not affixed to its mounting platform and which may be located where the base may undergo excitation in the horizontal and vertical directions. These situations are typically found in ocean and seismic situations where the 'base' oscillation can transfer unwanted motions to the equipment. That is, it can be shown that through the base support excitation, these "rocking blocks"

can also be set into highly nonlinear complex motions. Chapters 2 and 3 of this dissertation give a brief analysis of the complex oscillations exhibited by these disparate ocean structural systems.

The nonlinear dynamics of the ocean structural systems have been demonstrated to exhibit chaotic oscillations under certain environmental conditions. This phenomenon has been calibrated on data obtained from experiments for both systems under consideration. For this reason, the control of these oscillatory states is of interest. This study outlines a method for controlling these chaotic motions by small perturbations to the system trajectory. The method utilizes the structure of the chaotic time series to an advantage. By categorizing the nonlinear dynamics by mapping the time series to a Poincaré section and then obtaining the unstable periodic orbits through an exhaustive search of the Poincaré points, some of the interesting dynamics are obtainable. This methodology produces a locally linear map for which the pole placement method of feedback control can be applied. The method was then applied to the two different models to verify control.

An extension of the method was investigated to achieve a more robust controller under the circumstances that additive noise is present in the excitation force. This extension applies the same algorithm of control design to a series of Poincaré sections produced by stroboscopically sampling every $2\pi/r\Gamma$, where r is the number of sections desired and Γ is the fundamental frequency of the system. This yields r separate controllers evenly distributed about an unstable cycle, thus

decreasing the long term effects of the noise with respect to an individual controller. This extension appears to yield at least a linear growth in the intensity of noise that the system is able to handle. Meanwhile, a means of investigating the power required to maintain control of the nonlinear oscillations during a particular crossing of the Poincaré plane was presented as well. This analysis investigated the equilibrium equations of motion to formulate a form for the instantaneous power required to instigate the necessary shift in position and velocity in order to move the trajectory towards the stable eigenvector of the linearized system.

This method appears to be ideal for nonlinear systems for which there is little noise present. With small adjustments, the system can be driven to any desired state. This is particularly attractive if, for instance, it is undesirable for the nonlinear system to become locked in primary resonance. The controller can be used to ensure that the resulting oscillatory state is not one of these predefined undesirable modes of oscillations. The papers presented in Chapters 2 and 3 discuss the specific results of the two ocean structural systems in question. Recall that the important difference between these two nonlinear dynamical systems is that in the mooring system the nonlinear oscillations can be considered steady state (in a macro sense) while in the rocking system the nonlinear oscillations cannot be considered steady state due to the fact that the block can topple. However, the control algorithm works equally well for either case as long as in the later case, control is instigated prior to toppling.

Currently there are several limitations to the methodology outlined. First, as is evident in the controller design, it is necessary for the system trajectory to come arbitrarily close to the desired trajectory before the controller can be applied. However, means of targeting a trajectory do exist in linear control theory. These methods may be extended for this case also. More importantly though, the addition of increasing levels of system or structural noise is of concern. In order to combat this, the Iterated Kalman Filter was investigated to determine whether the noise could be mitigated. Because the first step of the control algorithm is to create a locally linear map of the system in question where all subsequent actions are taken, it was postulated that the theory of Kalman Filtering was applicable even though the overall dynamics are nonlinear in nature. Chapters 3 and 4 apply the Iterated Kalman Filter to the dynamical systems in order to investigate whether this notion with stood the implementation without proof. It was found through this work that the Iterated Kalman Filter behaved well under these conditions for both of the systems.

Finally, although the proposed methodology utilizes linear control theory, highly complex, nonlinear oscillations can be controlled in these systems. This is true because the methodology utilizes the systems sensitivity and topological transitivity to an advantage. Moreover, since the controller applies small perturbations to the system trajectory, on the scale of several orders of magnitude less then the forcing amplitude, little energy is required in the implementation.

More advanced control techniques, such as optimal control, etc., can be applied to achieve gains in cost or energy saving. Note that the methodology is equally applicable to many offshore and land-based structural systems where there is a potential for highly nonlinear and possibly chaotic responses.

APPENDIX A UNSTABLE PERIODIC ORBITS

A means of analyzing the complex motions of chaotic systems by using the time series alone has been introduced[1,2] The procedure utilizes the unstable periodic orbits of a system to an advantage. Since a chaotic attractor contains a multitude of UPO's of varying periodicities, much of the nonlinear characteristics can be identified through these special cycles. It is well known that UPO's are dense on a chaotic attractor,[3] and in fact this is a necessary condition for chaos to exist.[4] This characteristic of a chaotic system is exploited in the following discussions.

It is instructional to formalize the notion of a Poincaré section here. This method was originally devised by Henri Poincaré in the 1890's in an effort to understand the N-body problem of planetary motion.[5] The Poincaré section is a method of inspecting the

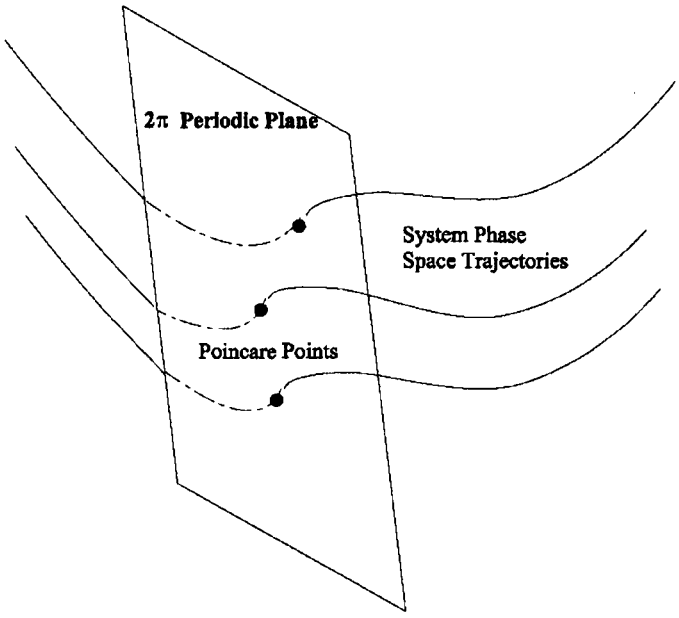

Figure A.1 - Periodic Sampling of a time series to create a Poincaré section.

continuous time phase space of a periodically driven system by projecting it onto a discrete time phase space by sampling the phase space variables at discrete time intervals. A natural choice for the discretization interval is that of the natural period, $T_f = 2\pi/\omega$, where ω is the driving frequency of the system. Figure A.1 is a schematic of this operation where the flow of the system, the 3-D phase portrait, is sampled at regular intervals. These sampling points are then plotted against one another. That is, if $Z(t)$ is a point sampled in this manner and $Z(t+T_f)$ is the next point, then $Z(t)$ is plotted against $Z(t+T_f)$. The relationship between the points $Z(t)$ and $Z(t+T_f)$ is called the Poincaré map. The Poincaré map proves to be a useful tool in understanding and manipulating chaotic dynamical systems. This method is sometimes called stroboscopic sampling for obvious reasons.

Since the nonlinear dynamical system is deterministic, so too is the Poincaré map. This is true due to the fact that any point on the continuous trajectory, $x(t)$, uniquely determines a point at a later time, $x(t+T_f)$. Thus, if $Z(t) = x(t)$, that is, the point is on the Poincaré plane, then $Z(t)$ uniquely determines $Z(t+T_f)$. $Z(t+T_f)$ is the image of $Z(t)$ on the Poincaré plane and there exists a deterministic map relating $Z(t)$ and $Z(t+T_f)$, $Z(t+T_f) = F(Z(t))$. It must be noted that the map, F, relating $Z(t)$ to $Z(t+T_f)$ is not easily determined in general.

Studying the dynamics on the Poincaré section has certain advantages. These

include the decrease in dimension. At least one of the variables is eliminated. In this case, time is eliminated explicitly from the dynamics. The Poincaré map transforms the points on the section according to the dynamics of the continuous nonlinear system. Therefore, the invariants of the three dimensional set are transformed to the Poincaré map as well. Because of this, remarkable insight can be gained by studying these lower dimensional systems. This is true for unstable periodic orbits as well. However, instead of having to study the flow in order to identify the unstable periodic orbits, all that is required is to study the reduced system.

An unstable periodic orbit of a chaotic system is defined as an orbit or cycle of the system which has the property that it is both periodic and unstable. That is, if a trajectory of the system is on a cycle, it will remain on it for all time. However, if there is any minute deviation from the cycle, then the chaotic trajectory will diverge from this unstable cycle at an exponential rate. Because of the "mixing property" of a chaotic attractor (topological transitivity), at some time later the trajectory will again come arbitrarily close to the UPO. It appears that a large portion of the unstable cycles in a chaotic system have low periodicity. For example, it is reported that 84% of the cycles in the Rössler System have period less then 16,[6] while 95% of the recurrence times (a measure related to periodicity) in the Belousov-Zhabotinskii (B-Z) chemical reaction are found in a small number of intervals, or equivalently, periodicities.[1]

The characteristic of an unstable periodic orbit returning arbitrarily close to a given unstable cycle, arbitrarily often, can be exploited. If the chaotic system is allowed to evolve long enough, then a trajectory will eventually come close to the UPO (in theory, there does exist a set of initial conditions of measure zero for which the time evolution of the chaotic attractor will never come close to the UPO). Because of this fact, one can obtain the stability characteristics of an unstable cycle through an analysis of the rate of divergence from the unstable cycle. At least locally, this can be accomplished by studying the eigenvalues of the linearized system about the cycle in question. Moreover, by examining a large number of the periodic cycles, certain global invariants of the chaotic attractor can be identified, including the topological entropy,[2] the Hausdorff dimension,[2] the multifractal spectrum,[3] and the Lyapunov spectrum.[7] These global invariants give a measure of the complexity of the system and hence are useful in its characterization.

Suppose that a time history of a chaotic system, x(t), is available. Let $\eta > 0$ be given, then at some time t in the time series, $|x_p - x_t| < \eta$ and the chaotic trajectory has come arbitrarily close to the UPO, x_p, of period p. At some time Y later $|x_p - x_{t+Y}| < \eta$ and the trajectory has come close to the UPO again. Often times, Y is selected as an integer multiple of the period of excitation. In order to identify the unstable cycle of period p, a search through the data set for all points separated by Y time steps that are

a distance of η apart is performed. Since η is arbitrary, it is possible for points of two distinct periodic orbits to be grouped as one. It is necessary to be able to tell these distinct periodic orbits apart hence, not only are the points that are identified used to characterize the unstable cycle, but their images under iteration are also used. This is done by restricting the points of interest to those with iterates within $\delta > \eta$ of each other, $|x_{p+l}-x_{t+l}| < \delta$. That is, all points such that $|x_p-x_t| < \eta$ and $|x_p-x_{t+Y}| < \eta$ are considered and that $|x_{p+l}-x_{t+l}| < \delta$ to ensure that only one cycle is included and not several nearby cycles.

In practice, this is typically performed on a Poincaré section. For continuous time dynamical systems with periodic driving force, a natural choice of the sampling interval is that of the driving period ($Y = \Gamma$). Let Z_i be a point on the Poincaré section and suppose Z_p is an unstable periodic point on the section representing the UPO of period p. Then, the algorithm for calculating the UPO consists of searching the data set on the section, $\{Z_i\}^N_{i=1}$, for all points that are within η of Z_p. Once these points have been identified, their corresponding image, or next iterate, is investigated. The set of points whose images are within δ, $|Z_p-Z_{i+p}| < \delta$, for some $\delta > \eta$, are considered to correspond to that UPO, otherwise they correspond to a different UPO and are not further considered for control purposes (Figure A.2).

A linear map representing the local dynamics of the UPO is constructed by

using a least squares procedure. This is accomplished by creating the vectors $D = \{d_i\}$ and $E = \{e_i\}$, where the d_i's are the deviations of the points from the UPO under consideration, $d_i = Z_i - Z_p$, and the e_i's are the deviations of the iterates from the image of the UPO, $e_i = Z_{i+\Gamma} - Z_{p+\Gamma}$. The point corresponding to the UPO, Z^*, is taken as the centroid of points under consideration. The linear map A (an n *x* n matrix, where n is the dimension of the Poincaré section, usually taken as 2) is calculated by a least squares method which minimizes the error orthogonal to the approximate solution of the matrix equation $||DA-E||^2$, which, since D and E are vectors, has a solution given by $A = \text{inv}(D^T D)\, D^T E$.[8]

The stability characteristics of the UPO are governed by the eigenvalues of the map A.

Now, for purposes of control, the length of time for the system to reach the η-ball from an arbitrary set of initial conditions is random.

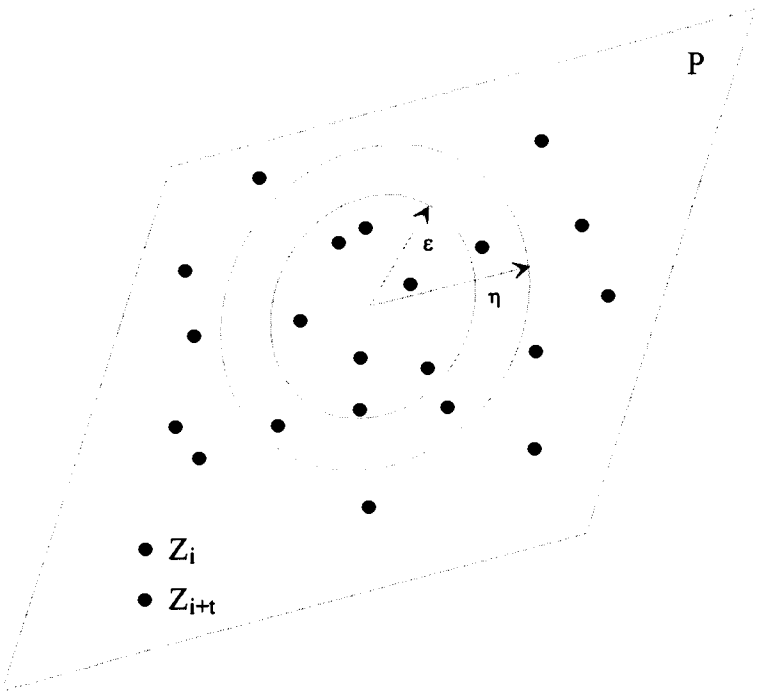

Figure A.2 - Estimating unstable periodic points on a Poincaré Plane

The probability distribution of this chaotic transient is exponential with average transient length $<\tau> \sim \Delta^{-\kappa}$ for $\kappa > 0$. κ is the scaling exponent and Δ is the maximum allowable deviation imparted by the controller.[9] For a two-dimensional diffeomorphism, the scaling exponent is expressed as[10]

$$\kappa = 1 + \frac{1}{2} \frac{\ln|\lambda_u|}{\ln(1/|\lambda_s|)} \qquad \text{(A.1)}$$

where λ_u and λ_s are the unstable and stable eigenvalues of the unstable periodic orbit, respectively.

References

1. Lathrop, D. P. and Kostelich, E. J., "Characterization of an Experimental Strange Attractor by Periodic Orbits.', Phys. Rev. A, Vol. 40, No. 7, pp 4028-31, Oct. 1989.

2. Auerbach, D., Cvitanovic, P., Eckmann, J.-P.,Gunaratne, G., and Procaccia, I., "Exploring Chaotic Motion Through Periodic Orbits", Phys. Rev. Lett., Vol. 58, No. 23, June 1987, pp 2387-89.

3. Grebogi, C., Ott, E., and Yorke, J. A. (1988). "Unstable Periodic Orbits and the Dimensions of Multi-fractal Chaotic Attractors," *Phys. Rev. A*, Vol. 37, No. 5, 1711-24.

4. Devaney, R. L. (1987). *An Introduction to Chaotic Dynamical Systems*, Addison-Wesley, New York, 320 pps.

5. Thompson, J. M. T. and Stewart, H. B. (1986). *Nonlinear Dynamics and Chaos*, John Wiley & Sons, New York.

6. Corney, S. (1997), "Control of Chaos in the Rössler System," *Aust. J. Phys.*, **50**, pps. 263-79.

7. Sano, M. and Sawada, Y. (1985). "Measurement of the Lyapunov Spectrum from a Chaotic Time Series", *Phys. Rev. Lett.*, No. 55, 1082-85.

8. Strang, G. (1986). *Introduction to Applied Mathematics*, Wellesley-Cambridge

Press, Wellesley, Massachusetts.

9. Grebogi, C. and Lai, Y.-C. (1997). "Controlling Chaotic Dynamical Systems", *Systems & Control Let.*, No. 31, 307-12.

10. Ott, E., Grebogi, C., and Yorke, J. A. (1990), "Controlling Chaotic Dynamical Systems", in *CHAOS/XAOS, Soviet-American Perspective on Nonlinear Science*, Ed. By D. Campbell, Am. Inst. Phys., New York.

APPENDIX B POLE PLACEMENT

Once a periodic cycle has been selected and the corresponding linear map, A, is calculated, control of the system about this cycle can be maintained by applying a state feedback control law to the system. Figure B.1 is a state feedback diagram indicating the flow of information through the dynamical system. For the problem under consideration, the state feedback controller applies a small perturbation to the chaotic trajectory about the UPO. This action is performed on the Poincaré plane and hence is a discrete controller for a continuous dynamical system. The system is allowed to oscillate chaotically until the first time the trajectory enters within the η-ball of the chosen UPO on the Poincaré plane. Once within this ball, the feedback controller applies a small perturbation to the measured signal, in the direction of the stable eigenvector of the linear map. This action ensures that upon the next return to the Poincaré section the trajectory is still within η of the UPO. Figure B.2 is a schematic of this operation on the

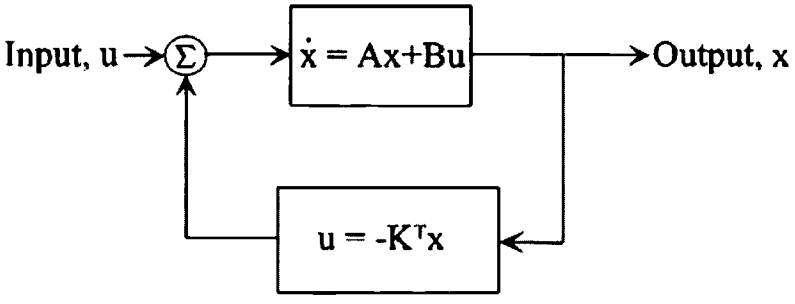

Figure B.1 - State feedback diagram for a linear (time varying) system.

Poincaré section in which the point Z_p, is perturbed toward the stable eigenvector of the UPO.

A means of finding the magnitude and direction of the perturbation is obtained by employing the pole placement method. The pole placement method is a state feedback rule devised to render the eigenvalues of the controlled system stable.[1] Mathematically,

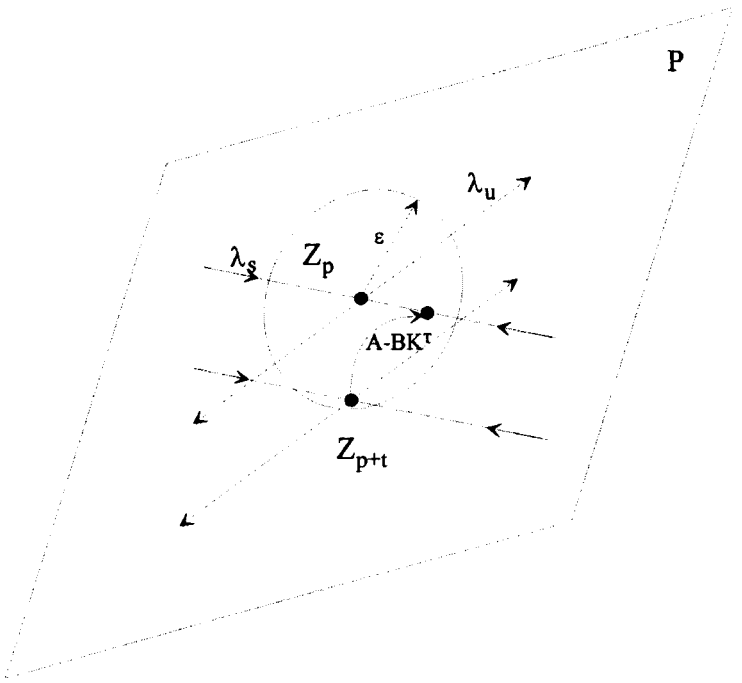

Figure B.2 - Control of the unstable periodic orbit on the Poincare Plane via Pole Placement.

the goal of this method is to construct a matrix, called a gain matrix, which assigns the poles of the controlled system in prescribed positions. The action of assigning the poles of the controlled system is sometimes called the spectral assignability problem. In order to solve the general problem of spectral assignability, the canonical single input case is first considered. Then, a means of constructing a transformation matrix from a general single-input system to the canonical single-input system is explored.

The general multi-input case becomes an exercise in transforming the multi-input case into the canonical single input case. Using the spectral assignability technique identified for the canonical single input case, a feedback matrix is constructed for this system and then the inverse transformations are applied to the feedback matrix to obtain the feedback matrix for the multi-input case. Since the transformation matrices are similarity transformations, the eigenvalues will remain the same for both the canonical single input case and the general multi-input case, ensuring that the system remains stable under these transformations.

The controllable canonical form is a convenient means of representing a linear dynamical system. The controllable canonical form is the system defined by the state model

$$\dot{x} = \hat{A}x + \hat{b}y \tag{B.1}$$

where the matrices $\hat{A}$ and $\hat{b}$ are given by the special forms

$$\hat{A} = \begin{bmatrix} 0 & 1 & 0 & \cdots & 0 & 0 \\ 0 & 0 & 1 & \cdots & 0 & 0 \\ \vdots & \vdots & \vdots & & \vdots & \vdots \\ 0 & 0 & 0 & \cdots & 0 & 1 \\ -\hat{a}_n & -\hat{a}_{n-1} & -\hat{a}_{n-2} & \cdots & -\hat{a}_2 & -\hat{a}_1 \end{bmatrix} \qquad \hat{b} = \begin{bmatrix} 0 \\ 0 \\ \vdots \\ 0 \\ 1 \end{bmatrix} \tag{B.2}$$

Then, by expanding the determinant of $\hat{A}$-λI about the bottom row, we see that the characteristic polynomial $\pi_A(\lambda) = \det\{\hat{A} - \lambda I\}$ is

$$\pi_A = (\lambda - \lambda_1)(\lambda - \lambda_2) \cdots (\lambda - \lambda_n) = \hat{a}_n + \hat{a}_{n-1}\lambda + \cdots + \hat{a}_1\lambda^{n-1} + \lambda^n \quad \text{(B.3)}$$

Consider the dynamical system (linearized within the η-ball) represented by the state-space system

$$\dot{x} = Ax + bu \quad \text{(B.4)}$$

where x is the response of the system, u is the external forcing, A is the linear mapping and b is the input vector. Assume, furthermore, that the pair (A, b) is in controllable canonical form. Suppose that the external forcing can be written as $u = u_c + u_e$ where u_c describes a control input and u_e is the usual external excitation. Next, consider a feedback law of the form $u_c = -K^T x$, then Equation (B.4) can be rewritten as

$$\dot{x} = (A - bK^T)x + bu_e \quad \text{(B.5)}$$

The homogeneous portion of Equation (B.5) determines the linear systems natural

behavior, hence if the external excitation is ignored and the subscript from u_c is dropped, then a feedback of the form $u = - K^T x$ can be considered and Equation (B.5) takes the form

$$\dot{x} = (A - bK^T)x \tag{B.6}$$

The goal is to find a gain vector K^T such that the eigenvalues of the matrix $(A - bK^T)$ are asymptotically stable,[2] i.e. $|\lambda_i| < 1$ for i=1...n, this ensures that the fixed points of the associated system are stable. The eigenvalues of the matrix $(A - bK^T)$ are called the regulator poles while the problem of placing these poles in an appropriate spot on the complex plane is called the pole placement problem.[3] The solution to this problem lies in the fact that one is free to choose K^T in an advantageous way, as long as the eigenvalues have the appropriate characteristics. Notice that since the system is assumed to be in controllable canonical form, the state feedback matrix is

$$A - bK^T =$$

$$\begin{bmatrix} 0 & 1 & 0 & \cdots & 0 & 0 \\ 0 & 0 & 1 & \cdots & 0 & 0 \\ \vdots & \vdots & \vdots & & \vdots & \vdots \\ 0 & 0 & 0 & \cdots & 0 & 1 \\ (-a_n - k_n) & (-a_{n-1} - k_{n-1}) & (-a_{n-2} k_{n-2}) & \cdots & (-a_2 - k_2) & (-a_1 - k_1) \end{bmatrix} \tag{B.7}$$

which has characteristic polynomial

$$\pi_{A-bK^T}(\lambda) = (a_n+k_n) + (a_{n-1}+k_{n-1})\lambda + \cdots + (a_1+k_1)\lambda^{n-1} + \lambda^n = (\lambda - \lambda_1)(\lambda - \lambda_2)\cdots(\lambda - \lambda_n) = \alpha_n + \alpha_{n-1}\lambda + \cdots + \alpha_1\lambda^{n-1} + \lambda^n \quad \text{(B.8)}$$

and where the α_i's specify the coefficient's of the desired characteristic polynomial. By specifying the position of the regulator poles, one can calculate the k_i's in the gain matrix, K^T, hence solving the spectral assignability problem (for the system in controllable canonical form).

Now, suppose the pair (A, b) is not in controllable canonical form. Assume that the system is still a single input system ($b = \hat{b}$) and that the system is controllable, then a solution to the pole placement problem always exists. It can be shown that (A, b) is controllable when the n x n controllability matrix, C, has full rank, where the controllability matrix is defined by

$$C = \left[\, b \mid Ab \mid A^2b \mid \cdots \mid A^{n-1}b \,\right] \quad \text{(B.9)}$$

and where the columns of C are made up of the column vectors b, Ab, A^2b, ... $A^{n-1}b$. The system (A,b) can be transformed into controllable canonical form by introducing

the transformation matrix constructed as follows. Let ν be the last row of C^{-1} (notice that C^{-1} exists by assumption). Define the state transformation matrix Υ such that $z = \Upsilon x$ by

$$\Upsilon = \begin{bmatrix} \nu \\ \nu A \\ \nu A^2 \\ \vdots \\ \nu A^{n-1} \end{bmatrix} \tag{B.10}$$

Then, Υ^{-1} exists by construction. Applying the state transformation to the original system yields the transformed system

$$\dot{z} = \Upsilon A \Upsilon^{-1} z + \Upsilon b u \tag{B.11}$$

Define $\hat{A}=\Upsilon A \Upsilon^{-1}$ and $\hat{b}=\Upsilon b$, then the pair $(\hat{A}, \hat{b})$ have the controllable canonical form and the spectral assignability follows as before. Should the pair (A, b) not be completely controllable as assumed, then the part that is not completely controllable can still be assigned an arbitrary spectrum. The solution here relies on a nonsingular transformation which converts the state model to the Kalman controllable canonical form. The Kalman controllable canonical form identifies and extracts the completely

controllable modes of the system and then builds a state feedback controller for this portion of the problem.[4] This is mentioned here for completeness, however, for the current problem, this generalization is not required.

The control law then consists of picking the entries in the gain vector K^T so that the roots of the characteristic equation are in prescribed positions. Since the λ_i's are known, this amounts to choosing the α_i's in the characteristic polynomial $\pi_{A\text{-}bK}{}^T(\lambda)$. Then, applying the inverse transformation yields the desired control laws for the original system. Notice that the eigenvalues for the original system and the transformed system are the same since the particular transformation matrix constructed is a similarity transformation matrix. This procedure is called Ackerman's formula for pole placement.[5] For the case where A is 2 *x* 2, it can be shown that an optimal choice (in the sense of time to control) for the gain vector is $K^T = [\lambda_u, -\lambda_u\lambda_s]$, where λ_u is the unstable eigenvalue and λ_s is the stable eigenvalue of A.[19,28]

One can now formulate an algorithm to control a chaotic system utilizing this control law on a Poincaré section. First, the linear map, A, of an unstable cycle is constructed as before and its eigenvalues identified. Then, setting $x = Z_i - Z^*$ and $\dot{x} = Z_{i+1} - Z^*$ in Eq. (B.6) yields the control law for the discrete UPOs on the Poincaré section as

$$Z_{i+1}=(A - bK^T)(Z_i - Z^*) + Z^* \qquad (B.12)$$

Calculating the eigenvalues of A, λ_u and λ_s, and either using Ackerman's formula to determine specified regulator poles or by choosing $K^T = [\lambda_u, -\lambda_u\lambda_s]$ and applying Eq. (B.12) whenever the trajectory comes within η of Z^* on the Poincaré section yields the desired stability characteristics.

The relative distance on the Poincaré section for which a trajectory can be from Z^* and still be able to guarantee that the controller will perform adequately can be calculated by combining the fact that since it was required that $|Z^* - Z_{i+1}| < \delta$, by construction, combining this with Eq. (B.12) yields

$$\Delta = | Z_i - Z^* | < \frac{\delta}{| A - bK^T |} \qquad (B.13)$$

Since K^T was constructed to render the eigenvalues of the matrix $A - bK^T$ stable, and $(A - bK^T)^{-1}$ exists, this defines an area of width $2\delta / | A - b K^T |$ about Z^* for which the control should be applied.

References

1. DeCarlo, R., A.(1989). *Linear Systems, A State Variable Approach with Numerical Implementation,* Prentice Hall, New Jersey.

2. Nitsche, G. and Dressler, U. (1992). "Controlling Chaotic Dynamical Systems Using Time Delay Coordinates," *Physica D*, Vol. 58, 153-64.

3. Franklin, G. F., Powell, J. D., and Emami-Naeimi, A. (1991). *Feedback Control of Dynamic Systems,* 2nd ed., Addison-Weseley, New York.

4. Romeiras, F., J., Grebogi, C., Ott, E., and Dayawansa, W., P. (1992). "Controlling Chaotic Dynamical Systems", *Physica D*, Vol. 58, 165-92.

5. Anderson, B. D. O., and Moore, J., B. (1979). *Optimal Filtering,* Prentice Hall.

APPENDIX C KALMAN-BUCY FILTER

The Kalman Filter[1] addresses the general problem of estimating the state of a first order, discrete time system that can be represented as a system of linear difference equations. (For the purposes here, it suffices to consider only the discrete time Kalman Filter.) Consider the system of equations

$$x_{k+1} = Ax_k + Bu_k + w_k \tag{C.1}$$

with the measurement equation

$$z_k = H\,x_k + v_k \tag{C.2}$$

where $x_k \in \Re^n$ is the state variable, A is an $n \times n$ matrix of state coefficients relating the state at time k to the state at time k+1 in the absence of either a driving force or process noise. $u_k \in \Re^n$ is the vector of control inputs while B is an $n \times l$ matrix that relates the control inputs to the state. w_k represents the process noise. Similarly, $z_k \in \Re^m$ is the measurement, H is an m x n measurement matrix which relates the state to the measurement and v_k is the measurement noise.

The process and measurement noise are assumed to be white noise with normal probability distributions given by

$$p(w) = N(0,Q) \tag{C.3}$$

$$p(v) = N(0,R) \tag{C.4}$$

and are assumed to be independent of one another. In practice, the noise covariance Q is either determined on some basis of intuition, or it is guessed. Similarly, the measurement covariance, R, is provided by a signal processing algorithm or is again guessed. And, in general, the noise levels are determined independently, hence there are no correlations between the two noise processes.

In order to estimate the state in the presence of the noise through the measurement, z, Kalman introduced the optimal recursive estimation procedure for linear discrete time systems. The method utilizes previous estimates of the state and the current measurement to estimate the state at the current time. That is, let $\hat{x}_k^- \in \Re^n$ denote the a priori state estimate at time step k given the knowledge of the system prior to step k. Notice that the "super minus" indicates that this is the estimate at this time. Then, let $\hat{x}_k \in \Re^n$ be our a posteriori estimate at step k given measurement z_k. We define the a priori and the a posteriori error estimate as follows:

$$e_k^- \equiv x_k - \hat{x}_k^- \tag{C.5}$$

and

$$e_k \equiv x_k - \hat{x}_k \tag{C.6}$$

The a priori error covariance is then

$$P_k^- = E\,[e_k^- e_k^{-T}] \tag{C.7}$$

and the a posteriori error covariance estimate is

$$P_k = E\,[e_k\, e_k^T] \tag{C.8}$$

In order to derive the equations that compute the a posteriori estimate $\hat{x}_k$ as a linear combination of an a priori estimate $\hat{x}_k^-$ and a weighted difference between an actual measurement z_k and the measurement prediction $H_k\,\hat{x}_k^-$, we must recall that the probability of the a priori estimate $\hat{x}_k^-$ is conditioned on all prior measurements, z_k (Bayes Rule). That is

$$\rho_{x|z} = \frac{\rho_{z|x}\ \rho_x}{\rho_z} \tag{C.9}$$

where $\rho_{x|z}$ is the probability of obtaining x conditioned on z, ρ_x is the prior estimate of x, $\rho_{z|x}$ is the likelihood estimate of z given prior measurements and ρ_z is independent of x. Thus, the estimate at time k is a combination of the known quantities.

Now, since the state estimate x_k is given as a linear combination of the a priori estimate and a weighted difference of the measurement and the predicted measurement, we have

$$\hat{x}_k = \hat{x}_k^- + K\left(z_k - H_k\hat{x}_k^-\right) \tag{C.10}$$

where the difference $z_k - H_k\,\hat{x}_k^-$ is the innovation (or, in some texts, the residual). The

innovation sequence reflects the discrepancy between the predicted measurement H_k $\hat{x}_k^-$ and the actual measurement z_k. A residual of zero indicates that the two are in complete agreement.

The *n x m* gain matrix K is chosen to minimize the a posteriori error covariance, Eq. (C.8). This is accomplished by substituting Eq. (C.10) into Eq. (C.6) and then substituting this result into Eq. (C.8). The indicated expectations are taken and then the derivative of the trace of the result with respect to K is taken and set to zero. One of the many forms of the gain, K, which minimizes the a posteriori covariance is given by

$$K_k = P_k^- H_k^T \left(H_k P_k^- H_k^T + R_k \right)^{-1} \tag{C.11}$$

where it is evident that as the measurement error covariance R_k approaches zero, the gain K weights the residual more heavily. That is, the actual measurement, z_k, is "trusted" more while the predicted measurement,

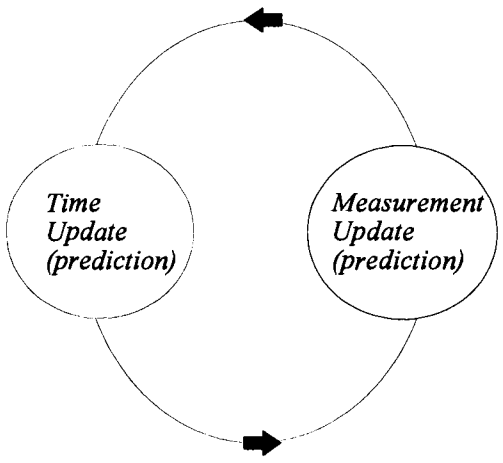

Figure C.1 - Time-measurement update cycle for the Kalman Filter.

$H_k \hat{x}_k^-$, is trusted less. On the other hand, as the a priori estimate error covariance P_k^- approaches zero, the gain K weights the residual less heavily. That is, the measurement is trusted less while the measurement is trusted more.

So, the Kalman Filter algorithm is a recursive data processing algorithm which, as it turns out, is optimal with respect to almost any criterion available. It incorporates all available measurements, regardless of their precision, to estimate the current state. The algorithm is depicted in Figure C.1 where we see that the filter cycle projects the current state estimate ahead in time and then the measurement update adjusts this prediction based on the measurement at that time.

Consider again Eqs. (C.1)-(C.2) where the system equations are allowed to vary with time:

$$x_{k+1} = A_k x_k + B_k u_k + w_k \tag{C.12}$$

with measurement equation

$$z_k = H_k x_k + v_k \tag{C.13}$$

The time update is then given by

$$\hat{x}_{k+1}^- = A_k \hat{x}_k + B_k u_k \tag{C.14}$$

$$P_{k+1}^- = A_k P_k A_k^T + Q_k \tag{C.15}$$

and the measurement update is then

$$K_k = P_k^- H_k^T \left(H_k P_k^- H_k^T + R_k \right)^{-1} \tag{C.16}$$

$$\hat{x}_k = \hat{x}_k^- + K\left(z_k - H_k \hat{x}_k^- \right) \tag{C.17}$$

$$P_k = \left(I - K_k H_k \right) P_k^- \tag{C.18}$$

Notice that the structure of the Kalman Filter is that of a predictor corrector method. The time update, Eqs. (C.11)-(C.12), calculates the a priori state estimate and error covariance matrix. Then, the measurement is made and incorporated into the corrector portion through Eqs. (C.16)-(C.18). The measurement update computes the new Kalman gain prior to the measurement, which is incorporated in Eq. (C.18) calculating the a posteriori estimate of the state. Finally, the a posteriori error covariance is calculated. After each time and

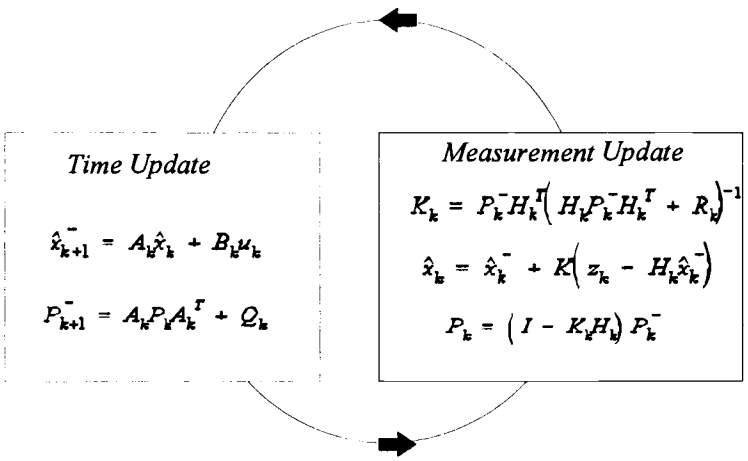

Figure C.2 - The Kalman Filter operation indicating the time update (project ahead) and measurement update (correct for the projection).

measurement update pair, the process is repeated with the prior a posteriori estimates used to project the new a priori estimate, recursively conditioning the current estimate on all of the previous measurements. Figure C.2 diagrams the complete recursive algorithm in the context of Figure C.1.

Initial conditions for the Kalman Filter can be given in order to start the algorithm. In general, we define the initial conditions as

$$\hat{x}_0 = E\,[x_0] \tag{C.19}$$

and the initial covariance matrix is

$$P_0 = E\,[(x_0 - \hat{x}_0)(x_0 - \hat{x}_0)^T] \tag{C.20}$$

In the implementation of the filter, either the measurement error covariance matrix R_k or the process noise covariance matrix Q_k could be measured prior to the filter operation. In particular, it is plausible for the measurement error covariance matrix to be measured since it is tacitly assumed that there is a measurement of the process. And, as such, there will be an off-line means of obtaining an estimate of the error covariance matrix, R_k prior to filter operation. In the case of the process noise covariance, the choice is often times less deterministic, especially since this noise source is often used to represent the uncertainty in the process. So, the process noise covariance can be used to "tune" the filter. For example, sometimes a poor model can be utilized as the state representation simply by injecting enough uncertainty into the

filter through Q_k. In any case, whether we have a rational basis for choosing the system parameters, superior performance of the filter can be obtained through judicious choices of the filter parameters R_k and Q_k.

It is important to remember that the Kalman Filter gives a linear, unbiased, minimum error variance recursive algorithm to optimally estimate the unknown state of the linear dynamics of a system whose noisy measurements are taken at discrete time intervals. The Kalman filter yields an optimal estimate of the state x_k, optimal in the sense that the spread of the estimate error probability density is minimized. That is, the Kalman Filter minimizes the cost function given by

$$J_k(\hat{x}_k) = E\left[(\hat{x}_k - x_k)^T M(\hat{x}_k - x_k)\right] \tag{C.21}$$

where M is some positive semi-definite matrix. The Kalman Filter also maintains the first and second order moments of the state distribution as we might imagine

$$E\,[x_k] = \hat{x}_k \tag{C.22}$$

and

$$E\,[(x_k - \hat{x}_k)(x_k - \hat{x}_k)^T] = P_k \tag{C.23}$$

Hence, in the case that the noise is Gaussian, the Kalman Filter gives the minimum variance estimate of the state. If the noise is not Gaussian, the Kalman Filter gives the linear minimum variance estimate having the smallest covariance of all such linear estimates. In this sense, the filter is optimal.

Also notice that $\hat{x}_{k+1}^-$ is a one-step ahead prediction. This is a very interesting fact in that should it be necessary to predict many steps ahead, the construct is already available. For N-step ahead prediction we consider the state transition from k+1 to N given by

$$x_{k+N} = \phi_{k+N,k+1} x_{k+1} + \sum_{i=k+1}^{k+N-1} \phi_{k+N,i} (B_i u_i + w_i) \qquad \text{(C.24)}$$

where $\phi_{N,k}$ is the state transition matrix.[2] Taking the conditional expectation yields

$$\hat{x}_{k+N/k} = \phi_{k+N,k+1} x_{k+1/k} + \sum_{i=k+1}^{k+N-1} \phi_{k+N,i} B_i u_i \qquad \text{(C.25)}$$

where it is explicitly shown that the expectation is taken with condition on k. Since the state transition matrix defines the evolution of the state from time i to time j > i, this gives a very simple means of computing the N-step ahead prediction of x_k. Similarly, the measurement variable is obtained by a strait substitution

$$z_{k+N} = H_{k+N} \hat{x}_{k+N/k} \qquad \text{(C.26)}$$

Hence, not only is the Kalman Filter the optimal estimate of the state of the system, but it can be used as an optimal predictor of the future state of the system.

C.2 The Extended Kalman Filter

Recall that the derivation of the Kalman Filter was based on linear systems. Fowler[3], in his dissertation showed that the Kalman Filter can be used with some success on certain nonlinear systems. He showed that a control system based upon the Kalman Filter estimator yields significant improvement with respect to covariance over other control systems. He also showed that for nondissipative systems, the improved performance translated to improved stability. However, in general, the covariance matrix will grow, particularly with respect to prediction, as the nonlinearities take effect. That is, while filtering in a linearized portion of phase space, the optimal filter performs well. As a trajectory strays from this linearized field, the performance of the filter will degrade.

In order to increase improvement under this more general case, the Extended Kalman Filter (EKF) and the Iterated Kalman Filter are investigated. The EKF is an extension of the Kalman Filter where the filter is continually updated by creating a linearization around the previous state estimate, starting with the given initial guess. A first order Taylor series approximation of the system dynamics is calculated at the previous state estimate as well as the measurement function at the corresponding predicted state. Consider the nonlinear difference equation

$$\tilde{x}_{k+1} = f(x_k, u_k, w_k) \tag{C.27}$$

with measurement update

$$\tilde{z}_k = h(x_k, v_k) \tag{C.28}$$

where, again, w_k and v_k represent the process and measurement noise, respectively. To estimate the process with these nonlinear state and measurements, we perform a linearization about the previous estimate. This is done by investigating the linearized versions of Eq. (C.27) and (C.28), which are seen to be given by

$$x_{k+1} = \tilde{x}_{k+1} + A(x_k - \hat{x}_k) + Ww_k \tag{C.29}$$

and

$$z_k = \tilde{z}_k + H(x_k - \hat{x}_k) + Vv_k \tag{C.30}$$

where A is the Jacobian matirx

$$A_{i,j} = \frac{\partial f_i}{\partial x_j}(x_k, u_k, 0) \tag{C.31}$$

W is the Jacobian

$$W_{i,j} = \frac{\partial f_i}{\partial w_j}(x_k, u_k, 0) \tag{C.32}$$

H is the Jacobian

$$H_{i,j} = \frac{\partial h_i}{\partial x_j}(x_k, 0) \tag{C.33}$$

and V is the Jacobian

$$V_{i,j} = \frac{\partial f_i}{\partial v_j}(x_k, 0) \tag{C.34}$$

Now, define the notation for the prediction error to be

$$\tilde{e}_{x_k} = x_k - \tilde{x}_k \tag{C.35}$$

and the measurement error to be

$$\tilde{e}_{z_k} = z_k - \tilde{z}_k \tag{C.36}$$

Substituting Eq. (C.35) and (C.36) into Eq. (C.29) and (C.30) we obtain

$$\tilde{e}_{x_k} \approx A\ (x_k - \hat{x}_k) + \varepsilon_k \tag{C.37}$$

and

$$\tilde{e}_{z_k} \approx H\ \tilde{e}_{x_k} + \eta_k \tag{C.38}$$

where ε_k and η_k are ensembles of independent random variables with zero mean and covariance matrices $W\ Q\ W^T$ and $V\ R\ V^T$.

Notice that these last two equations closely resemble the difference equations for the discrete Kalman Filter defined in the previous section. This suggests that we use the measured residual, Eq. (C.36), and a second, hypothetical Kalman Filter to estimate the prediction error Eq. (C.35). This estimate is then used to obtain the a posteriori state estimates for the nonlinear process. Suppose that this interim estimate is given as $\hat{e}\tilde{}_k$, then the a posteriori state estimate is

$$\hat{x}_k = \tilde{x}_k + \hat{e}_k \tag{C.39}$$

The random variables defined in this process have the following probability density functions

$$
\begin{aligned}
p(\tilde{e}_{x_k}) &\approx N\left(0,\ E[\tilde{e}_{x_k}\ \tilde{e}_{x_k}^T]\right) \\
p(\varepsilon_k) &\approx N\left(0,\ W\ Q_k\ W^T\right) \\
p(\eta_k) &\approx N\left(0,\ V\ R_k\ V^T\right)
\end{aligned}
\tag{C.40}
$$

Given this, the predicted value of the interim estimate, $\hat{e}^{-}_{k}$, is zero and the (hypothetical) Kalman Filter used to estimate it is simply

$$\hat{e}_k = K_k \tilde{e}_{z_k} \tag{C.41}$$

Substituting this back into Eq. (C.39) and then using the measurement residual Eq. (C.36) we obtain

$$\hat{x}_k = \tilde{x}_k + K_k(z_k - \tilde{z}_k) \tag{C.42}$$

where it is evident that we don't really need the hypothetical Kalman Filter. We can now use this for the measurement update in the Extended Kalman Filter with $\tilde{x}_k$ and $\tilde{z}_k$ as defined in Eqs. (C.27) and (C.28) and the Kalman gain, K_k from Eq. (C.16) and the appropriate substitution for the measurement error covariance. The complete EKF algorithm is shown in Figure C.3 and the complete set of EKF equations are given by

$$\hat{x}_{k+1}^{-} = f(\ x_k,\ u_k,\ 0) \tag{C.43}$$

$$P_{k+1}^{-} = A_k P_k A_k^T + W Q_k W^T \tag{C.44}$$

with the measurement update equations given by

$$K_k = P_k^- H_k^T \left(H_k P_k^- H_k^T + V R_k V^T \right)^{-1} \tag{C.45}$$

$$\hat{x}_k = \hat{x}_k^- + K\left(z_k - h\left(\hat{x}_k^-, 0 \right) \right) \tag{C.46}$$

$$P_k = \left(I - K_k H_k \right) P_k^- \tag{C.47}$$

where, as with the discrete Kalman Filter, Eqs. (C.45)-(C.47) correct the state and covariance estimates with the measurement z_k. Notice that the Jacobian, H_k, in the equation for the Kalman gain K_k serves to correctly propagate only the relevant components of the measurement information, that is, the observable components of the state.

Now, taking this one step further, we define the Iterated Kalman Filter by noticing that an iteration technique can be applied to update the state estimate and covariance matrix, consequently improving performance. That is, within a given time step, the sequences $\{x_k^i\}$ and $\{P^i\}$ can be defined inductively as follows:

$$x_k^{i+1} = \hat{x}_k + K^i \left(z_k - h(x_k^i) - H_k^i (\hat{x} - x_k^i) \right) \tag{C.48}$$

$$P_k^{i+1} = \left(I - K_k^i H_k^i \right) P_k^i \tag{C.49}$$

where

$$H_k^i = \frac{\partial h}{\partial x_k}(x_k^i) \tag{C.50}$$

and

$$K_k^i = P_k^i H_k^{i\,T}\left(H_k^i P_k^i H_k^{i\,T} + R_k\right)^{-1} \tag{C.51}$$

are the updates for the linearized measurement matrix and the Kalman gain. The induction process begins with the initial conditions

$$x_k^0 = \hat{x}_k\,, \qquad P_k^0 = P_{k-1} \tag{C.52}$$

where the initial covariance matrix is taken to be the last one calculated in the previous step. This gives the update for the IKF as

$$\hat{x}_{k+1} = x_k^i\,, \qquad P_{k+1} = P_k^i \tag{C.53}$$

It is evident that for $i = 0$ in Eqs. (C.48)-(C.49) we obtain the EKF. Also notice that both methods reduce to the ordinary Kalman Filter in the case that the measurement function is affine.

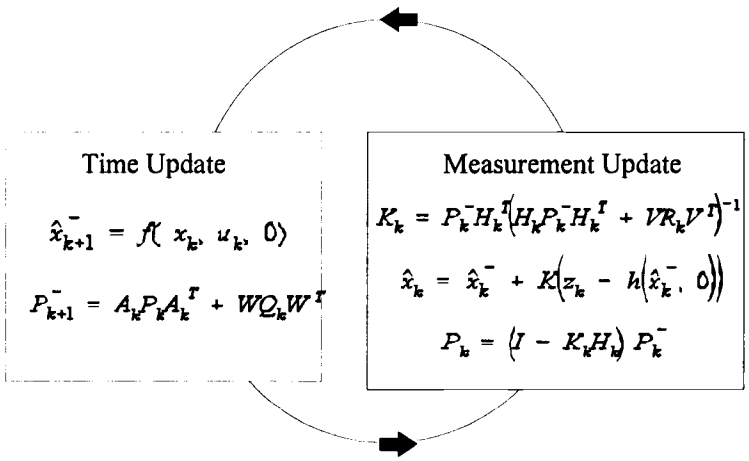

Figure C.3 - The Extended Kalman Filter with the time update (project ahead) and the measurement update (correct for the projection).

It can be shown that the IKF is capable of providing better performance then the ordinary Kalman Filter in the presence of significant nonlinearities since the IKF introduces a reference trajectory which is incorporated into the iteratively estimates.[4] Notice that the iterations can be stopped by any number of convergence criteria such as when two consecutive values $\hat{x}_k^i$ and $\hat{x}_k^{i+1}$ differ by a pre-defined amount or after a predetermined number of iterations. Notice that this iteration technique becomes a Gauss-Newton process under these conditions.[5] The trade-off for this technique, of course, is computational power required to perform the iterations within each time step.

References

1. Anderson, B. D. O., and Moore, J., B. (1979). *Optimal Filtering,* Prentice Hall.

2. DeCarlo, R., A.(1989). *Linear Systems, A State Variable Approach with Numerical Implementation,* Prentice Hall, New Jersey.

3. Fowler, T. B. (1988) "Stochastic Control Techniques Applied to Chaotic Systems," *Proc.1988 IEEE Int. Symp. on Cir. and Sys.*, Vol. 1, Helsinki, Finland.

4. Bell, B. M. and Cathey, F. W. (1993). "The Iterated Kalman Filter Update as a Gauss-Newton Method," *IEEE Trans. on Automatic Control*, Vol. 38, No. 2, 294-297.

5. Bell, B. M. (1994). "The Iterated Kalman Smoother as a Gauss-Newton Method," *SIAM J. Optimization*, Vol. 4, No. 3, 626-636.